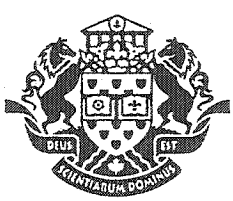

Université d'Ottawa · University of Ottawa

Université d'Ottawa · University of Ottawa

FACULTÉ DES ÉTUDES SUPÉRIEURES ET POSTDOCTORALES

FACULTY OF GRADUATE AND POSTDOCTORAL STUDIES

MALEK, Sameh

AUTEUR DE LA THÈSE - AUTHOR OF THESIS

M.Sc. (Neuroscience)

GRADE - DEGREE

Cellular and Molecular Medicine

FACULTÉ, ÉCOLE, DÉPARTEMENT - FACULTY, SCHOOL, DEPARTMENT

TITRE DE LA THÈSE - TITLE OF THE THESIS

Aberrant Chloride Transport Contributes to Anoxic Injury in Central Myelinated Axons

P. Stys

DIRECTEUR DE LA THÈSE - THESIS SUPERVISOR

EXAMINATEURS DE LA THÈSE - THESIS EXAMINERS

M. Hogan

B. Hu

J.-M. De Koninck, Ph.D.

LE DOYEN DE LA FACULTÉ DES ÉTUDES SUPÉRIEURES ET POSTDOCTORALES

SIGNATURE

DEAN OF THE FACULTY OF GRADUATE AND POSTDOCTORAL STUDIES

ABERRANT CHLORIDE TRANSPORT CONTRIBUTES TO ANOXIC INJURY IN CENTRAL MYELINATED AXONS

By

Sameh A Malek

A Thesis submitted to the
School of Graduate Studies and Research
in partial fulfillment of the requirments for the degree of
Master of Science

Department of Cellular and Molecular Medicine
University of Ottawa
Ottawa, Ontario
July, 2003

Your file Votre référence
ISBN: 0-612-89900-4
Our file Notre référence
ISBN: 0-612-89900-4

ABSTRACT

Rundown of ionic gradients is a central feature of white matter anoxic injury. However little is known about the contribution of anions such as Cl^- . Previous studies have shown that Na^+-blockade during anoxia was in adequate in preserving K^+-loss. We hypothesized that run down of the K^+-gradient during anoxia/Na^+-channel inhibition proceeds in conjunction with an anion and more specifically Cl^-. We used the *in vitro* rat optic nerve to study the role of aberrant Cl^- transport in anoxia/ischemia. After 30 min of anoxia (NaN_3 2mM), axonal membrane potential (V_m) decreased to 42 ± 11% of control, and to 73 ± 11% in the presence of TTX (1 μM). TTX + DIDS 500μM (a broad spectrum anion transport blocker) abolished anoxic depolarization (95 ± 8%). Inhibition of the K-Cl cotransporter (KCC) (furosemide 100μM) together with TTX was also more effective than TTX alone (84±14%). Compound action potential (CAP) area recovered to 26±6% of control after 1 h anoxia. KCC blockade (furosemide 10μM) improved outcome (40±4%) and TTX (100nM) was even more effective (74±12%). In contrast, the Cl^- channel blocker niflumic acid (50 μM) worsened injury (6±1%). Co-application of TTX (100 nM) + furosemide (10 μM) was more effective than either agent alone (91±9%). Furosemide was also very effective at normalizing the shape of the CAPs. The KCC3a isoform was localized to astrocytes. KCC3 and weaker KCC3a was detected in myelin of larger axons. KCC2 was seen in oligodendrocytes and within axon cylinders. Cl^- gradients contribute to resting optic nerve membrane potential, and transporter and channel-mediated Cl^- fluxes of during anoxia contribute to injury, possibly due cellular volume changes and disruption of axo-glial integrity, leading to propagation failure and distortion of fiber conduction velocities.

ACKNOWLEDGMENTS

First, I would like to thank GOD for his abundant grace and uncountable gifts. I am also extremely grateful to my supervisor Dr. Peter Stys for offering me the opportunity to be trained at an intellectually stimulating environment, for his constant encouragement and support and excellent guidance. Dr. Stys has provided me with outstanding training in the scientific research philosophy; not to mention my writing skills have improved extensively.

I would like to thank my advisory committee members, Dr. Leo Renaud and Dr. Petro Doroshenko for their valuable advice and comments. I also had the pleasure of working with a number of well trained lab colleagues: Dr. Quibo Jiang, Dr. Mohammed Ouardouz. I thank Dr. Ouardouz for the numerous hours spent critically evaluating my thesis and paper, and for having those intellectually stimulating discussions; your help is very much appreciated. The technical assistance of Elaine Coderre in producing the immunohistochemical results with KCC was invaluable and greatly appreciated.

My deepest gratitude has to go towards my mother and late father for always supporting me and constantly encouraging me to excel in life. I would like to thank my brother and sister for their support. I can't forget the person that has kept my sanity through the rough times; Amy your presence in my life was certainly a gift from GOD. Thanks goes out to the gang (Rafik, Rami and George) for their support.

Finally, I would like to acknowledge the Ontario Neurotrauma Foundation for their financial assistance.

TABLE OF CONTENTS

LIST OF TABLES

LIST OF FIGURES

LIST OF ABBREVIATIONS

$[\ ]_i$: intracellular concentration

$[\ ]_o$: extracellular concentration

aCSF; artificial cerebral spinal fluid

Ca^{2+}_i: intracellular calcium

Ca^{2+}_o: extracellular calcium

CAP: compound action potential

CNS: central nervous system

CN^-: cyanide

DIDS: 4,4`-Diisothiocyanatostilbene-2,2`-disulfonic acid disodium salt

DNDS: 4-acetamido-4'-isothiocyanatostilbene-2,2'-disulfonic acid

ECS: extracellular space

E_K: K^+ equilibrium

EPMA: electron probe X-ray microanalysis

i_g: trans-gap current

I_{CaCl}: Calcium-activated Cl^- current

$I_{Cl,h}$: Inwardly-rectifying Cl^- current

$I_{Cl,Swell}$: Swelling-activated Cl^- current

$I_{Cl,Vol}$: Volume-activated Cl^- current

IAA: Iodoacetic acid-Na^+ salt

K^+_i: intracellular potassium

K^+_o: extracellular potassium

K_{fast}: fast K^+ channel

K_{slow}: slow K^+channel

KCC: K^+-Cl^- cotransporter

N_3^-: Azide

Na^+_i: intracellular sodium

Na^+_o: extracellular sodium

NFA: Niflumic Acid

NKCC: Na^+-K^+-Cl^- cotransporter

NPPB: 5-Nitro-2-(3-phenylpropylamino)benzoic acid

ORCC: outwardly rectifying Cl^- current

pH_i: intracellular pH

P_K: K^+ permeability

P_{Na}: Na^+ permeability

R_b: baseline resistance

R_e; external resistance

R_g: trans-gap resistance

R_i: internal axoplasmic resistance

R_p: parallel resistance

RON: rat optic nerve

SITS: 4,4'-dinitrostilbene-2,2'-disulfonic acid

TTX: tetrodotoxin

V_g: recorded membrane potential

V_m: absolute membrane potential

VGCC: voltage-gated calcium channel

WM: white matter

"We shall not cease from exploration
And the end of all our exploring
Will be to arrive where we started
And know the place for the first time.
Through the unknown, unremembered gate
When the last of earth left to discover
Is that which was the beginning"

T.S. Elliot: Little Giding, 4th quartet

To my Mother
And
In memory of my late Father

CHAPTER 1

INTRODUCTION

Axons of central nervous system (CNS) are highly specialized structures whose membranes are capable of producing currents and maintaining potentials. This in turn allows them to fulfill the purpose of signal transmission between neurons. Axonal functionality relies on the integrity of their cylindrical structure. While the use of squid axons has allowed for the elucidation of nonmyelinated axon electrical attributes, the following pertains to myelinated axons.

The complexity of the CNS is attributed to the physiological intricacies of the axon/neuronal relationship, and in particular myelinated axons. The presence of myelin wrapping around a population of axons allows for an increase in conduction speed, such that electrical impulses propagate in a saltatory fashion. Interrupting the segments of myelin along the axon are highly specialized regions known as nodes where the axolemma is exposed to the extracellular fluid. These domains were first described by Ranvier in 1875, however it wasn't until the 1980s when they were studied in detail. Indeed, a deep appreciation of these structures has risen from the invaluable role they play in action potential conduction. This site involves three significant cellular elements, which are the axon, the oligodendrocyte and the perinodal astrocyte (Black *et al*, 1995).

Oligodendrocytes and astrocytes are collectively called neuroglia, a term first coined by Virchow in 1846. The histological characterization of each of these components was the result of the microscopic studies of Ramon y Cajal and Rio Hortega. In 1913, the former successfully utilized gold impregnation to identify astrocytes and another element, which was not sensitive to this technique. In fact, a few years later, in 1928 Rio Hortega distinguished the oligodendrocyte cells using silver carbonate. It is now well established that oligodendrocytes are myelin forming cells of the CNS (Hirano 1968; Waxman and Sims 1984) In many mature white matter tracts original oligodendroglial cells keep the connectivity to their corresponding myelin sheaths via thin cytoplasmic bridges (Waxman and Sims 1984). Another integral part of the node is the astrocyte whose processes extend to come in close proximity with the nodal axonal membrane (Black *et al.* 1995). Hildebrand (1971) suggested that these cells participate in

nodal metabolism and control ionic concentrations at the nodal extracellular microenvironment. The optimum environment created by glial components to facilitate saltatory conduction underlines the critical functionality of the nodal domain. Axonal nodal membrane, seats a number of important channels and other ionic transporters, each having a major impact on axonal physiology. Equally as important are the specific channels at the internodal region. A diagram of outlining the node domain is shown in figure 1.1.

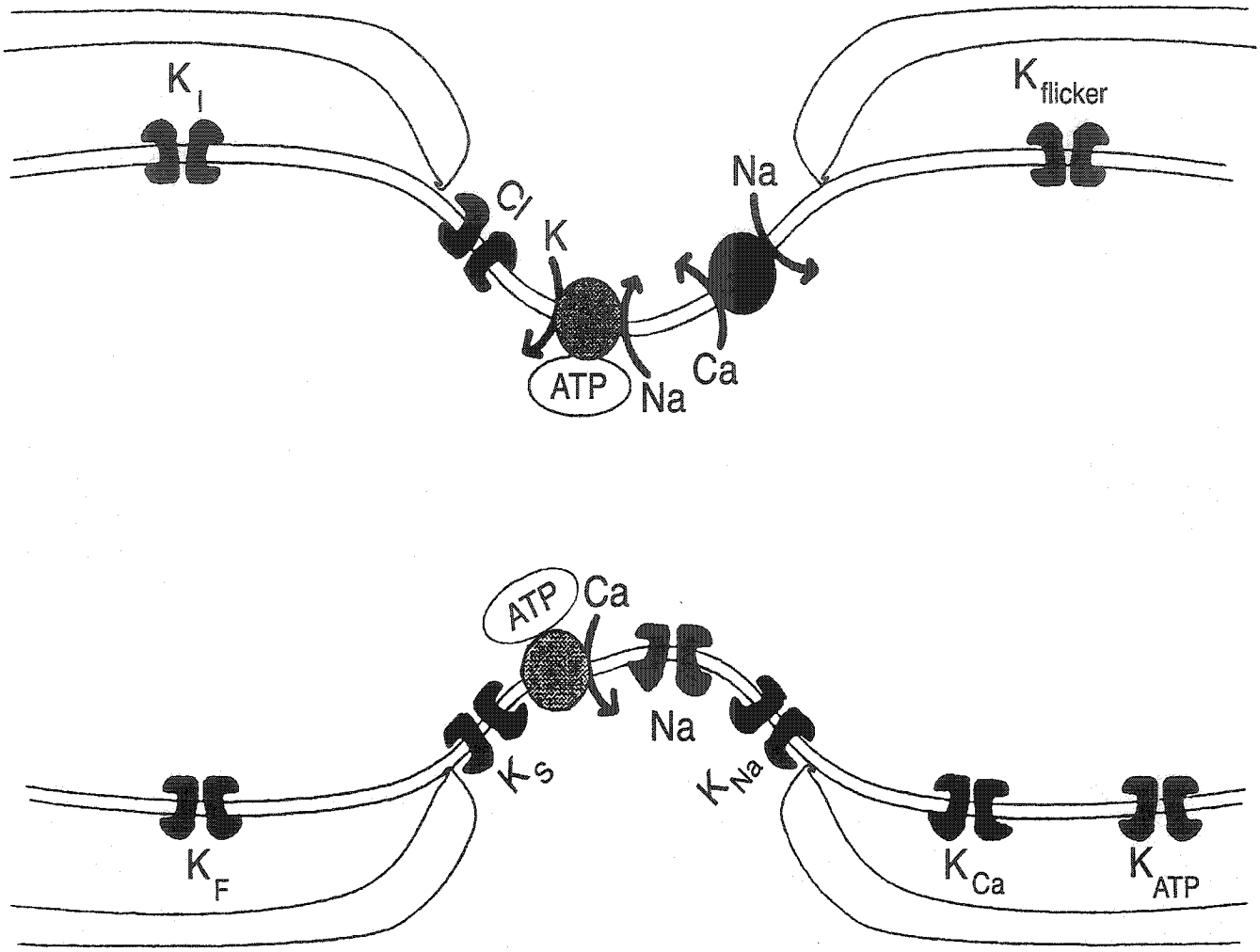

Figure 1.1: Diagram of channel and transporter distribution in myelinated axons at the node of Ranvier. Nodal Na^+ channels found in high density carry the inward depolarizing current at the onset and during the action potential. Potassium channels have a more diverse subtype and distribution within this area. There are fast(K_F), intermediate(K_I) and slow (K_S) kinetics, chemically modulated K^+ channels (by axoplasmic ATP, Ca^{2+}, or Na^+ ions) and voltage-independent "flicker" channels. These are involved in setting membrane potential, modulating the firing patterns and in some fibers aid in action potential repolarization. Independent pumps such as Na^+-K^+ and Ca^{2+} -ATPase pumps are involved in maintaining the ionic homeostasis as well as the Na^+-Ca^{2+} antiporter. Precise location and distribution of these channels varies among species and within the peripheral and central nervous system. There is a tight seal at the paranodal area which creates the isolation needed for quick, reliable signal propagation. Modified from Vogel and Schwarz, 1995.

1.1 Axon: Basic Physiology

1.1.1 Membrane Potential determinants

Resting axonal permeability is biased towards K^+ over other ions, due to the opening of K^+-channels. As a result, a concentration gradient develops across the membrane to create a potential. However, the potential across the membrane is not equal to E_K. The resting V_m results from the interaction of the permeabilities for the different ions. Quantitatively the Goldman-Hodgkin-Katz (GHK) equation gives an expression for V_m from the permeabilities in the following form:

$$V_m = \left(\frac{RT}{F}\right) \ln\left(\frac{P_K[K^+]_o + P_{Na}[Na^+]_o + P_{Cl}[Cl^-]_i}{P_K[K^+]_i + P_{Na}[Na^+]_i + P_{Cl}[Cl^-]_o}\right)$$

where P_K, P_{Na}, P_{Cl} are membrane permeabilites for the specific ion. In the case of the rat optic nerve, the equation can be modified to:

$$V_m = \left(\frac{RT}{F}\right) \ln\left(\frac{P_K[K^+]_o + P_{Na}[Na^+]_o}{P_K[K^+]_i + P_{Na}[Na^+]_i}\right)$$

because Cl^- was found to have minimal influence on V_m in the adult rat optic nerve, due to its insignificant membrane permeability at rest (Connors and Ransom 1984).

1.1.2 Action Potential Processes

An action potential originating at the axon hilock is relayed to other neurons via the axon and synaptic bouton. Initial work by Hodgkin and Huxley in 1952, done in the squid giant axon, determined the ionic basis of the action potential. An electrical stimulus produces increases in Na^+ conductance, which at sufficient levels allows for the rising

phase of the action potential. Coordinated interplay between fast Na^+-channel inactivation at the peak of the action potential and the delayed rise in K^+ conductance are both responsible for membrane repolarization. K^+-channels, K^+_{fast}, present are poised to attenuate depolarizations once activated. In fact experiments done using 4-AP, a K^+-channel blocker, in the rat optic nerve showed a broadening of the action potential waveform (Gordon et al. 1988). Some fibers also displayed repetitive firing with longer lasting depolarization post spike (Gordon *et al.* 1988; Waxman and Ritchie 1993). In addition to repolarizing V_m, this type of channel functions to prevent re-excitation brought about by additional Na^+-channel activation (Ritchie, 1995). There exists a second pathway responsible for repolarization.

TEA-sensitive, kinetically slower K^+-channels, K^+_{slow}, are present in nodal axolemma of mammalian myelinated fibers (Waxman 1995). Blockade of the channels had little effect on the action potential waveform in RON (Gordon *et al.* 1988). Yet when combined with 4-AP, TEA abolished the observed prolonged depolarization associated with 4-AP (Gordon *et al.* 1988).Therefore 4-AP sensitive channels respond to single stimulus while TEA-sensitive ones will repolarize V_m under high activity conditions. However, an excitatory pathway balances these inhibitory ones.

The inward rectifier, a voltage dependent ion channel with mixed permeability to Na^+ and K^+ has been shown to exist in optic nerve (Birch *et al.* 1991; Eng *et al.* 1990). Activated by hyperpolarizing effects such as increase Na^+/K^+-ATPase activity after high frequency transmission (Gordon *et al.* 1988; Lux *et al.* 1970), the channel mediates a depolarization, which re-establishes axonal V_m towards resting potential (Waxman 1995) and in turn facilitates impulse transmission.

In myelinated axons a high density of Na^+-channels (>1000/μm^2) is concentrated at the nodes (Neumcke and Stämpfli 1982; Waxman and Ritchie 1993). The internodes are covered by myelin, which creates a high resistance, low capacitance patch of membrane. Thus after depolarization and Na^+-channel activation the excitation signal will "jump" to the subsequent node along the length of the axon propagating in a saltatory fashion.

1.1.3 Channels and Pump

1.1.3.1 K-channel:

The fast activating.

Paranodal regions of axon membrane under myelin have been shown to contain a 4-AP sensitive K^+-channel (Foster *et al.* 1982; Kocsis *et al.* 1982). Blockade of the channel was shown to have a significant effect on action potential in premyelinated axons compared to mature myelinated ones. For example Kocsis *et al.* 1987 showed that external application of 4-AP to premyelinated axons caused prolongation of action potential as seen by significant delay in repolarization. Furthermore, voltage-clamp recordings from acutely demyelinated axons revealed similar results. This indicates the masking of the channels by myelin. In fact paranodal K^+-channels, have been described genetically in the rat optic nerve by Rasband *et al.* (1999), who were able to demonstrate that pore forming α-subunit protein Kv1.1, 1.2, 1.6 and the cytoplasmic subunit Kvβ2.1 were colocalized at juxtaparanodal regions (Rasband *et al.* 1999).

SlowK-channel.

Cellular localization for slow channels was shown in the internodal and paranodal zones as well as at the node of myelinated fibers (Baker *et al.* 1987; Chiu and Ritchie 1980; Waxman and Ritchie 1993). Eng and colleagues (1988) induced a TEA-sensitive afterhypolarization by high frequency stimulation in both developmental stages, young and mature nerves. Myelination of fibers abolished the 4-AP effect yet it had no effect on the TEA-sensitive afterhyperpolarization, which persisted even after complete myelination (Eng *et al.* 1990). Consequently, it was concluded that the channel is located at the node. Others such as Roper and Schwarz (1989) demonstrated a high density of slow K^+-channels at the node with a decline to $1/30^{th}$ of the density at the internodal region. Safronov *et al.* (1993) put forth the estimate of 110 slow channels/μm^2 in rat axonal membrane.

Study of K^+_{slow} channel activation revealed that 35% of the channels are open at rest (Roper and Schwarz 1989). This provides a route for continued K^+ entry at rest. Others such as Chiu and Ritchie (1981) suggested that 13% of the nodal K^+ leakage at rest is the result of K^+_{slow} channels.

1.1.3.2 Na-channel:

Early ultrastructural studies using freeze fracture electron microscopy revealed a difference in particle density between internode and nodal regions with the latter having a higher concentration (Black *et al.* 1982). Subsequent, studies established that there is a high clustering of Na^+-channel at the nodal gap (Novakovic *et al.* 1996; Shrager 1989; Vabnick *et al.* 1996). Anchoring of the Na^+-channel is established via specific cytoskeletal proteins namely Spectrin and Ankyrin (Srinivasan *et al.* 1988). According to the authors, Ankyrin was found to interact specifically with the cytoplasmic domain of the Na^+-channel. These localization studies addressed the presence of the rapidly activating-inactivating Na^+-channel, similar to the type seen in squid giant axon.

The Slowly Inactivating Na^+ Current

Early reports outlining the presence of slowly inactivating Na^+-conductance surfaced at the beginning of the 1980's through the work of Llinas, Shoukimas and French. In Cs-perfused squid axons, Shoukimas and French (1980) were able to observe under voltage-clamp an non-inactivating Na^+-conductance. Deduction of this phenomenon in nonperfused axons was achieved by comparing recorded membrane properties before and after TTX addition to the bath. In fact the difference between current records with and without TTX denotes the contribution of Na^+ conductance to the total current. Thus over a time scale of tens of milliseconds, they reported that the Na^+ conductance did not inactivate in nonperfused axons. Moreover, Cs-perfused and nonperfused membrane recordings were similar at depolarized potentials attesting to the fact that these channels remain active even at positive potentials. Others working with DRG neurons and using whole cell patch clamp, outlined the presence of both fast and slow Na^+-currents in the axon (Honmou *et al.* 1994). Inference about the existence of these channels in white matter tracts came from observations on burst activity, produced from persistent depolarization following primary spike post 4-AP exposure (Bowe *et al.* 1985; Kocsis *et al.* 1982; Stys *et al.* 1993). Moreover, Stys *et al.* (1993), recorded a noninactivating –TTX sensitive Na^+-conductance at various levels of K^+-induced depolarization, in the rat optic nerve.

Second to K^+ is the Na^+ permeability at rest, which causes V_m to deviate from E_K. Channel blockade produced a hyperpolarizing effect on the V_m of RON even at depolarized potentials reflecting the nonclassical behaviour of the channel. Molecular analysis of the channel localized the responsible gene in humans, rats and mouse CNS.

Mouse Scn8a and its rat ortholog NaCh6, fall under the type 1 channel and more specifically the Nav1.6 gene (Goldin 1999) . Nav1.6 has been shown to be responsible for persistent currents in Purkinje cells (Raman *et al.* 1997; Smith *et al.* 1998). The lack of inactivation displayed by the channel is attributed to the β subunit, which possesses modulatory properties, since in the absence of the subunit the channel inactivates more rapidly than other isoforms (Smith *et al.* 1998). In comparison to other CNS isoforms, namely Nav1.1 and 1.2, Nav1.6 showed the greatest percentage of persistent current which increased linearly with more positive potentials (Smith *et al.* 1998). The presence of such type of conductance has in turn introduced questions concerning its functionality.

Stys *et al* (1993) put forth the interesting possibility that the channel serves to fuel the Na-K-ATPase pump with necessary Na^+_i needed for the proper functioning of the pump. This notion is based on the work of Nakao and Gadsby (1989) who elucidated that the pump requires a finite $[Na^+]_i$ for proper activity. In fact RON axonal Na^+-pump behaves in such a way, in that it is sensitive to changes in $[Na^+]_i$ (Ransom *et al.* 2000) similar to pumps present in other types of neurons (Rose and Ransom 1997; Thomas 1972b).

1.1.3.3 Na-K-ATPase.

It is estimated that 50-60% of total brain ATP is used for ionic regulation (Erecinska and Silver 1989). One of the main ionic regulators is the Na^+-pump. Identified by Caldwell *et al.* (1960) , the protein utilizes ATP to drive the exchange of Na^+ and K^+ with a stoichiometry of $3Na^+$ extruded simultaneously with $2K^+$ admitted. Two polypeptide chains, 112kD α-subunit and 35kD β-subunit make up the protein. The function of the α-subunit is believed to be ion binding while the β participates in the assembly of the complex and the cellular localization at the axolemma (McDonough *et al.* 1990).Using immunocytochemistry with mammalian and fish CNS axons, Wood *et al.* (1977) and Ariyasu and Ellisman (1987) demonstrated the presence of the Na^+-K^+

ATPase pump in nodal regions of the axons, with no detectable signal from at the internodal region (Ariyasu and Ellisman 1987; Wood *et al.* 1977). On the other hand, Mata *et al.* (1991) showed an exclusive internodal localization of the Na^+-K^+ ATPase pump in both CNS and PNS fibers. Thus it seems that the protein might be present in both regions of the axon. In any case, due to the stoichiometry of the exchange, the net effect on V_m will be a hyperpolarizing effect estimated at 1-2 mV in squid giant axon (De Weer and Geduldig 1973), and 7-10 mV in myelinated mammalian fibers (Leppanen and Stys 1997a; Thomas 1972a).

1.1.3.4 Inward Rectifier.

Activated by hyperpolarization to mediate a depolarizing effect on membrane potential, the inward rectifier channel was shown to have mixed permeability to Na^+ and K^+ and to be blocked by Cs^+ (Baker *et al.* 1987). It is thought to exist in areas spanning both nodal and internodal regions with the functional role of stabilizing membrane potential during periods of intense electrical activity, since electrogenic activity of the Na^+-ATPase pump results in excessive hyperpolarization (Eng *et al.* 1990). Activation of inwardly rectifier channel would tend to depolarize the axon and prevent conduction block (Waxman 1995)

1.2 Cl^- Homeostasis in CNS: A brief overview

The functional effects of Cl^- transport in the CNS underscores the importance of Cl^-regulatory mechanisms. Disruption of Cl^- homeostasis could trigger a wide range of processes such as over-excitability occurring during epileptic discharges, pH deregulation and deregulated cell volume. Maintaining Cl^- at its respective level requires the presence of transport systems capable of ensuring a homeostatic distribution. To this end, vertebrate neurons are equipped with cotransporters such as K-Cl and Na-K-Cl, exchangers such as Na^+-dependent and independent Cl^-/HCO_3^- and channels be it voltage, ligand gated and/or Ca^{2+}-activated.

1.2.1Chloride Carriers:

1.2.1.1 K-Cl cotransport(KCC).

Work done by Lux *et al.* (1976) in spinal motor neurons was the first to indicate the existence of this type of transport in nervous system. Thompson *et al.* (1988) described a K-Cl cotransport system capable of maintaining E_{Cl} at more negative potentials than V_m in pig cingulate cortical neurons. Their conclusions were based on the observations that Cl^- extrusion following a Cl^-_i load is blocked by furosemide, a loop diuretic and a relatively specific blocker for the protein. The transport system was found to be K^+_o sensitive such that increases in $[K^+]_o$ caused a subsequent increase in $[Cl^-]_i$. Interestingly, no change in cell input resistance or V_m accompanied Cl^- shifts indicative of an electroneutral mechanism that is not dependent on opening of a channel. Interestingly, maintaining E_{Cl} at more negative potentials than V_m via the uphill extrusion of Cl^- is an energy dependent process. Yet the cotransporter is capable of facilitating this process without catalyzing ATP in the following manner.

While mediating the cotranport of K^+ and Cl^- across the membrane in a 1:1 stiochiometry, the K-Cl cotransporter, though reversible, uses the K^+ gradient to control Cl^- levels. Under physiological conditions, the Na^+/K^+-ATPase allows for an energetically favourable net outward driving force on the KCC because of the difference between $[K^+]_i$ and $[K^+]_o$ (Alvarez-Leefmans, 1990), allowing for net Cl^- and K^+ extrusion. Quantitavely, the net driving force on the cotransporter ($\Delta\mu_{KCC}$) is the sum of the chemical potential differences of K^+ ($\Delta\mu_K$) and Cl^- ($\Delta\mu_{Cl}$) (Kakazu *et al.* 1999).

$$\Delta\mu_{KCC} = \Delta\mu_K + \Delta\mu_{Cl}$$

which simplifies to : $[K^+]_i \times [Cl^-]_i = [K^+]_o \times [Cl^-]_o$

given the 1:1 stoichiometry. From this relationship we see the dependence of Cl^- on the K^+ gradient.

The KCC is subject not only to transmembrane K^+ and Cl^- gradients, but is also modulated by several signaling pathways. The protein depends on a conserved carboxy

terminus for proper functioning (Strange *et al.* 2000). In addition, protein phosphatase-1 (PP-1), which has been shown to be essential in KCC activation (Mercado *et al.* 2000), maintains a dephosphorylated active state of the protein. Other signals such as intracellular Mg^{2+} and ATP were found to modulate the cotransporter. Presence of both compounds showed synergistic maximal inhibition on KCC activity in low-K^+ sheep red blood cells, indicating that MgATP interferes with phosphoryltation/dephosphorylation processes required for normal protein activity (Ortiz-Carranza *et al.* 1996).

During the last few years there has been a surge in the interest in KCC because of the development of molecular techniques allowing for the cloning and the functional characterization of this protein. Up to date, there have been 4 identified cloned isoforms of the cotransporter, KCC1-4 (Gillen *et al.* 1996; Hiki *et al.* 1999; Mount *et al.* 1999; Payne *et al.* 1996; Race *et al.* 1999). Phylogenetic comparison grouped KCC1 with 3 and KCC2 with 4 (Mercado *et al.* 2000). Cellular localization of the cotransporter is determined by the protein isoform. KCC1 has a ubiquitous distribution and is believed to be the "housekeeping" isoform responsible for cell volume regulation (Gillen *et al.* 1996). KCC3 is found predominantly in heart, skeletal muscle, brain and kidney (Race *et al.* 1999) while KCC4 is mostly in heart and kidney (Mount *et al.* 1999). KCC2, the neuronal specific isoform (Payne *et al* 1996) is believed to be the regulatory pathway by which Cl^- gradient is maintained favourably in the CNS for GABA-hyperpolarizing effects (Williams *et al.* 1999). Yet the GABA response at different developmental stages produces opposite responses.

During early neuronal development $GABA_A$-receptor mediated responses are often depolarizing (Ben-Ari *et al.* 1994; Owens *et al.* 1996) because of the Cl^- gradient favouring Cl^- extrusion due to the high initial levels of intracellular Cl^-. Upregulation of KCC2 expression postnatally, shown in the rat brain (Delpire *et al.* 1999), regulates Cl^-_i in such a way as to allow reversal of the GABA-response from depolarizing to hyperpolarizing (Rivera *et al.* 1999).

1.2.1.2 Na-K-Cl cotransport(NKCC).

The Na-K-Cl cotransporter is an electrically silent protein, which translocates Na^+, K^+ and Cl^- with a stoichiometry of 1:1:2; one exception is the squid giant axon

isoform having a ratio of 2:1:3 (Russell 2000). Molecular studies revealed the existence of 2 isoforms with the NKCC1 having a wide tissue distribution (Delpire *et al.* 1994; Xu *et al.* 1994) while NKCC2 has only been found in vertebrate kidney (Payne and Forbush 1995). *In situ* hybridization and immunocytochemical studies revealed an abundant distribution of NKCC1 on the plasma membrane of rat neocortex as well as CA1-CA3 neurons of pyramidal cells in hippocampus (Plotkin *et al.* 1997a; Plotkin *et al.* 1997b).

Work done by Russell (1979) in internally dialyzed squid axons, examined the effects of ATP on the transporter. Subsequent to the reduction of ATP was the loss of ion translocation. Even though the protein is not itself an ATPase, it is thought that ATP is needed for phosphorylation, rendering the protein active (Lytle 1997). Cl^-_i has been shown to modify cotransporter activity. Raising Cl^-_i blocked both inward and outward flux modes of the cotransporter in a concentration dependent manner (Breitwieser *et al.* 1990). Neurotransmitter modulation of NKCC was demonstrated by (Sun and Murali 1999). The conclusion was based on the finding that NMDA receptor activation causes increases in Ca^{2+}_i and subsequent stimulation of ser/thr protein kinases, such as the Ca^{2+}/CAMK II (Hollmann and Heinemann 1994), which in turn phosphorylates the cotransporter. In addition, BAPTA-AM, a Ca^{2+}-chelator, completely abolished the stimulation of the cotransporter by NMDA. The cotransporter mediates regulatory volume increase, serving the function of net salt and water transport into the cell (Cala, 1990).

NKCC has been shown to contribute to active Cl^-_i accumulation in neurons both in early (Sun and Murali 1999) and adult stages (Alvarez-Leefmans *et al.* 1988; Ballanyi and Grafe 1985; Misgeld *et al.* 1986). Early development of the NKCC coupled with the delayed expression of KCC in neuronal tissue (Lu *et al.* 1999; Sun and Murali 1999) results in high Cl^-_i levels. Thus it is the interplay between KCC and NKCC that dictates the levels Cl^-. Expression levels of NKCC1 mRNA in rat brain assessed using *in situ* hybridization, revealed a strong signal from choroid plexus epithelial cells, forebrain and hippocampal regions (Kanaka *et al.* 2001). Specific cellular localization will be outlined in greater detail in the section on Cl^- transport in glia.

Thermodynamically the driving force on the transporter can be written as (Russell 2000):

$$\Delta\mu_{NKCC} = \Delta\mu_{Na} + \Delta\mu_{K} + 2\Delta\mu_{Cl}$$

Simplified, the equation reduced to (Alvarez-Leefmans, 1990):

$$[Na^+]_i \times [K^+]_i \times [Cl^-]^2_i = [Na^+]_o \times [K^+]_o \times [Cl^-]^2_o$$

The Cl^- gradient is a major contributor to the driving force since it depends upon the square of $[Cl^-]$. Similarly, $[Na^+]_i$ and $[K^+]_o$ are smaller relative to $[Na^+]_o$ and $[K^+]_i$ making the cotransporter more sensitive to changes in $[Na^+]_i$ and $[K^+]_o$ (Cala, 1990).

1.2.1.3 .Na^+-dependent Cl^-/HCO_3^- exchanger

Recovery from pH_i shifts has been shown to occur via Na^+-dependent Cl^-/HCO_3^- exchanger in squid giant axons (Boron and De Weer 1976). The process is Na^+-dependent as it is driven by the Na^+-gradient with a requirement for ATP_i, not for energetic duties (Russell and Boron 1990) but for modulatory purposes. 4,4'-diisothiocyanatostilbene-2,2'-disulfonic acid (DIDS) completely inhibits the transporter as do other stilbene derivatives such as 4,4'-dinitrostilbene-2,2'-disulfonic acid (SITS) and 4-acetamido-4'-isothiocyanatostilbene-2,2'-disulfonic acid (DNDS) (Boron and Knakal 1989).

Given the coupling of Cl^- to ions related to pH, Cl^- concentrations and transport may have important consequences for cellular acid-base balance. In 1983, Boron and Russell investigated the role of Cl_i^- on the recovery from an acidic load in squid axons. They reported that in order for Cl^- efflux to occur pH_i must be acidic in the presence of ATP_i with Na^+ and extracellular HCO_3^- (Boron and Russell 1983). In vertebrate preparations, such as pyramidal neurons from CA1 rat hippocampus, the existence of this type of Cl^- mediated pH regulation was confirmed by (Schwiening and Boron 1994). Their results indicate that similar to invertebrates, CA1 neurons recover from acidic loads by the same means outlined for the squid axon and depending upon similar parameters. In

fact loss of Cl^-_i during recovery from the acidic load will also impact neurotransmission by changing the GABA response.

1.2.2 Cl^- Channels

One of the functions Cl^- channels play a role in, is the control of cytoplasmic ionic composition, which in turn is a function of cellular volume. Shifts in Cl^- gradient through channels can also impact electrical excitability. The purpose of the following review is to examine four classes of Cl^- channels namely voltage-gated, ligand gated, Ca^{2+}- and swelling activated.

1.2.2.1 Voltage-Gated Cl^- channels

Cloning of voltage-gated Cl^- channel gene (ClC-0) from electric organ of marine electric ray Torpedo initiated the identification of the ClC- chloride channel family (Jentsch *et al.* 2002). ClC-2 expression in brain was found using *in situ* hybridization and immunocytochemistry in pyramidal cells of the hippocampus and Purkinje cells of the cerebellum (Sik *et al.* 2000) with a less abundant signal in other neurons and glia (Smith *et al.* 1995). Immunoelectron microscopy revealed a more defined localization for ClC-2 found close to inhibitory synapses in adult rat brain (Sik *et al.* 2000). ClC-2 currents activate slowly upon hyperpolarization (Park *et al.* 1998) and display a dependence on $[Cl^-]_i$ (Dinudom *et al.* 1993) suggesting a regulatory function for Cl^- gradient. In fact as seen in hippocampal neurons, $[Cl^-]_i$ facilitates ClC-2 activation to prevent Cl^- accumulation occurring during high-frequency neuronal activity (Staley 1994) . DIDS is a poor blocker of the current (Thiemann *et al.* 1992) while the inorganic blockers, Cd^{2+} and Zn^{2+} show a higher potency (Schwiebert *et al.* 1998). Hypotonicity induces cell swelling, which has been shown to activate ClC-2 (Schwiebert *et al.* 1998) causing Cl^- efflux. Functionally, the channel has been shown to participate in neuronal physiology. ClC-2 currents contribute to the hyperpolarization-activated Cl^- currents in neurons (Clark *et al.* 1998; Smith *et al.* 1995). The current is thought to depress excessive hyperpolarizations (Chesnoy-Marchais 1983) and thus facilitate neuronal excitability.

1.2.2.2 Swelling Activated Cl^- channels

Volume shifts, particularly cell swelling, activates an anion-selective conductance called $I_{Cl,Swell}$. The current is outwardly rectifying displaying a sensitivity to $[Cl^-]_i$,which causes a decrease in rate of activation at high levels (Doroshenko 1999). The precise mechanism by which volume changes are translated into conductance activation is unknown. However, there are studies which suggest that second messengers are involved because of the time lag observed between hypotonic swelling and $I_{Cl,Swell}$ activation (Estevez *et al.* 2001). Most effective blockers are DIDS and NPPB (Dick *et al.* 1999) while others such as niflumic acid, flufenamic acid and IAA-94 are an order of magnitude less potent (Jentsch *et al.* 2002).

1.2.2.3 Ca^{2+}-activated Cl^- Channels

Cl^- currents dependent on Ca^{2+} were established in neurons by a number of studies (Frings *et al.* 2000; Currie *et al.* 1995; Scott *et al.* 1995). Their characteristic features are outlined below. Time dependent activation of the channel by depolarizing voltage steps, though slow in nature, has been demonstrated in spinal cord and sensory ganglia (Mayer 1985). Inactivation is absent during voltage steps ranging in several seconds (Mayer *et al.* 1990). In any case upon activation, the current is typically outwardly rectifying. Furthermore, sensitivity of the channel to Ca^{2+} was detected by either removal or blockade of Ca^{2+}-channels with Cd^{2+} or Co^{2+} (Mayer 1985).These manipulations reversibly abolished the Cl^- current (Mayer 1985).The precise nature of this dependence was outlined by Ayar and Scott (1999) working with rat DRG neurons. Calcium entry through voltage-activated channels produces increases in $[Ca^{2+}]_i$ via release from internal Ca^{2+}-stores which in turn promotes the Cl^- conductance. Typical blockers are disulfonic stilbene derivatives such as DIDS or fenemates such as niflumic acid (NFA) (Firestein and Shepherd 1995; Lancaster *et al.* 2002). Physiologically, the channel exerts a modulatory function on excitability.

In neurons activation of Cl^- conductance by Ca^{2+}-release from stores or by action potential may have excitatory effects depending upon the equilibrium potential for Cl^- in

relation to V_m. In DRG neurons, because E_{Cl} lies more positive to V_m, channel activation is thought to cause a depolarization that physiologically facilitates action potential genesis and/or maintains voltage-gated Ca^{2+}-channel activation (Dichter and Fischbach 1977). However, these experiments were done in neonatal preparations having a reversed Cl^- gradient. Others have suggested a more depressive role for the channel allowing hyperpolarizing effects in neurons not loaded with Cl^- (Owen *et al.* 1986). Consequently, this would reduce the probability for an action potential and limit the frequency of spikes. Therefore, channel activity directly modulates synaptic transmission.

1.2.2.4 Ligand Gated Cl^- channels

Physiological effects of $GABA_A$, and glycine receptor activation are mediated by Cl^- . Evidence for GABA acting as an inhibitory transmitter substance in mammalian CNS dates back to 1967 when Krnjevic and Schwartz concluded that actions of both IPSPs and GABA are Cl^- dependent (Krnjevic and Schwartz 1967). GABA acts at 3 subtypes of receptors the classical ionotropic $GABA_A$, the metabotropic $GABA_B$ and the newly identified ionotropic $GABA_c$. $GABA_A$ receptor is a Cl^- channel with well characterized physiological properties (Sivilotti and Nistri 1991). Glycine, which also exerts inhibitory effects on neurotransmission, acts via Cl^- channel.

In mammalian nerve cells, the uneven Cl^- distribution dictates the nature of the current, be it inward or outward, produced upon receptor activation. The direction of ion flow is a function of the electrochemical driving force determined in part by V_m and Cl^- gradient. In addition to the inhibitory effects, the receptor may produce excitatory actions. For example, $GABA_A$-mediating neonatal depolarization arises because of the high Cl^-_i levels that dictate an E_{Cl} more positive than V_m (Cherubini *et al.* 1991). Moreover, this phenomenon is observed in adult preparations of hippocampal neurons (Misgeld *et al.* 1986) dorsal root ganglion (Alvarez-Leefmans *et al.* 1988) as well as sympathetic ganglion neurons (Ballanyi and Grafe 1985). A specific characteristic of these areas is their ability to maintain high levels of Cl^-_i over and above those values predicted for passive distribution. The molecular mechanism for this effect is thought to proceed via NKCC1, since the active Cl^- accumulation was blocked by bumetanide (Alvarez-Leefmans *et al.* 1988). Thus it is the interplay of the Cl^- regulatory mechanisms,

which establish the physiological response of the receptor. It is thought that the depressive nature of the receptor channel contributes to the stability of resting potential by increasing Cl^- conductance. The depolarizing response developmentally initiates mechanisms necessary for growth.

1.2.3 Cl^- transport in Glia

Initial work done by Kuffler and colleagues (1966) concluded that Cl^- conductance of glial cells was insignificant when compared with that of K^+. It wasn't until the work of Kimelberg *et al.* (1982), Walz and Schlue (1982) surfaced that this initial idea was challenged. For example Kimelberg and colleagues noticed a 10mV depolarization upon Cl^- replacement with an impermeant anion in cerebral cortical astrocytes. Working with leech neuropil glia, Walz and Schlue reported a significant depolarization when external Cl^- was removed. Others such as Kettenmann (1987) working on cultured oligodendrocytes observed a 27% increase in input resistance upon bath Cl^- removal. Thus these results emphasize the significant contribution of Cl^- transport, occurring through the variety of systems available.

1.2.3.1 Glia Cl^- Channels

$GABA_A$-receptors have been reported in astrocytes (Bormann and Kettenmann 1988). The other class of Cl^- channels present in glia are the voltage-gated channels whose members include inwardly rectifying Cl^- conductance (I_{Clh}), volume activated conductance ($I_{Cl,Vol}$), and the outwardly rectifying Cl^- current (ORCC).

I_{Clh} was found to exist in reactive astrocytes and thought to contribute to the resting Cl^- conductance (Ferroni *et al.* 1995). Genetically, the channel is encoded by the ClC-2 gene (Jentsch *et al.* 2002) and located in astrocytic endfeet around capillaries (Sik *et al.* 2000). ClC-2 channels are activated by hyperpolarization, swelling or extracellular acidification (Walz 2002). The second type of current termed $I_{Cl,Vol}$ is known to be blocked by DIDS, DNDS, Zn^{2+} and Cd^{2+} and displays outward rectification upon activation by cell swelling (Ullrich and Sontheimer 1996). Genetic origin of the channel is still unknown. As for the ORCC, activation occurs following a change in cellular

morphology as depicted by Lascola and Kraig (1996). Mechanistically, channel activation following cellular shape alterations, is thought to be associated with change in actin cytoskeleton (Lascola *et al.* 1998).

1.2.3.2 Glia Cl^- Carriers

Movement of Cl^- across glial membrane occurs via most of the same carriers outlined for neurons. In fact $[Cl^-]_i$ in cultured astrocytes from rat cortex has been shown to be considerably higher than passive distribution levels reflecting active Cl^- accumulation (Kimelberg 1981), which may occur via NKCC. Immunocytochemistry confirmed the existence of NKCC in cultured astrocytes of the rat cerebellum (Zalc *et al.* 1984). A more involved localization study, undertaken by Yan and colleagues (2001) (Yan *et al.* 2001) revealed intense immunoreactive NKCC signal originating from CA1-CA3 hippocampal pyramidal neurons. The signal was colocalized with GFAP (astrocytic marker) suggesting astrocytic localization. Functionally, the cotransporter plays a role in K^+_o buffering during periods of intense electrical activity (Walz 1992). High K^+ will stimulate the cotransporter and cause Na^+_i accumulation, which is extruded by the Na^+/K^+-ATPase. The end result of the process is KCl uptake along with osmotically obliged H_2O (Walz 1992). This finding was confirmed by MacVicar and colleagues (2002) who, using the rat optic nerve, reported NKCC colocalization with GFAP-immunopositive astrocytes. Furthermore, imaging techniques allowed them to assess the effect of K^+_o on the transporter where an increase in optical signals attested to KCl uptake in astrocytes. Yet this does not exclude the presence of the transporter in axons. Alvarez-Leefmans and colleagues (2001) conducted a detailed immunolocalization study of NKCC in PNS of vertebrate tissue. NKCC in DRG neurons, resided in both axoplasmic and membrane regions of the axon, as well as in three distinct areas of Schwann cells: the paranodal region, the myelin sheath attachment segment and at the Schmidt-Lanterman incisures.

In contrast with astrocytes the Cl^- gradient across oligodendrocytes is maintained by a simpler mechanism. Kettenmann in (1987) was the first to demonstrate Cl^- activity

across oligodendrocytic membranes. Based on the finding that input resistance of the cell increased in low or zero $[Cl^-]_o$ he proposed that oligodendrocytes are highly permeable to Cl^-. As a result, the model put forth establishes passive events, driven by Donnan forces, as the primary mode of co K^+ and Cl^- uptake via their respective channels in response to increases in K^+_o (Kettenmann 1987). Physiologically K^+_o buffering during neuronal activity has been attributed largely to astrocytes, because of their extensive electrical coupling and ability to redistribute K^+; however, oligodendrocytes might present local buffering capacities for K^+_o, in turn aiding with extracellular space preservation (Kettenmann 1987).

1.3 Anoxic/Ischemic Injury in CNS WM

1.3.1 Energy Metabolism

The purpose of CNS is to generate and transmit impulses. These activities depend on the tight control of ionic gradients, through specific energy-dependent mechanisms. Estimates put forth indicate that 50-60% of total brain ATP production is utilized in supporting ionic movements (Erecinska and Silver 1994).

Energy production at the glycolytic stage generates 2 moles of ATP/mole of glucose and either pyruvate or lactate depending on the availability of oxygen (Stryer, 1988). Aerobic or anaerobic conditions, produce pyruvate or lactate respectively (Stryer, 1988). Subsequent metabolism of pyruvate through the TCA cycle and electron transport chain (ETC) in mitochondria yields the bulk of ATP. Pyruvate conversion to AcetylCoA and subsequent entry to the mitochondrial matrix starts the TCA cycle, which yields the reduced compound Nicotinamide Adenine Dinucleotide (NADH). Electrons from NADH flow through enzyme complexes namely NADH-Q, cytochrome reductase and cytochrome oxidase, which are embedded in the inner mitochondrial membrane. These complexes function as proton pumps, acting in series with respect to the electron flux, in order to extrude H^+ from the matrix (Nicholls and Budd 2000). Subsequently an electrochemical potential gradient is created which has in it the stored energy required for ATP production at complex V, known as ATP synthase.

The proton-motive force allows H^+ reentry into the matrix down its gradient while simultaneously forcing ATP-hydrolyzing pump to run in reverse and synthesize ATP (Nicholls and Budd 2000). Therefore the passage of one molecule of glucose through the TCA and oxidative phosphorylation process yields 34 of 36 ATP molecules (Erecinska and Silver 1994). In fact the continuous reliability on aerobic metabolism is needed for tight control of ionic homeostasis during periods of rest and electrical activity.

1.3.2 Acute Events: Ionic deregulation

Loss of energy substrate due to disruption of its production by oxygen deprivation induces acute cellular injurious events such as marked loss of membrane polarization and sustained excitability. Decreased levels of ATP causes dysfunction of Na-K-ATPase and thus increasing levels of intracellular Na^+. Further accumulation of Na^+ occurs through TTX sensitive Na^+ channels. Large amounts of K^+ is simultaneously lost down its electrochemical gradient leading to rise from 3mmol/L to 14mmol/L of external K^+ (Ransom and Philbin 1992). Electron probe microanalysis data confirmed the marked loss in K^+_i declining to approximately 10% of control after 60 min of anoxia in RON (LoPachin and Saubermann 1990). Blockade of TTX sensitive channels has been shown to exert protective effects as judged by a variety of parameters such as V_m and CAP recordings, ultrastructure and biochemical determinations (Jiang and Stys 2000; Leppanen and Stys 1997a; b; Stys *et al.* 1992a; Waxman *et al.* 1994). The reason for this protection lies in the fact that Na^+ overload secondarily triggers increases in $[Ca^{2+}]_i$ via reverse operation of Na^+/Ca^{2+} exchanger (Stys *et al.* 1992b). Other Ca^{2+} entry pathways in white matter such as AMPA receptors when blocked allowed for functional recovery from anoxic insult in rat dorsal column slices (Li *et al.* 1999). Calcium induces further injury to the tissue by activating sensitive pathways known to lead to cell demise; however knowledge of the precise mode of entry will lead to development of specific blockers capable of deterring cellular damage.

1.3.3 Calcium Entry pathways

A fundamental step in the injurious cascade of events is the Ca^{2+} overload since it leads to necrotic cell death (Orrenius *et al.* 1996; Schanne *et al.* 1979; Siesjo 1986).

Physiological studies on RON carried out in absence of Ca^{2+} from the perfusate with concomitant addition of a chelator prevented anoxic injury (Stys *et al.* 1990).Ultrastructural analysis of the anoxic rat optic nerve (RON) perfused with $0Ca^{2+}$ revealed a sparing of the axonal cytoskeleton from disintegration (Waxman *et al.* 1994) as increases in $Ca^{2+}{}_i$ has been shown to activate enzymes responsible for cytokeletal destruction (Jiang and Stys 2000). Furthermore, examination of Ca^{2+} levels during anoxia, conducted using Electron Probe X-ray Microanalysis (EPMA) on RON, showed a persistent rise in $Ca^{2+}{}_i$ throughout the 60min anoxic insult (LoPachin and Stys 1995). The modes of entry are several and range from voltage or transmitter gated channels, nonspecific cation channels, and/or coupled transporters (Stys and Lopachin 1998).

Entry of Ca^{2+} through the NMDA and AMPA receptors during injury has been shown in grey matter (Choi *et al.* 1988) while in white matter areas only AMPA/Kainate glutamate receptors are involved (Li and Stys 2000). However, in *in vivo* spinal cord ischemia, blockade of AMPA and NMDA receptors was effective in attenuating injury causing mechanisms (Bowes *et al.* 1996; Madden *et al.* 1993). There may also be a role for voltage-gated calcium channels (VGCC) in mechanisms causing cellular injury during anoxia/ischemia. Although original work done by Stys *et al.* (1990) on RON, showed lack of protection with either organic or inorganic blockers. This result was later confirmed using EPMA where neither nifedipine nor nimodipine was found to reduce Ca^{2+}-accumulation during anoxia (Stys *et al.* 1997). However, Fern *et al.* (1995) reexamined this phenomena and reported protective effects of voltage-sensitive Ca^{2+} channel blockade during white matter injury. Later, a study by Brown *et al.* (2001) identified axonal L-type Ca^{2+}-channels as one of the routes for the observed overload during anoxia based on the effect of diltiazem in attenuating suspected Ca^{2+} influx. Furthermore, using immunocytochemistry, α- subunits of Cav 1.2 and 1.3 colocalized with axonal and astrocytic markers. One potential problem with this interpretation is the nonspecific effect of diltiazem that also blocks Ca^{2+} release from a subtype of intracellular store (Genazzani *et al.* 1996). In fact, presence of the α- subunit in the cytoplasmic compartment is not a potent reflector of the availability of the channel within the membrane. In essence, the protein subunits could be present in the cytoplasm for

transport purposes, presumably from the site of production at the soma to their final destination at the nerve terminal.

Other studies have shown the importance of the Na^+/Ca^{2+} exchanger in white matter injury cascade using exchanger blocker during axonal injury (Stys and Lopachin 1998; Stys *et al.* 1992b; Verbny *et al.* 2002; Wolf *et al.* 2001). Immunohistochemical localization of the exchanger by Steffensen *et al.* (1997) outlined the presence of the protein in central and peripheral white matter tracts. Bath replacement of Na^+ with either choline or Li^+ allowed for complete recovery of the compound action potential area after a 60min anoxic insult. Furthermore, EPMA data confirmed the existence of a Na^+-dependent mechanism for Ca^{2+} entry as Na^+-channel blockade with TTX diminished Ca^{2+} accumulation (Stys and Lopachin 1998). Taken together these observations established that the exchanger operates in the reverse mode during injury to cause Na^+-dependent Ca^{2+}-entry.

1.3.4 Cl^- shifts: Grey Matter *vs.* White Matter

Following pathophysiological conditions such as anoxia/ ischemia in grey matter areas, changes in Cl^- gradient are contrary to those seen in white matter tracts where Cl^-_i levels were found to remain unchanged during anoxia (LoPachin and Stys 1995). For example, hypoglossal neurons of rat brain slices subjected to anoxia showed an increase in Cl^-_i by 20.6 ± 7.2 mM (Jiang *et al.* 1992). Furthermore, using EPMA in OGD treated adult hippocampal slices, Taylor *et al.* (1999) were able to show that there is an increase in Cl^-_i in CA1 area cell bodies. Others have shown the effects of Cl^- deregulation on hypoxic depolarization. Current-clamped CA1 pyramidal cells subjected to hypoxia, in presence of Cl^- transport inhibitors, caused a delay of the hypoxia depolarization (Muller 2000). Another observation was that Cl^-_o reduction shifted the potential for the hypoxic depolarization to more positive levels thus facilitating the process (Muller 2000). Since Cl^- regulation in cell body, dictates a more negative E_{Cl} than Vm for the proper functioning of GABA receptors, the positive shift in E_{Cl} will suppress GABA-mediated IPSCs as shown in anoxic hippocampal slices (Katchman *et al.* 1994). The shift in Cl^- gradient has been shown to cause a novel response after neuronal trauma. GABA whether exogenously released or synaptically applied caused excitatory depolarizing responses

which in turn activated L and N-type voltage-activated Ca^{2+} channels allowing an increase intracellular Ca^{2+} (van den Pol *et al.* 1996). The mechanism for this reversed action of GABA was attributed to the change in Cl^- gradient favoring an outward movement of Cl^- (van den Pol *et al.* 1996) presumably because of the increase in Cl^- levels following injury. Recently, *in vivo* axonal injury was shown to impact $GABA_A$-receptor response in dorsal motor neurons of the vagus. Axotomy was found to cause a $GABA_A$-receptor mediated excitation caused by a shift in Cl^- gradient due to the dysfunction of Cl-regulatory pathways in the somatodendritic region (Nabekura *et al.* 2002). *In situ* hybridization and pharmacological manipulations, revealed that KCC2 mRNA decreased following injury and it is this lack of Cl^- regulation via KCC2, which causes elevated Cl^-_i levels (Nabekura *et al.* 2002). This in turn allows for a switch in GABA response to excitatory.

1.3.5 Glial cell Injury

The notion put forth by a number of earlier reports such as Goldberg and Choi (1993) that astrocytes are resistant to aglycemic or anoxic injury, was challenged by the finding that astrocytic ischemic damage was sensitive to Ca^{2+}_o levels implying a direct connection between increases in Ca^{2+}_i and cellular demise (Haun *et al.* 1992). Blockers of L-Type Ca^{2+} channel, such as verapamil (Yu *et al.* 1989) and nimodipine (Haun *et al.* 1992) attenuated astrocytic cellular damage emphasizing the role of these channels in astrocytic injury. Another interesting finding by Yu *et al.* (1989) was that furosemide partially protected astrocytes against ischemic insult which reflects the aberrant activity of anion cotransporters during injury. The authors used the release of lactate dehydrogenase(LDH) from astrocytes as one of the markers for biochemical cellular injury. With furosemide release of LDH from cultured astrocytes into the medium decreased by over 60%. They accounted for this result by providing a generalized explanation that hypoxic astrocytic cell damage involves Cl^-.

Nevertheless another important target for cellular injury is myelin. Conduction block as a result of an anoxic insult, is associated with a loss of ultrastructural integrity characterized by empty zones between axolemma and myelin layer along with detachment of myelin loops (Waxman *et al.* 1992). Following from such findings,

Imaizumi *et al.* 1998 reported that demyelinated axons displayed a reduced sensitivity to anoxic injury. Functional assessment of the normal and demyelinated axons revealed that compound action potential was totally abolished in normal axons after 12 min of anoxic onset as opposed to 50 min in demyelinated axons. Moreover, compound action potential area recovery following the insult was significantly greater in demyelinated versus normal axons. Mechanistically, the observation by Waxman *et al.* (1992) that Ca^{2+}_o removal preserved normal morphology following anoxia suggests that Ca^{2+} is the instigator of the damage.

In oligodendrocytes, membrane depolarization induced by 60mM K^+, produces small changes in $[Ca^{2+}]_i$ (Dyer and Benjamins 1990) inferring the lack of voltage-activated Ca^{2+}-channels or strong buffering capacity. Indeed the influx seems to be mediated by voltage-insensitive, nonselective cation-channels, which are sensitive to arachidonic acid (Soliven *et al.* 1993), as it is known to be released from anoxic neurons (Sanfeliu *et al.* 1990). Thus arachidonic acid might be the stimulus needed to initiate the cascade of injury events in oligodendrocytes as hypothesized by Ransom and Fern (1996).

1.4 Research objectives

The main goal of this project was to gain a fundamental understanding of Cl^- transport during white matter injury. To address the following objective we assessed two parameters, membrane potential and compound action potential of the rat optic nerve, to elucidate cellular ionic mechanisms. The membrane potential was measured using the grease gap technique while the functional integrity of the axonal bundle was measured using the suction electrode, which provided compound action potential recordings. Based on previous studies (Leppanen and Stys 1997b; Stys and Lopachin 1998) we hypothesized that during the setting of anoxia/Na^+-channel blockade, continued K^+-loss proceeds in conjunction with anion and more specifically Cl^-, thereby causing an additional volume change and mechanical injury. Therefore concomitant inhibition of anion transport pathway(s) responsible for these anion fluxes may be additionally protective against anoxia/ischemia in white matter.

1. Membrane depolarization in white matter tracts resulting from ionic deregulation during anoxic insults has direct impact on axonal functionality. Other much simpler injury paradigms, such as Na-K-ATPase pump inhibition, has also been shown to cause loss of membrane potential and lead to cellular injury. Our aim was to study the ionic mechanisms behind the depolarization observed in both ouabain and chemical anoxia models within the context of Cl^- transport.

2. After establishing the involvement of Cl^- transport during chemical anoxia, we then analyzed the role of specific Cl^- regulatory mechanisms and how blockade of such pathway(s) impacts recovery of functional parameters, such as resting membrane potential and compound propagated action potentials.

CHAPTER 2

MATERIALS & METHODS

2.1 Preparation & Dissection

The RON is a representative central white matter (WM) tract composed of approximately 100,000 myelinated axons ranging in diameter between 0.3μm to 3μm (De Juan *et al.* 1992). The average inner diameter is of the order 0.77μm (Foster *et al.* 1982). In addition, once excised it is devoid of neuronal cell bodies or synaptic structures (Foster *et al.* 1982). Male Long-Evans rats (175-200g), obtained from Charles River Canada, were anesthetized with 80% CO_2-20% O_2 and decapitated. At the age used (>28 days old) the RON has developed mature physiological properties (Foster *et al.* 1982). The optic nerves were then dissected free from chiasm.

2.2 Grease Gap

2.2.1 Membrane Potential Recording

Conventional electrophysiological techniques such as patch or sharp electrodes have been used to measure V_m, as allowed for by the size of the preparation. However, the small diameter of optic nerve axons (mean <1μm (Foster *et al.* 1982), precluded the use of microelectrodes. Thus indirect recording methods have been devised of which the grease gap provides the most stable readings at physiological temperatures (Eng *et al.* 1990). The grease gap setup, as outlined in figure 2.1A contains two wells, one of which is continuously perfused with aCSF or drug solutions while the other with an isotonic K^+ solution. Table 2.1 summarizes solution makeup for aCSF and Isotonic-K^+ solutions. Axonal compound resting membrane potential was recorded in vitro as follows. A silastic tube, with the dimensions of 2mm long 0.64mm in diameter, was slit horizontally, filled with petroleum jelly to allow for electrical isolation and to minimize solution intermixing from the two wells (Fig. 2.1A). The middle segment of one nerve was inserted into the vaseline filled tube.

Signals were recorded across the two wells through the use of an Ag/AgCl wire bathed in 3M KCl and 5% agar in 3M KCl. The electrodes are then connected to a high impedance operational amplifier. The complete breakdown of this type of electrode is shown in Figure 2.1C. For the period of at least 2hrs, drift and noise were low, allowing stable recording of resting compound membrane potential (Vg) and the reliable recognition of any transient membrane changes in the order of millivolts.

One nerve was recorded immediately using a grease gap chamber at 37°C as previously described (Leppanen and Stys 1997a) while the second was stored in oxygenated aCSF; pH 7.45) at room temperature for later study. No consistent differences were noted between nerves recorded immediately and those held for later study. Raw baseline gap potentials (V_g) varied from nerve to nerve (typical range -45mV to -50mV) due to differences in the short circuit factor (see section 2.2.2) (Stämpfli 1954). Therefore for display purposes all potentials were normalized (denoted V_m) to the true resting potential of CNS myelinated axons of -80 mV (Stys *et al.* 1997). Quantitative comparisons over time were performed using *ratios* of recorded potentials; therefore this normalization had no effect on such calculations. Data were acquired using WaveTrak software for Macintosh Computers (Stys 1994) and the analysis was done using Igor Pro (Wavemetrics, Lake Oswego, OR).

2.2.2 Grease Gap Electrical Model

The grease gap does not measure absolute membrane potential but rather a gap potential, V_g, which reflects changes in the potential across the gap between the two nerve endings perfused with different solutions. The value of V_g approaches the true membrane potential V_m but it is never equal to it because of a short circuit factor which will be explained using the outlined electrical model.

The electrical model of the grease gap, represented in Fig 2.1B, dictates the extent to which the recorded potential V_g, approaches the real value of the RON membrane potential. The difference between V_m and V_m', which denotes the absolute membrane potential at each end of the nerve, creates a current, i_g, which generates the recorded potential:

$$V_g = i_g R_e \quad (1)$$

V_g is the recorded gap potential . R_e defines the external resistance, which is composed of extracellular space, nerve sheath, residual solution and other parallel leakage pathways. R_i is the internal axoplasmic and combined membrane resistances.

Solving for the gap current, yields:

$$i_g = \frac{V_m - V_m`}{R_e + R_i} \quad (2)$$

If in isotonic KCl solution, V_m' tends to zero and at the same time i_g is eliminated from equations 1 and 2, then the net expression will be in the form of (Stämpfli , 1954)

$$V_g = \frac{V_m R_e}{R_e + R_i} \quad (3)$$

The strength of this equation is manifested in its ability to relate the recorded potential, V_g, to the true membrane potential while at the same time accounting for one of the setbacks of this technique. V_g, is lower in value than V_m by a constant fraction Re/(Re+Ri) known as the short circuit factor (Stämpfli 1954).

Under conditions where R_e is assumed to be much greater than R_i, usually the case in sucrose gap recordings of single fibers (Julian *et al* 1962), V_g will approach V_m. However, under our conditions the above assumption may not be completely valid. Stys *et al* in 1997 estimated that the true V_m for optic nerve axons was approximately –80mV, which differs from representative grease gap potentials, which normally ranging between -45 to -50mV. Thus the difference factor is approximately 0.6, which defines our short circuit factor in Eqn 3.

Even though absolute transmembrane potentials could not be recorded using this technique, if the short circuit factor remains stable over the recording period, then the acquired potentials represent a constant fraction of the true membrane potentials. In terms of Eqn 3, V_g will vary linearly with V_m and will act as a reliable indicator of the latter.

According to the circuit outlined in Fig. 2.1B, V_g is the result of a differential potential across R_e which creates i_g. The flow of this current through the constituent fibers, varies inversely with the axial resistance and thus directly relates to the square of axon diameter. Our preparation is a composition of parallel fibers with diameters ranging from 0.3 to 3μm (De Juan *et al.* 1992) and from the above analysis it follows that the current contribution to the total i_g, and therefore V_g will be biased towards larger fibers

2.3 Suction Electrode Electrical Model & Recording

With large fibers or even axon bundles, extracellular field recordings with glass microelectrodes presented a powerful technique to examine conduction properties relatively noninvasively. The suction electrode utilizes field microelectrodes to record propagated electrical activity in a quantitative reproducible manner. An electrical circuit was developed by Stys *et al.* 1991 to outline the origin of recorded potential. Figure 2.2A,B presents an outline of the recording setup and the electrical circuit in consideration.

Even though the optic nerve contains more than 100,000 axons along with glia, nevertheless the nerve could be approximated by a single large fiber with an extracellular potential near the inserted end denoted by V_e and intracellular potential outside the electrode denoted by V_m. The following equations summarizes the different relationships:

$$E_m = -V_m \tag{1}$$

$$E_e = V_o - V_e \tag{2}$$

where E_m is the transmembrane potential of exposed tissue. E_e is transmembrane potential at inserted end and V_o is the recorded potential. By Kirchoff's law:

$$E_m = iR_o + E_e + iR_i \tag{3}$$

where R_o and R_i are external and internal resistance respectively. After simplification, i- the current flowing around the loop, could be quantified by the following equation obtained from (1,2,3):

$$i = \frac{V_e - V_m - V_o}{R_o + R_i} \tag{4}$$

Resting conditions dictates that V_m and V_e be similar and thus no potential change occurs across R_o and R_i to produce a V_o close to zero. However, in the case when $V_m \neq V_e$, which occurs during and action potential, the recorded potential V_o is deduced mathematically through the following explanation.

Action Potential will cause V_m and V_e to become unequal, resulting in momentary current i which flows through R_o. Thus i can be also be quantified as:

$$i = \frac{-V_o}{R_o} \tag{5}$$

Equating (4) and (5) to solve for V_o yields:

$$V_o = \frac{R_o(V_m - V_e)}{R_i} \tag{6}$$

From this relationship one could deduce the following:

(1) $V_o \neq 0$ only under the condition $V_m - V_e \neq 0$ and that $V_m - V_e$ cannot be measured in isolation.

(2) $V_o \propto R_o$ and $V_o \propto 1/R_i$. R_o increases with tighter insertion of nerve as this eliminates the electrolytes at the electrode/nerve junction.

(3) R_o and R_i cannot be directly measured.

However there exists a measurable parameter, R_p, which denotes the parallel resistance relationship between R_o and R_i through the following equation:

$$R_p = R_o \| R_i = \frac{R_o R_i}{R_o + R_i} \tag{7}$$

R_p is easily measured. A stimulating current, i, is injected into the electrode then the resultant voltage is measured. From these parameters a total resistance is calculated. R_b, denoting resistance of the electrolyte within the electrode, bath and chlorided wire is obtained by allowing the electrode to sit in bath, nerve-free. A simple subtraction of R_b from total resistance will produce R_p.

If we were to combine (6) and (7) and eliminate R_o, we obtain:

$$V_o = \frac{R_p (V_m - V_e)}{R_i - R_p} \tag{8}$$

The condition where $R_i >> R_o$ as it offers more information pertinent to our tissue under study. Consequently, from (7) $R_p \approx R_o$ and by substituting R_p for R_o in (4,5,6) the following equation is achieved:

$$V_o = \frac{R_p}{R_i} * (V_m - V_e) \tag{9}$$

If our assumption about $R_i >> R_o$ is correct, then V_o and the measured R_p should be linearly proportional. Fitting a linear function to the data set (R_p, V_o) will provide

information about the entity V_m- V_e in such a way that the slope of the linear function will be (V_m- V_e)/ R_i. The line will be proportional to V_m- V_e only when R_i remains constant.

Propagated compound action potentials were recorded using suction electrodes as previously described (Stys *et al.* 1991). Briefly, nerves were placed in an interface perfusion chamber, perfused with aCSF (2 ml/min, 37°C) and gassed with either 95% O_2, 5% CO_2. One end of the nerve is fit snugly into a stimulating glass capillary electrode filled with a CSF, which delivers supramaximal constant voltage stimuli. At the other end, a gentle suction is applied and the nerve in inserted into another glass capillary, responsible for recording optic nerve responses. Anoxia was achieved by switching to 95% N_2, 5% CO_2, and ischemia was simulated by exposure to anoxia with equimolar replacement of glucose by sucrose (oxygen-glucose deprivation, OGD).

2.4 Immunohistochemistry

Deeply anesthetized Long Evans rats (200-300g) were perfused trans-cardially with 0.9% saline followed by 2% paraformaldehyde containing 20mM L-lysine, 2.5mM sodium periodate and 2.5% potassium dichromate. The optic nerves were post-fixed for 2hrs and immersed in 0.1M PBS for 24 hrs. Protocol: wash 3x10min in Tris buffer containing 1.5% NaCl and 0.3% Triton x-100 (TBS-T) incubate for 30 min at 4C in methanol. Wash 3x10min in TBS-T. Block with 10% normal goat serum in TBS-T for 1 hr at room temperature. Overnight incubation with primary antibody diluted in TBS-T containing 2% normal goat serum. All KCC primary antibodies (Chemicon) were diluted to 1:10 and neurofilament 160 (Sigma) to 1:2000. Next day, wash 3x10min in TBS –T. Secondary antibody used were goat anti-rabbit Cy2 (1:200) and anti-mouse Texas Red (1:100) from Jackson ImmunoResearch diluted in TBS-T. Sections were imaged on a BioRad 1024 or Nikon C1 confocal with 60x oil immersion objective.

2.5 Pharmacological Agents

Tetrodotoxin (TTX) (Alomone Labs) was prepared as a stock solution in distilled water. Iodoacetic Acid (IAA), 4,4`-Diisothiocyanatostilbene-2,2`disulfonic acid disodium

salt (DIDS), furosemide, bumetanide, niflumic acid(NFA), NMDG and Choline-HCO_3 salt were purchased from Sigma (St Louis, MO). NMDG, DIDS and IAA were added directly to the desired volume of aCSF solution to make up the required concentration. Furosemide was first dissolved in DMSO. Both bumetanide and niflumic acid were dissolved in ethanol. NaCN was acquired from BDH (Toronto, Ont). NaN_3 was purchased from Fisher Scientific. Ouabain was bought from Calbiochem. All other salts were purchased from Sigma. All stock solutions had a concentration factor of 1000x.

Table 2.1 Composition of standard solutions used in the grease gap recording chambers. Test drugs where perfused through the aCSF well while keeping a continuous perfusion of isotonic-K^+ solution bathing the other end of the nerve.

	aCSF (mM)	Iso-K^+ (mM)
NaCl	126	0
KCl	3	129
$NaHCO_3$	26	26
$NaHPO_4$	1.25	1.25
$CaCl_2$	2	0.5
$MgSO_4$	2	2
Dextrose	10	10

Figure 2.1: (A) Diagram of the grease gap recording apparatus setup. A nerve was inserted into the silastic tube containing petroleum jelly. One side was perfused with aCSF or test solutions, while the other end with isotonic-K^+ solution. A potential V_g is created and recorded using an Ag/AgCl wire bathed in 3M KCl and 5% agar. (B) Electrical model of the grease gap showing the major circuits involved. V_g represents the potential drop across the gap and it is the parameter being measured. V_m and V_m' are the absolute transmembrane potentials at their respective ends. R_e denotes the external resistance, comprised of extracellular space, nerve sheath, residual solution and other parallel leakage pathways. R_I, the internal resistance parameter, denotes the combined internal axoplasmic resistance and membrane resistance. The potential drop across V_m and V_m' creates V_g across R_e, which represents a stable reliable, constant fraction of the absolute transmembrane potential. (C) Diagram of the electrodes used for recording. A capillary tube, glued to a ceramic disk magnet, is filled from the bent end with a 5% agar 3M KCl solution. The other end of the capillary holds the Ag/AgCl wire that is stripped of the teflon coating approximately 1cm from the end. The crimped end of the wire is connected to an operational amplifier.

A

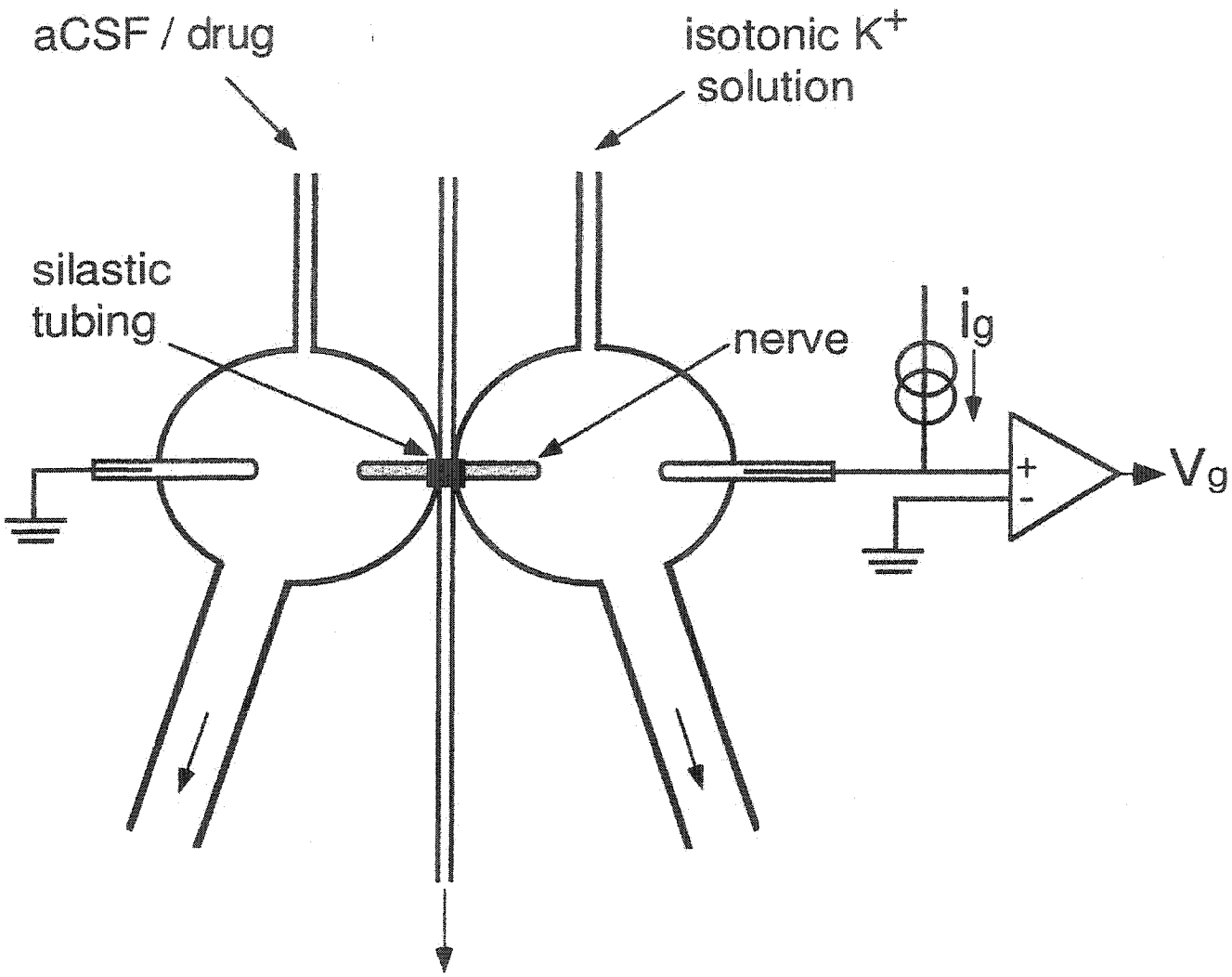
aCSF / drug
isotonic K+ solution
silastic tubing
nerve
ig
+
-
Vg

B

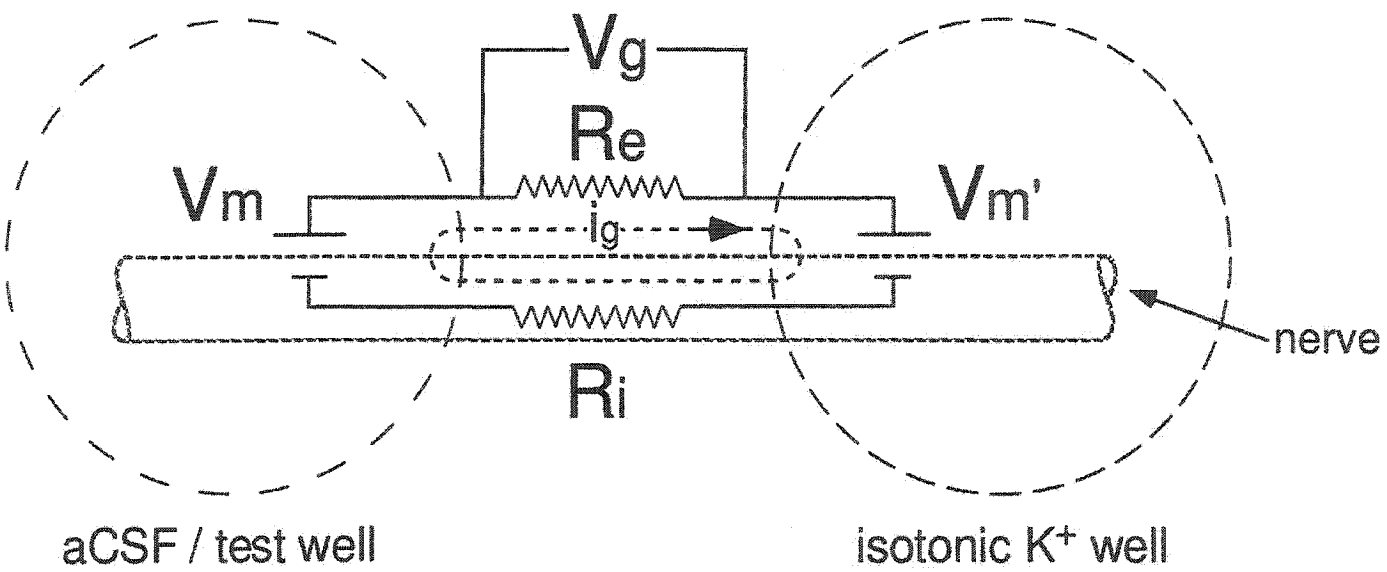
Vg
Re
Vm
Vm'
ig
Ri
nerve
aCSF / test well
isotonic K+ well

C

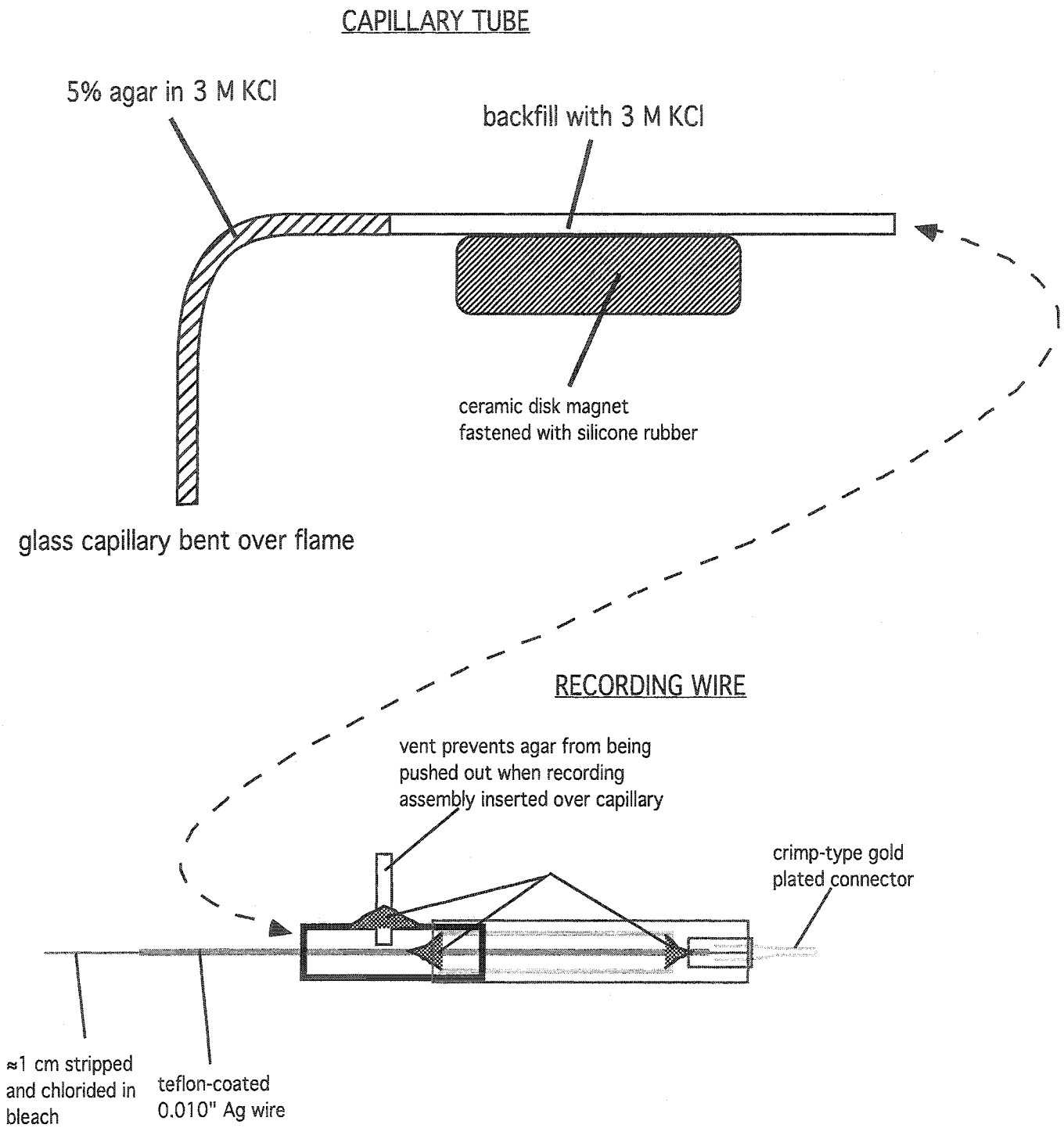
CAPILLARY TUBE
5% agar in 3 M KCl
backfill with 3 M KCl
ceramic disk magnet
fastened with silicone rubber
glass capillary bent over flame
RECORDING WIRE
vent prevents agar from being
pushed out when recording
assembly inserted over capillary
crimp-type gold
plated connector
≈1 cm stripped
and chlorided in
bleach
teflon-coated
0.010" Ag wire

Figure 2.2 Schematic diagram of experimental setup. Suction electrode recording was used to assess the functional injury in the rat optic nerve, a representative model of CNS white matter tracts. (A) Gentle suction was applied to one end of the nerve and constant voltage pulse stimulated this end while at the opposite end a similar electrode recorded the compound action potential. The signals were amplified, digitized and transformed to a computer for analysis. (B) Electrical circuit summarizing elements contributing to producing potentials at the recording end of a suction electrode with the nerve inserted. R_p, parallel resistance is a function of the combination, R_o, outside resistance and R_i, inside resistance. The diagram depicts technique used to measure R_p. R_b, baseline resistance of the fluid in the electrode barrel and surrounding bath, which is subtracted from total measured resistance to obtain R_p.

A.

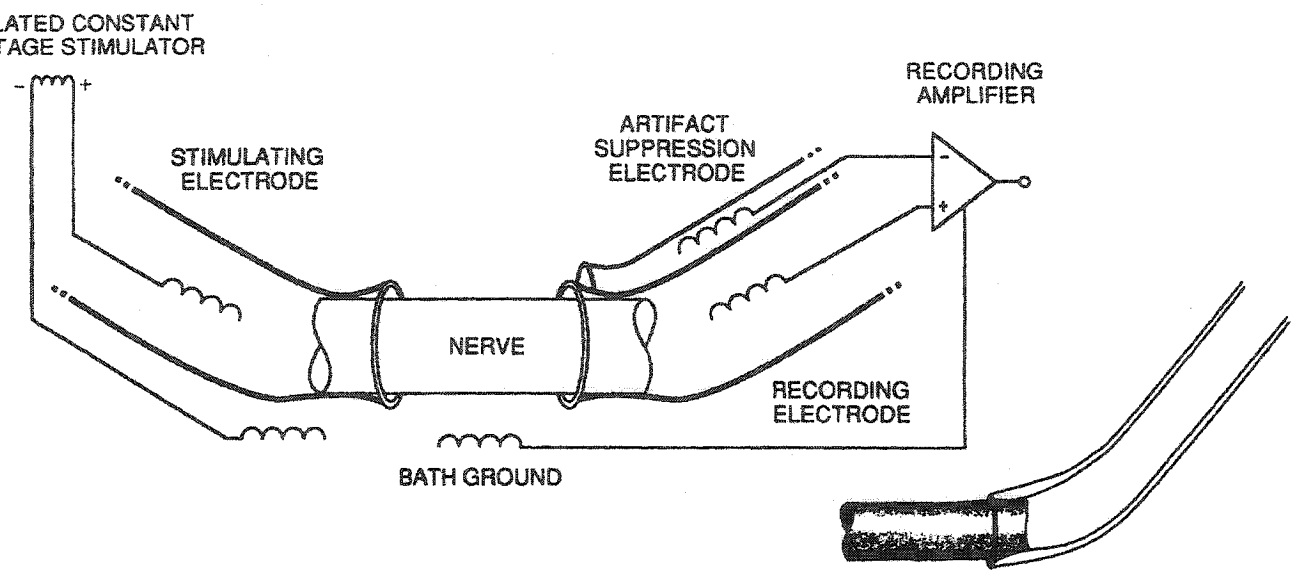
ISOLATED CONSTANT
VOLTAGE STIMULATOR
RECORDING
AMPLIFIER
STIMULATING
ELECTRODE
ARTIFACT
SUPPRESSION
ELECTRODE
NERVE
RECORDING
ELECTRODE
BATH GROUND

B.

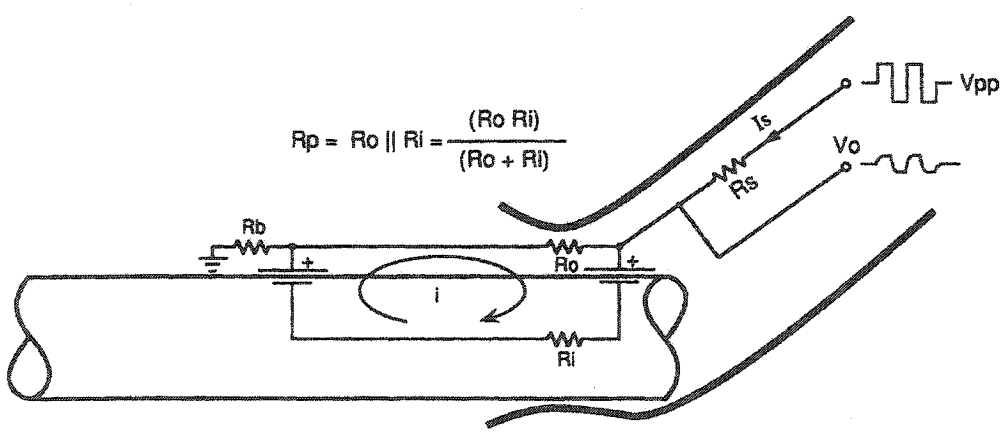
Rp = Ro || Ri = (Ro Ri) / (Ro + Ri)
Vpp
Is
Vo
Rs
Rb
Ro
i
Ri

CHAPTER 3

Differential effects of Ouabain versus Chemical Anoxia on Membrane Potential of Rat Optic Nerve

3.1Introduction

Na-K-ATPase is a ubiquitous plasma membrane protein entrusted with the transport of $2K^+$ into and $3Na^+$ out of the cell through the use of energy derived from ATP hydrolysis. This enzyme plays a crucial role in maintaining cellular ionic homeostasis necessary for the proper functioning of neurons and ultimately the CNS. Moreover, pharmacologically the pump is a receptor for cardiac glycosides known for their inhibitory action. Fuelling the pump is ATP produced to a large extent from the mitochondria.

Several studies have used Na-K-ATPase pump inhibition as a paradigm to examine the acute ionic deregulation occurring following oxygen and/or glucose deprivation(Brines *et al.* 1995; Lees *et al.* 1990; Li and Stys 2001; McCarren and Alger 1987; Omar *et al.* 2001; Ross and Soltesz 2000). The general finding was that pump inhibition leads to ionic deregulation followed by activation of Ca^{2+}-dependent injury mechanisms. On the other hand, tissue anoxia could be mimicked by blockade of aerobic metabolism with cyanide. Inhibition of mitochondrial respiratory chain will subsequently halt ATP production and cause failure of homeostatic ionic regulatory mechanisms (Leppanen and Stys 1997b; Sher 1988). In both paradigms there has been little known about the effects of Cl^- shifts on the membrane potential of the rat optic nerve, an extensively well studied model for CNS white matter.

With this in mind we set out to examine the role of Cl^- transport in both Na-K-ATPase pump inhibition and chemical anoxia injury paradigms. Our results showed a persistent activation of Cl^-transport pathways during chemical anoxia in the presence of Na^+-channel blocker as evident by the effect of broad spectrum anion transport blockers on the V_m residual depolarization of the RON.

3.2Results

3.2.1.Effects of Ouabain *vs.* Chemical Anoxia on Membrane Potential of RON

Figs 3.1A,B, 3.5 displays an example of ouabain and chemical anoxia and their effects on RON V_m. Table 3.1 summarizes the obtained V_m values for the different

manipulations. RON perfused with 1mM ouabain showed a pronounced loss of V_m allowing only 42±2% (30min) and 42±4% (60 min, n=7), of control V_m to remain. Chemical anoxia induced by either NaCN(2mM) or NaN_3 (2mM) (both have same effect on V_m) depolarized V_m to 42±11% (30min) and 32±10% (60 min, n =14 pooled data) of control. Comparing effects of ouabain and chemical anoxia on V_m showed statistical significance only after 60min of perfusion ($p>0.05$ at 30min Ouabain vs. Chemical anoxia, $p<0.01$ at 60min).

3.2.2.Effects of Na^+-channel inhibition or Na^+-substitution on Membrane Potential of RON during either Na-K-ATPase blockade or Chemical anoxia

Blockade of TTX-sensitive channels significantly attenuated V_m depolarization and maintained 68±4% and 60±4% at 30min and 60min during ouabain perfusion as displayed in Figures 3.2A and 3.5 ($p<0.001$ for both time points vs. Ouabain alone, n=8). In the chemical anoxia model, similar values were obtained with TTX(1μM) perfusion during 1hr chemical anoxia insult (Figs 3.2B and 3.5. 73±10% and 63±18% at 30min and 60min, both $p<0.001$ vs. Chemical anoxia alone, n=12). Bath Na^+ replacement with the membrane impermeant NMDG resulted in almost complete V_m maintenance during ouabain application (Figs 3.2C and 3.5. 87±5% at 30min vs. 68±4% with TTX, $p<0.001$, 87±5% at 60 min vs. 60±4%, $p<0.001$, n=6). During chemical anoxia, values obtained with Na^+ replacement were not statistically different in comparison with TTX (1μM) perfusion in presence of chemical anoxia (Figs 3.2D and 3.5. 77±9% vs. 73±10% at 30min, $p=0.54$, 73±10% vs. 63±18% at 60min, $p=0.25$, n=3).

3.2.3.Effects of concomitant Na^+-channel or Na^+-replacement and Cl^-transport blockade on Membrane Potential of RON during either Na-K-ATPase blockade or Chemical anoxia.

A broad spectrum anion transport blocker, DIDS(500μM), was used to assess the effect of Cl^-transport inhibition in both depolarization models. During ouabain perfusion, TTX+DIDS showed a slight but statistically significant improvement of V_m (74±5 vs 68±4% at 30min, $p<0.05$, 68±5 vs 60±4% at 60min, $p<0.01$, n=8, Figs 3.3A, 3.5). DIDS

has no reported effects on NKCC and thus a relatively specific blocker, bumetanide 10μM was used to examine the effect of the cotransporter as a possible Na^+ entry pathway. Addition of bumetanide to TTX during ouabain perfusion mildly but significantly improved V_m values to 76±3% at 30min (Fig 3.4, 35. n=4, $p<0.01$ vs TTX+Ouabain) and 65±1% of control V_m at 60min ($p<0.05$ vs TTX+Ouabain). A more robust effect was observed during chemical anoxia with DIDS, maintaining to a large extent V_m in the face of the insult (Figs 3.3B and 3.5. 95 ± 8% TTX+DIDS vs 73 ± 10% in TTX alone at 30min, $p<0.001$ and 89 ± 6% vs 63 ± 18% at 60min, $p<0.001$, n=13).

Figures 3.3C,D and 3.5 display responses obtained with combined $0Na^+$ Choline/NMDG perfusion in presence of DIDS. During Ouabain/$0Na^+$ application, addition of DIDS (500μM) showed no significant changes on the V_m (n=4, 90 ± 3% $0Na^+$/Choline/NMDG +DIDS vs 87 ± 5% in $0Na^+$/Choline/NMDG, alone at 30min, p=0.36; 86 ± 5% vs 87 ± 4% at 60min, p=0.85). With chemical anoxia, as with TTX+DIDS application, showed a stronger maintenance of V_m than $0Na^+$-perfusion (V_m maintained at 92 ± 3% of control after 30min in zero-Na^+ and DIDS vs. 77 ± 9% in zero-Na^+ alone, p=0.11 and 84 ± 5% of control after 60min. vs 73 ± 10%, p=0.2, $n_{0Na/Choline/NMDG/DIDS}=5$, $n_{0Na/Choline/NMDG}=3$).

3.3Discussion

It has been suggested that specific blockade of the Na^+-K^+-ATPase pump generates events overlapping those seen with oxygen deprivation (Brines *et al.* 1995; Ross and Soltesz 2000). Our findings agree partly with such a result as the levels of membrane depolarisation during either Na^+-K^+-ATPase pump or chemical anoxia were similar to a large extent at 30min post insult application, differing only after approximately 1hr. However, to our knowledge, there is no detailed account of Cl^- shifts in central mammalian axons during either Na^+-K^+-ATPase pump inhibition or anoxia. Hence, we investigated the effect of Cl^-transport blockade on the membrane of RON, during both paradigms. Our most significant finding was that blockade of Cl^- transport by DIDS was more effective in reducing membrane depolarization in the presence of TTX during chemical anoxia, compared to Na^+/K^+-ATPase pump inhibition.

While there is lack of studies outlining quantitatively the collapse of ion gradients during both anoxia and Na^+-K^+-ATPase pump blockade in central axons, work done by Lehning and colleagues (1995) in peripheral axons outlines such changes associated with both paradigms. Using EPMA, the Na^+ and K^+ gradients collapsed in both ouabain and *in vitro* anoxia. In fact both paradigms inhibit the Na^+-K^+-ATPase pump but to varying degrees. Ouabain perfusion targets specifically Na^+-K^+-ATPase pump and thus the blockade is faster. On the other hand, during anoxia the block is more gradual since Na^+-K^+-ATPase pump could be fuelled by limited energy substrates other than glucose such as astrocytic glycogen (Dringen and Hamprecht 1992). Another possibility is that glycolysis is upregulated during anoxia (Kauppinen and Nicholls 1986) possibly to fuel energy dependent processes responsible for maintaining homeostatic ionic gradients such as Na^+-K^+-ATPase pump. In any case, total pump failure should occur after running down of these alternative energy substrate concentrations. In both cases there is dissipation of the Na^+-gradient and thus one would expect that blockade of Na^+-entry pathways should attenuate depolarization in both conditions

Blunting of membrane depolarisation during anoxia, using Na^+-channel blockers has been shown and our findings are in total agreement (Agrawal and Fehlings 1996; Imaizumi *et al.* 1997; Jiang and Stys 2000; Leppanen and Stys 1997b). Curiously, we found that bath Na^+-replacement with NMDG, has different V_m maintenance effects in both models, of chemical anoxia and Na^+-K^+-ATPase pump inhibition. Almost complete preservation of V_m with ouabain/ $0Na^+$ perfusion suggests that the depolarisation is strictly Na^+-dependent. The precise routes of entry have been examined previously with TTX-sensitive channels emerging as the main pathway (Leppanen and Stys 1997b). On the other hand, with chemical anoxia the presence of a residual depolarization during either TTX or $0Na^+$ perfusion, indicates an alternative mechanism responsible for the continued decay. Indeed one might expect that with the prevention of Na^+-entry there will be no further K^+-loss and ultimately no depolarization. However, previous work suggested that even during Na^+-channel blockade there was a persistent run down of the K^+-gradient, but in this case simultaneously with loss of Cl^- (Stys and Lopachin 1998).

Our membrane potential data results suggest that Cl^- shifts occur only during chemical anoxia and more precisely under conditions of anoxia/Na^+-channel blockade.

Lack of effect with co-blockade of anion transport and Na^+-channels during Na^+-K^+-ATPase pump inhibition might be the result of proper functioning of anion transport processes during ouabain perfusion. For example, Lehning *et al.* (1995) showed an absence of Ca^{2+}changes during ouabain application explained by the fact that Ca^{2+} homeostatic processes are still functioning during Na^+-K^+-ATPase pump inhibition unlike with anoxia. We propose the same type of response to occur with Cl^- transport mechanisms dependent on ATP as an energy substrate or as a cofactor, to offset any Cl^- shifts brought about by the dissipation of Na^+ and K^+ gradients. In fact, the reason for additional sparing of anoxic depolarization with either DIDS +TTX or Bumetanide+TTX vs. TTX alone is probably a result of blocking a Na^+, Cl^- coupled entry pathway such as NKCC and/or Na^+-dependent Cl^-/HCO^-_3 exchanger. The latter protein has been described as the acid-extruding mechanism in central neurons including rat hippocampal CA1 region (Schwiening and Boron 1994) and is know to be DIDS-sensitive (Sakai and Tosaka 1999). This system in addition to regulating pH, is probably also mediating Na^+-influx. On the other hand, our results with concomitant blockade of Na^+-influx and Cl^- transport pathways, prevented to a large extent the anoxic depolarisation. Thus taken together these data ascertain to the fact that with chemical anoxia, there seems to be changes in Cl^- levels which have not been outlined before in white matter. To this end we attempted to outline some of these mechanisms in the following chapter.

Figure 3.1 Recorded (V_g) and normalized (V_m) in rat optic nerve measured using grease gap technique during either mitochondrial or Na-K-ATPase pump inhibition with CN^- and ouabain respectively. Time 0 denotes insult application (A) Over a 1hour ouabain perfusion, V_m depolarized to 42±2% of control at 30min and 42±4% of control at 60min since drug application. (B) Similar pronounced loss of V_m was seen with chemical anoxia, performed by NaCN application for 1hour. Quantitatively RON depolarized to 42±11% and 32±10% of control at 30 and 60min respectively.

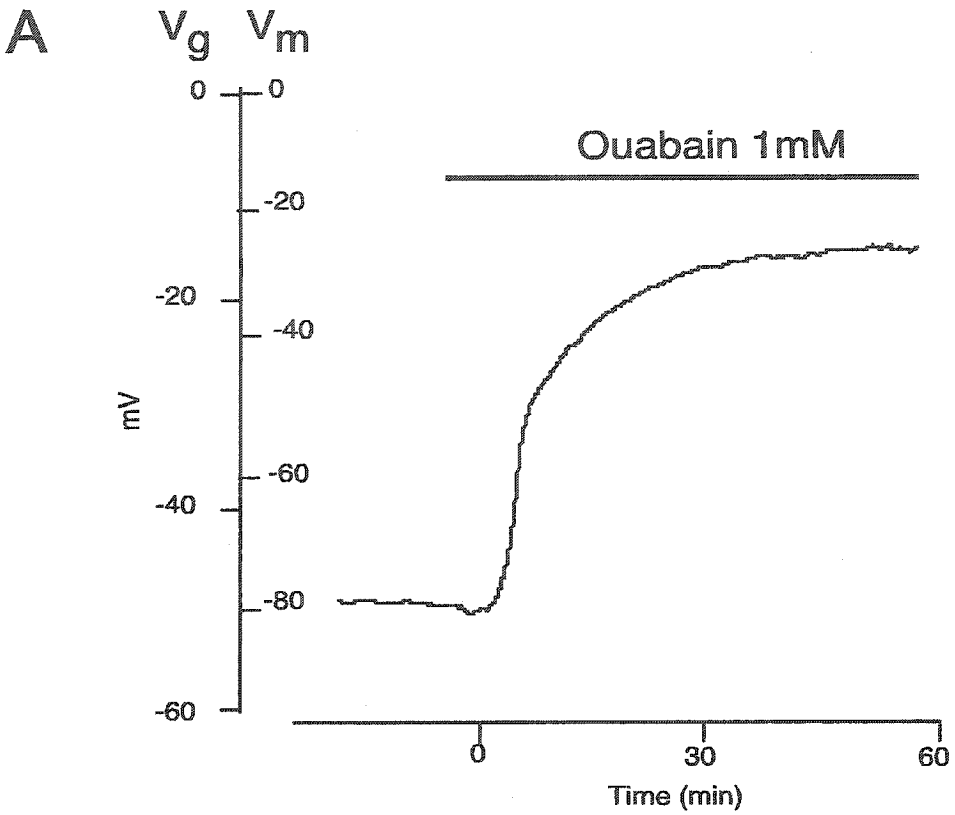
A
Vg Vm
0
0
-20
-20
-40
-60
-40
-80
-60
mV
Ouabain 1mM
0
30
60
Time (min)

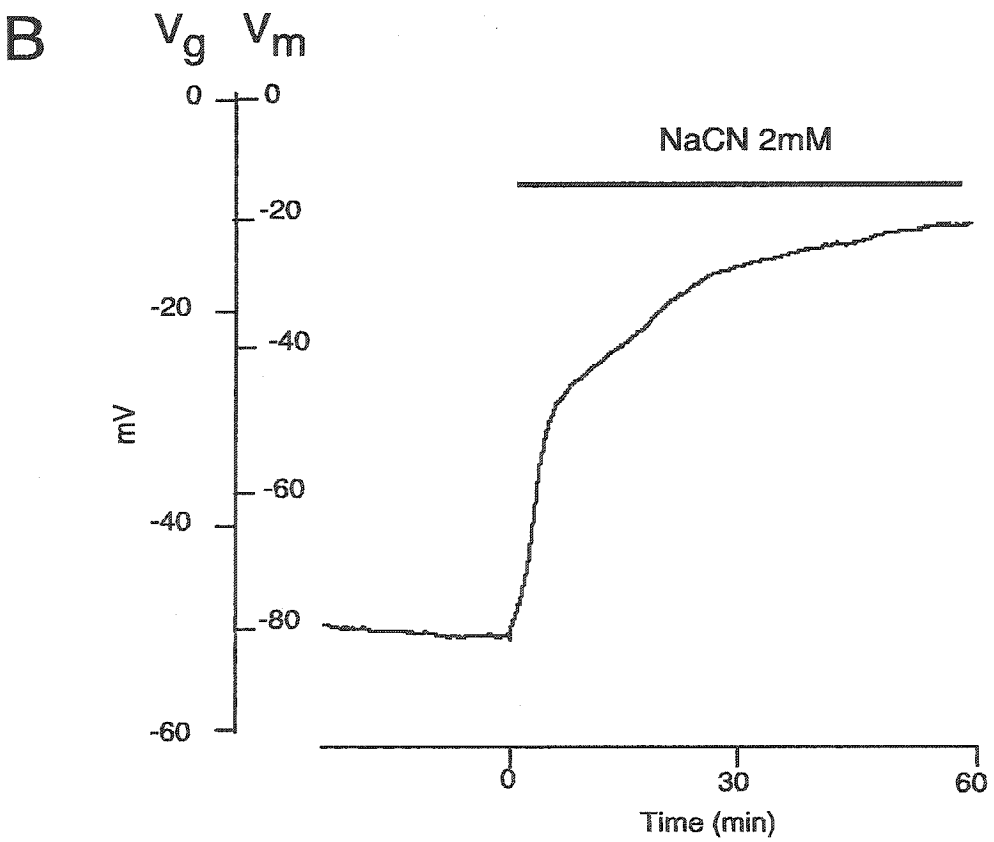
B
Vg Vm
0
0
-20
-20
-40
-60
-40
-80
-60
mV
NaCN 2mM
0
30
60
Time (min)

Figure 3.2 Effect of Na^+-channel blockade or Na^+-substitution on V_m of RON during mitochondrial or Na-K-ATPase pump inhibition. TTX(1μM) was pre-applied for 1hour then co-applied with either NaCN(2mM) or Ouabain (1mM). (A) Displays blunting of ouabain induced depolarization such that 68±4% and 60±4% of control V_m was maintained at 30min and 60min during ouabain application. (B) Similar response was observed with CN^- where less depolarization was observe in presence of TTX (73±10% and 63±18% at 30 and 60min respectively). As with TTX, $0Na^+$/NMDG/Choline was pre-applied for 1hr then continued with either the presence of ouabain or CN^-.

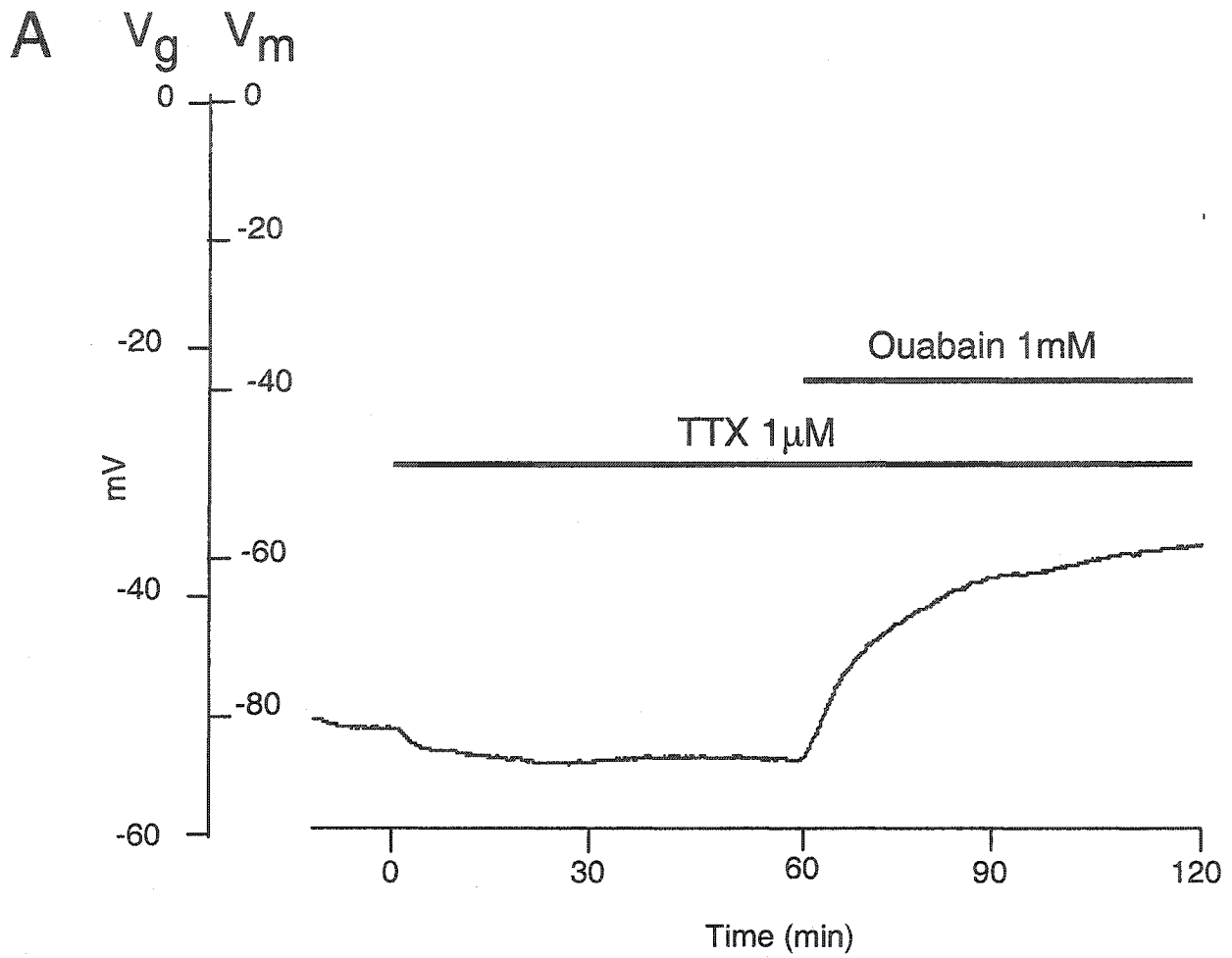
A
Vg Vm
0
0
-20
-20
-40
-40
-60
-80
-60
mV
Ouabain 1mM
TTX 1μM
0
30
60
90
120
Time (min)

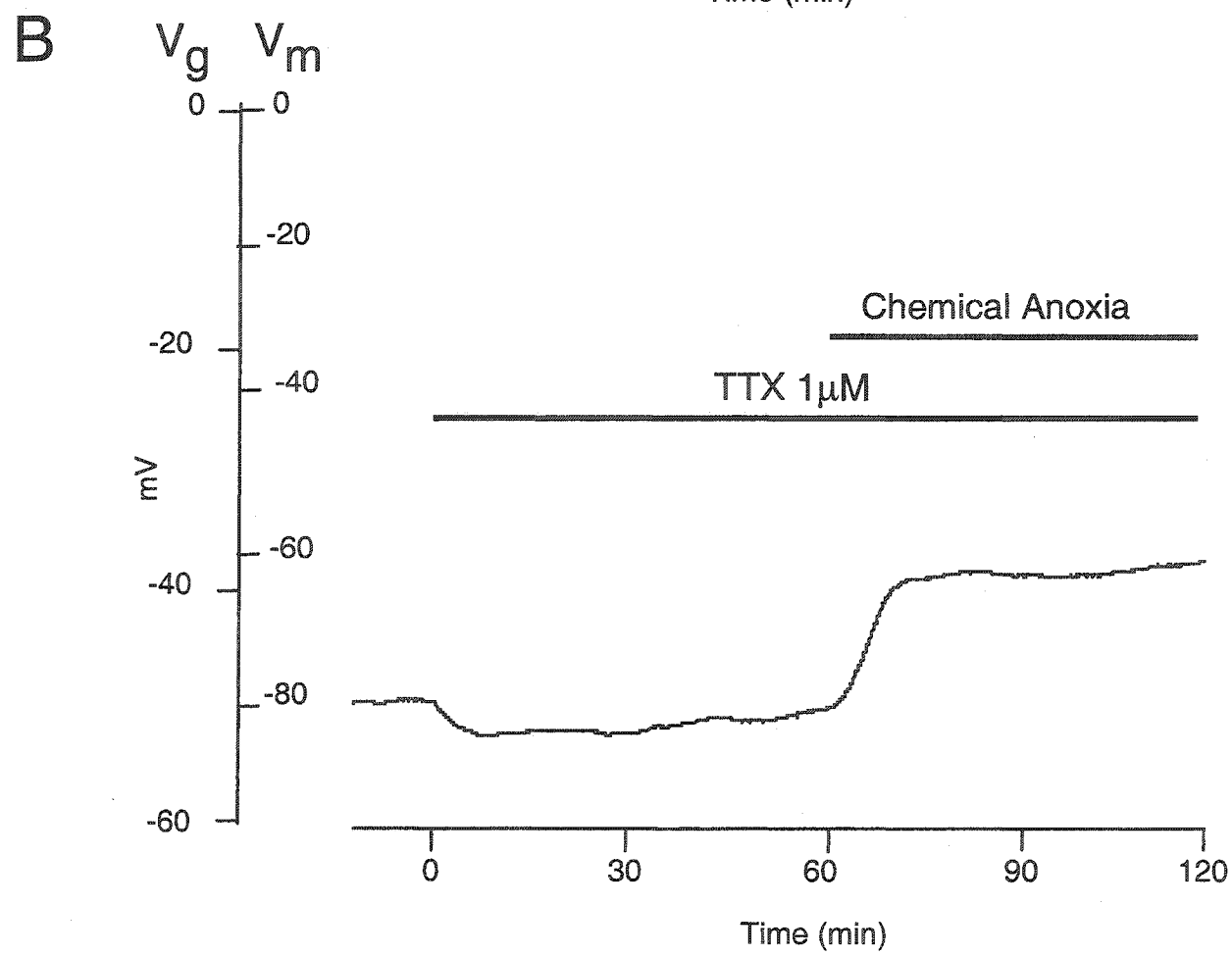
B
Vg Vm
0
0
-20
-20
-40
-40
-60
-80
-60
mV
Chemical Anoxia
TTX 1μM
0
30
60
90
120
Time (min)

Figure 3.2 (C) Na^+ replacement efficiently reduced the ouabain-induced depolarisation more so than TTX alone (87±5% at 30min vs 68±4% with TTX, $p<0.001$, 87±5% at 60 min vs 60±4%, $p<0.001$, n=6). (D) CN^- response to $0Na^+$ perfusion was not significantly different from that encountered with TTX perfusion (77±9% vs 73±10% at 30min, $p=0.54$, 73±10% vs 63±18% at 60min, $p=0.25$, n=3).

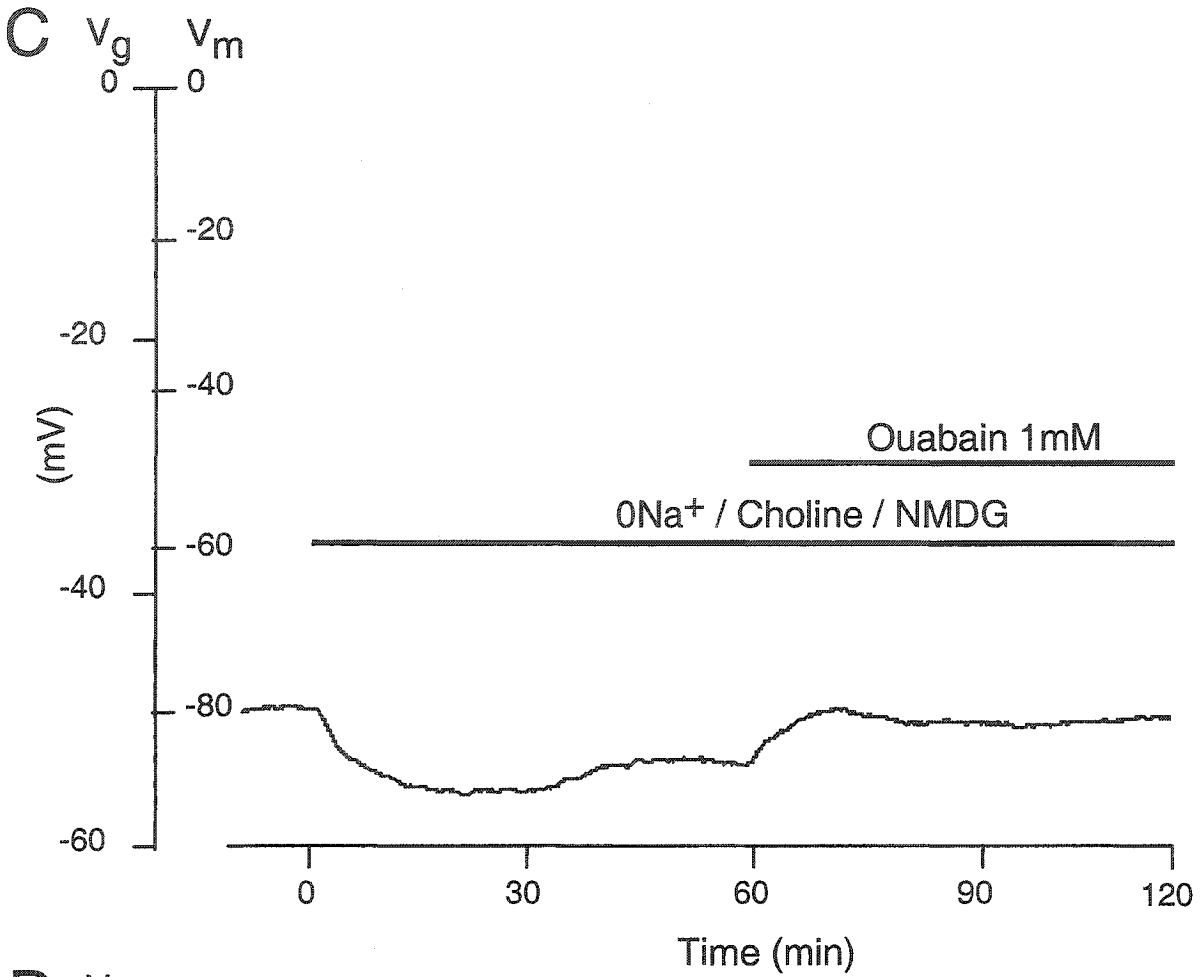
C
Vg
Vm
0
0
-20
-20
-40
-40
-60
-80
-60
(mV)
Ouabain 1mM
0Na+ / Choline / NMDG
0
30
60
90
120
Time (min)

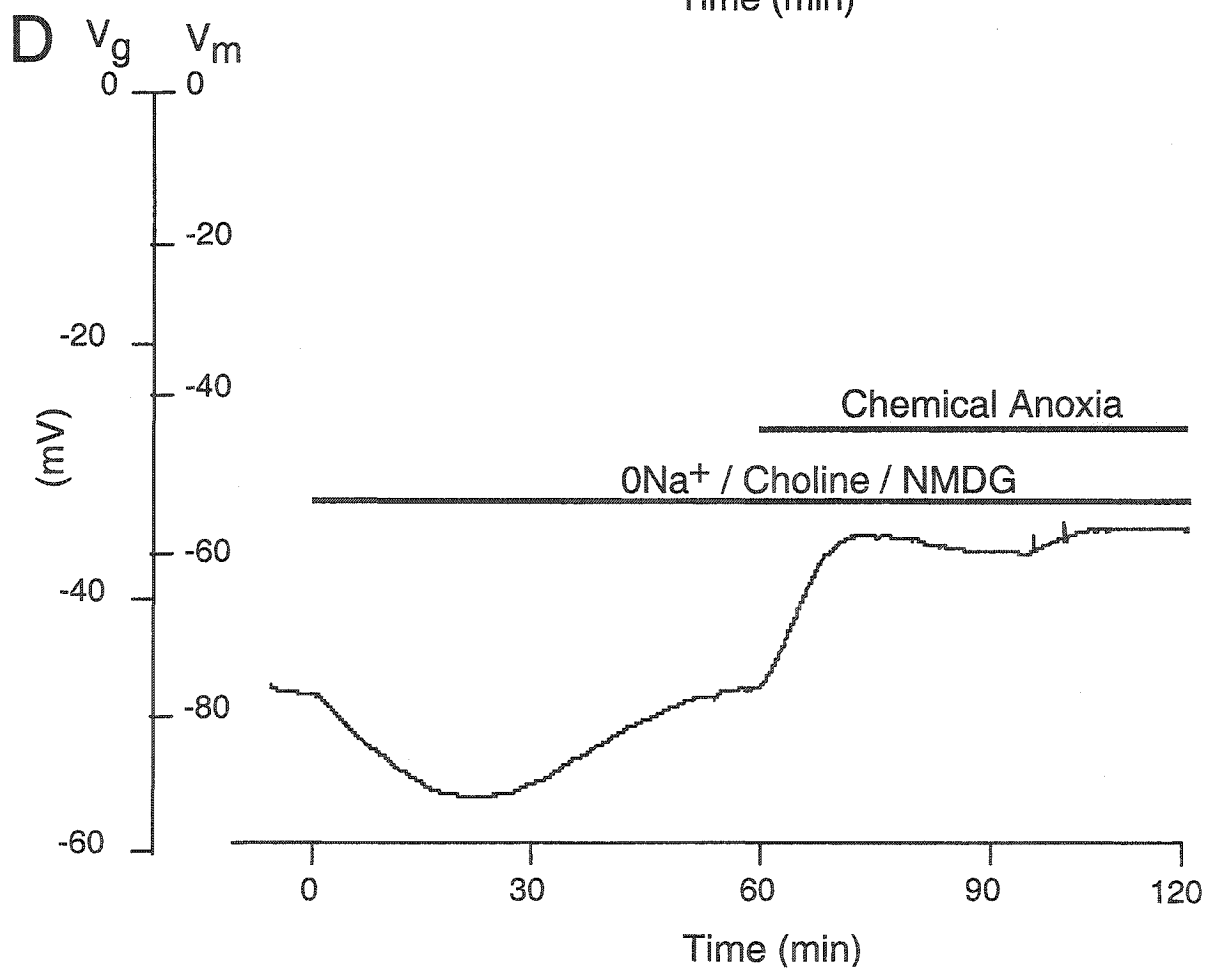
D
Vg
Vm
0
0
-20
-20
-40
-40
-60
-80
-60
(mV)
Chemical Anoxia
0Na+ / Choline / NMDG
0
30
60
90
120
Time (min)

Figure 3.3 Effect of concomitant blockade of Na^+-channel or Na^+-substitution and Cl^- transport on the V_m of RON during chemical anoxia or Na-K-ATPase pump inhibition. (A) Displays the observed response of TTX(1μM) and DIDS(500μM) during Ouabain perfusion. There was a slight, but significant blunting of the Ouabain(1mM) induced depolarization (74±5 vs 68±4% at 30min, $p<0.05$, 68±5 vs 60±4% at 60min in TTX alone, $p<0.01$). (B)Blockade of Na^+-channels and DIDS sensitive transporters during CN^- application preserved to large extent V_m (95 ± 8% TTX+DIDS vs 73 ± 10% in TTX alone at 30min, $p<0.001$; 89 ± 6% vs 63 ± 18% at 60min, $p<0.001$, n=13).

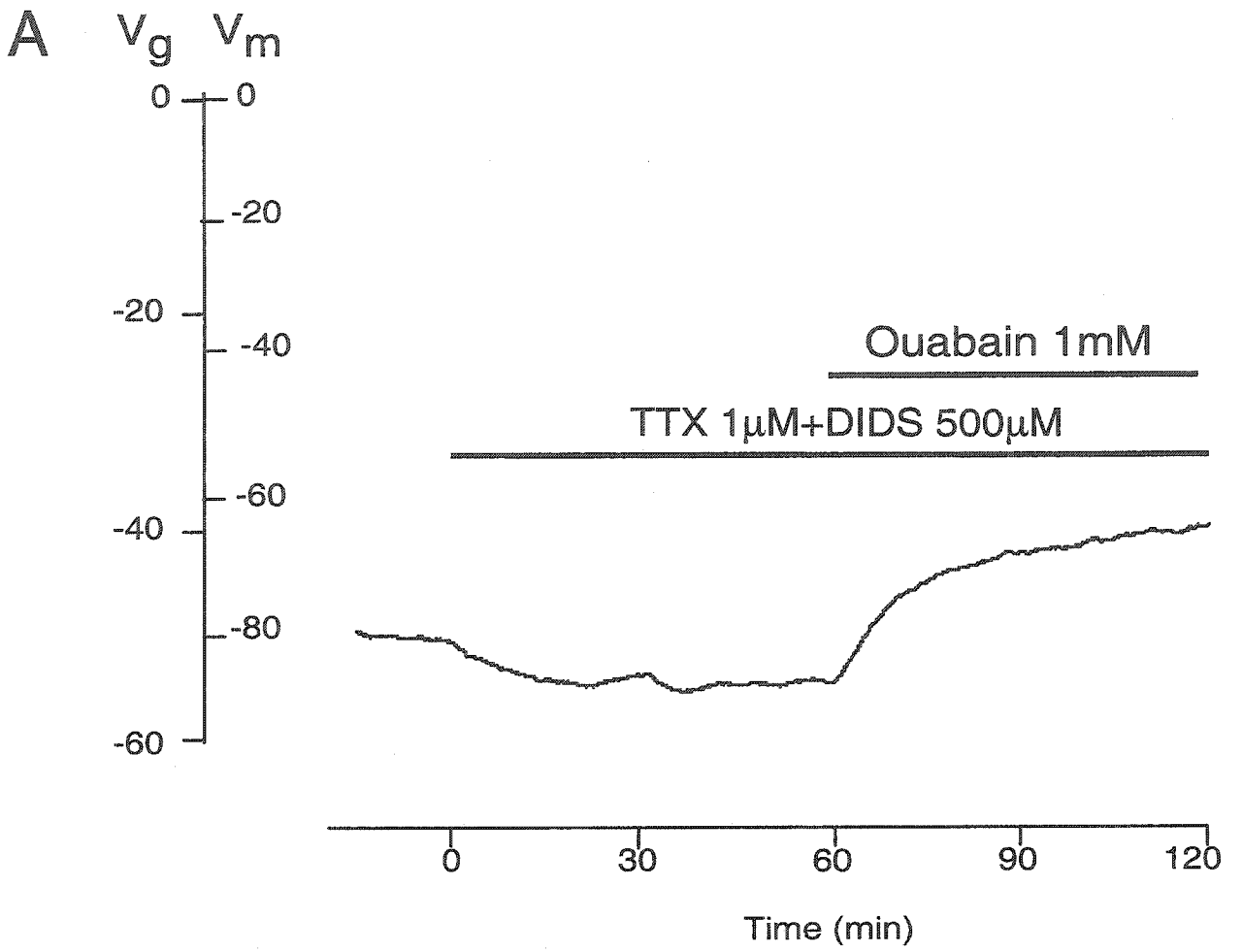
A
Vg Vm
0
0
-20
-20
-40
-40
-60
-80
-60
Ouabain 1mM
TTX 1μM+DIDS 500μM
0
30
60
90
120
Time (min)

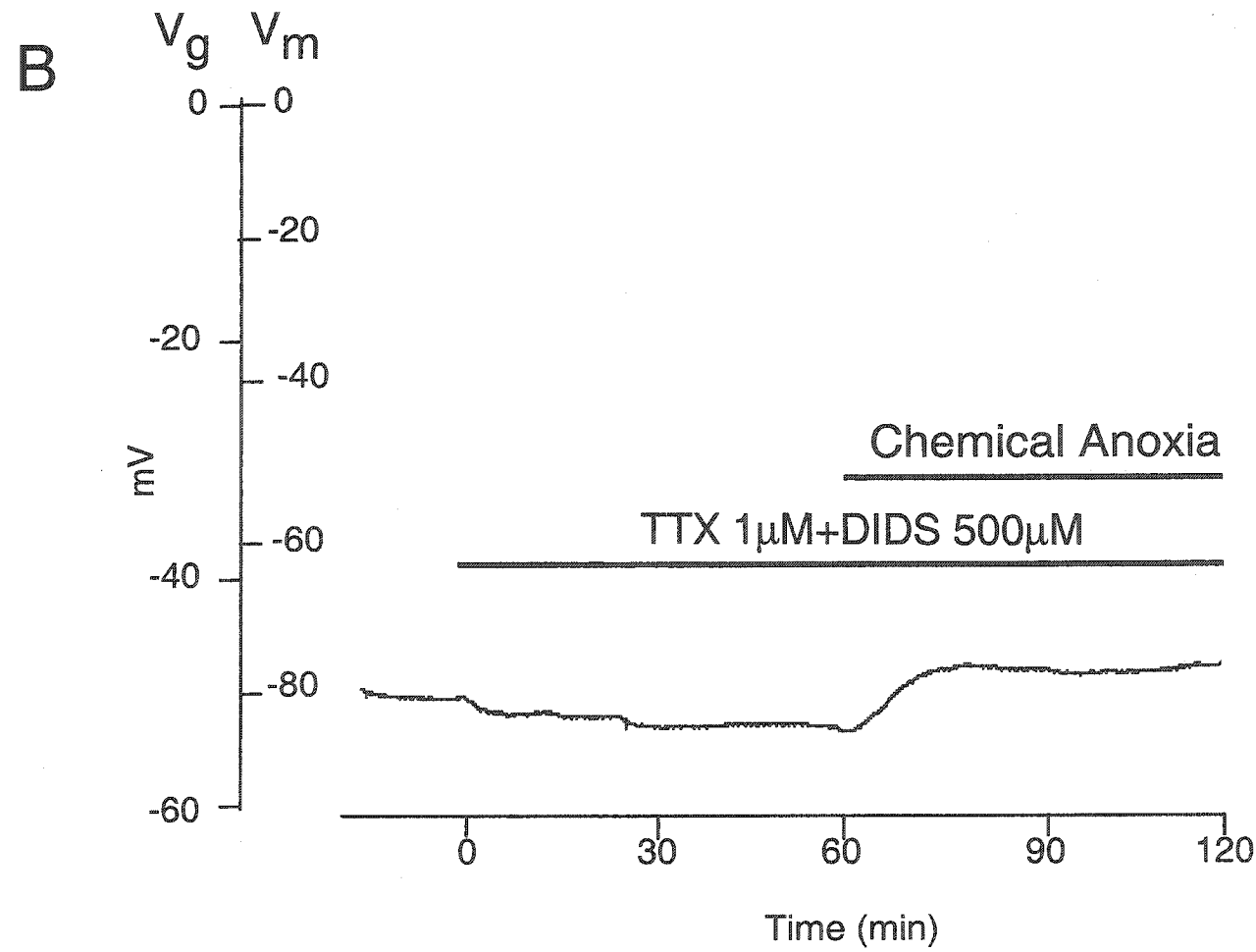
B
Vg Vm
0
0
-20
-20
-40
-40
mV
-60
-80
-60
Chemical Anoxia
TTX 1μM+DIDS 500μM
0
30
60
90
120
Time (min)

Figure 3.3 (C)Na^+-replacement, with NMDG, as well as DIDS application under Na-K-ATPase pump inhibition, did not produce statistically significant effects on V_m (n=4, 90 ± 3% $0Na^+$/Choline/NMDG +DIDS vs 87 ± 5% in $0Na^+$/Choline/NMDG, alone at 30min, p=0.36; 86 ± 5% vs 87 ± 4% at 60min, p=0.85). (D) With DIDS and Na^+-replacement manipulation during anoxia, V_m was maintained at 92 ± 3% of control after 30min in zero-Na^+ and DIDS and 84 ± 5% of control after 60min.

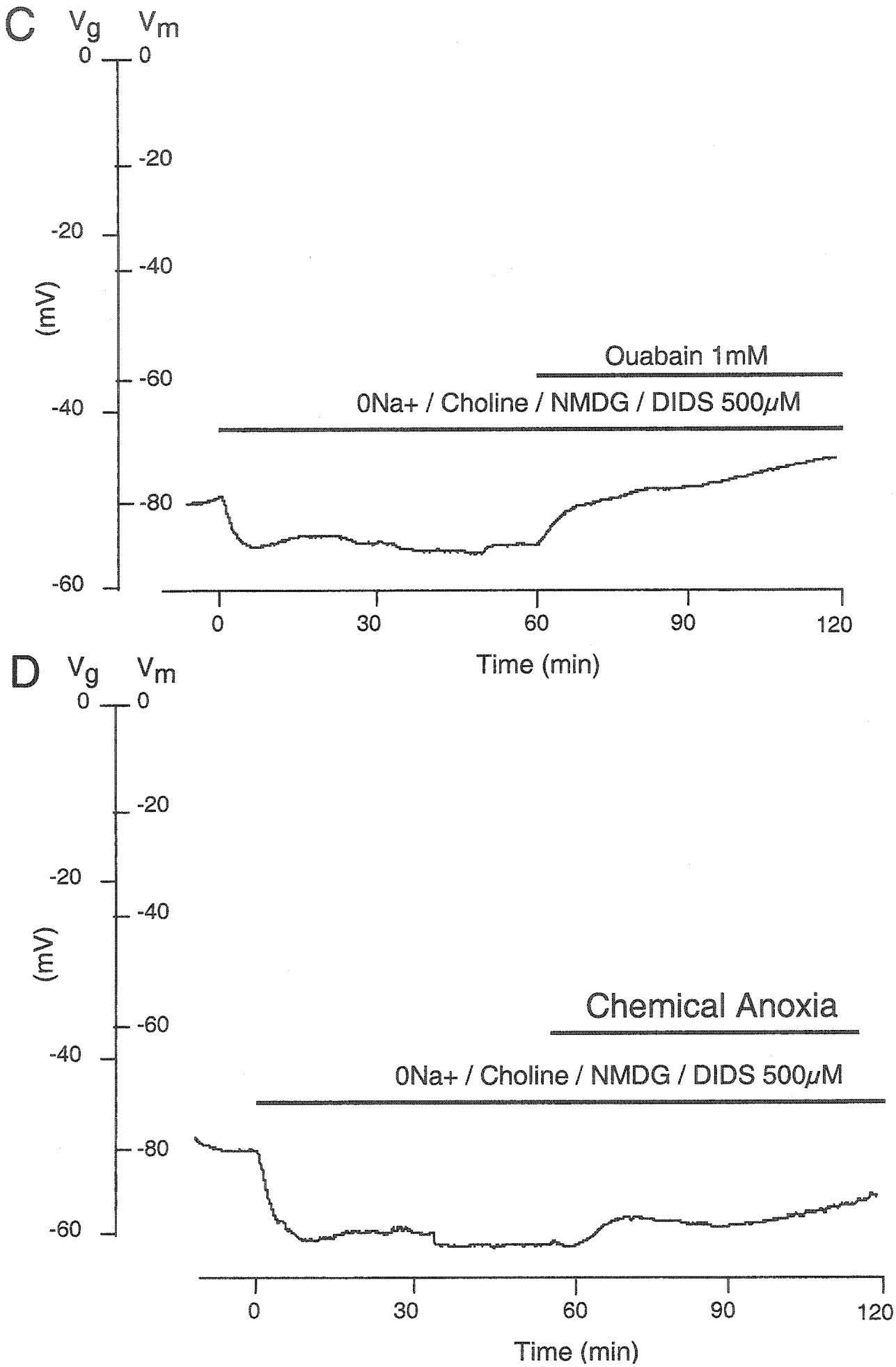
C
Vg
Vm
0
0
-20
-20
-40
-40
-60
-80
-60
(mV)
Ouabain 1mM
0Na+ / Choline / NMDG / DIDS 500μM
0
30
60
90
120
Time (min)
D
Vg
Vm
0
0
-20
-20
-40
-40
-60
-80
-60
(mV)
Chemical Anoxia
0Na+ / Choline / NMDG / DIDS 500μM
0
30
60
90
120
Time (min)

Figure 3.4 Co-blockade of Na^+-channels and Na-K-Cl cotransporter during Na-K-ATPase inhibition and its effect on membrane potential of rat optic nerve. Co perfusion of TTX(1μM) and Bumetanide(10μM) and relative specific blocker for NKCC, mildly improved V_m during ouabain application. Though small, the effect was statistically significant (n=4, 76±3% at 30min vs TTX+Ouabain, $p<0.01$; 65±1% of control V_m at 60min , $p<0.05$ vs TTX+Ouabain).

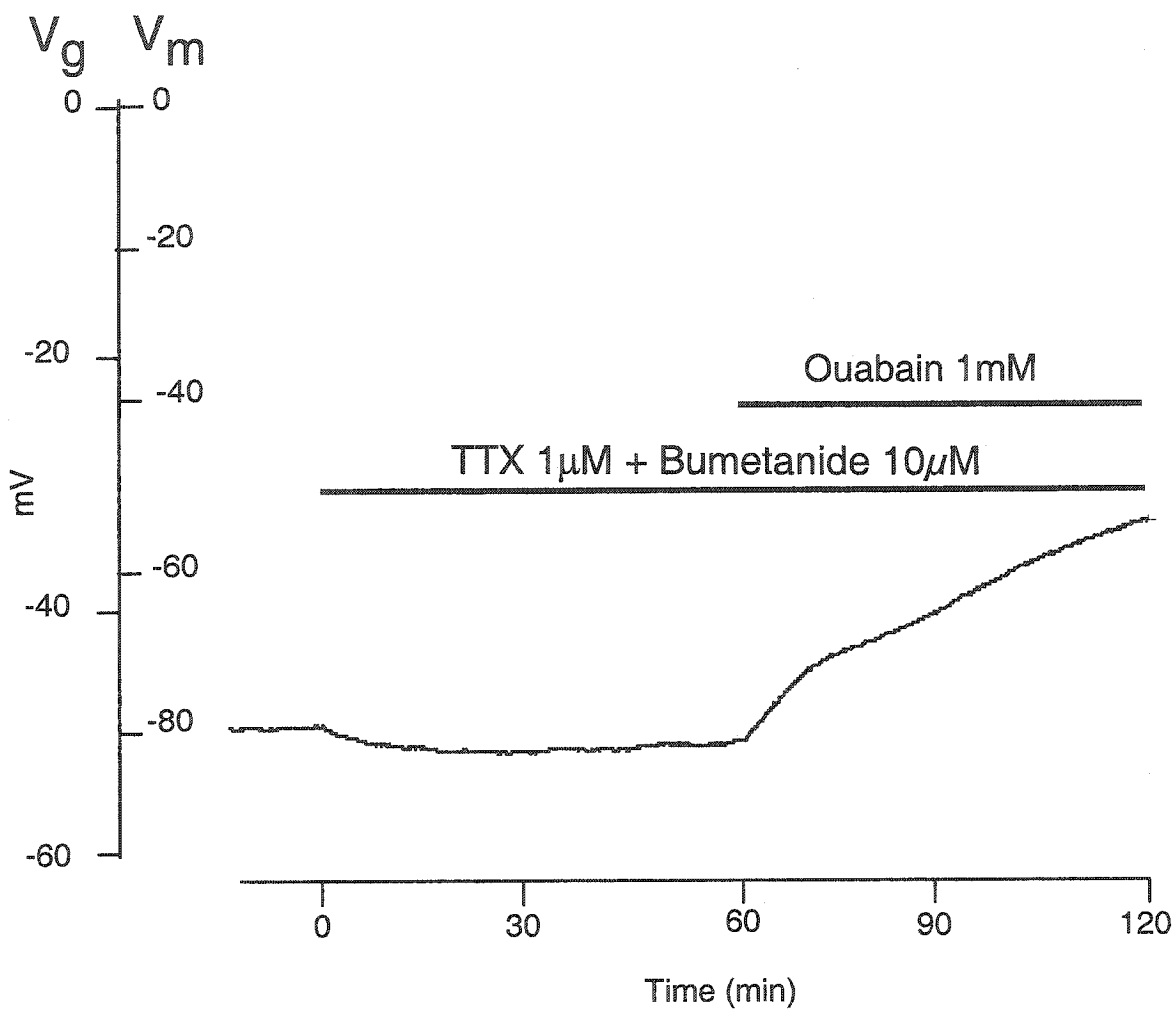
Vg
Vm
0
0
-20
-20
-40
-40
-60
-60
-80
mV
Ouabain 1mM
TTX 1μM + Bumetanide 10μM
0
30
60
90
120
Time (min)

Figure 3.5 Summary of pharmacological manipulations and their effects on V_m of RON. Error bars denote standard deviation. Pronounced V_m loss was observed with either Ouabain(1mM) or chemical anoxia (2mM). Blunting of the depolarization in both conditions was seen with addition of TTX(1μM). Addition of DIDS(500μM) mildly maintained V_m over levels seen with TTX+Ouabain. A similar effect was observed with addition of Bumetanide(10μM) to TTX during ouabain application. On the other hand, addition of DIDS to TTX during anoxia was effective in maintaining V_m to levels above those seen with TTX alone. Further experiments with Na^+-substitution with NMDG, allowed for a higher level of V_m maintenance than TTX alone during ouabain. DIDS, however, did not cause any further change on V_m when added to $0Na^+$/NMDG/Choline during ouabain application. Na^+-replacement in the chemical anoxia also maintained a large portion of control V_m while DIDS addition improved levels over those seen with $0Na^+$ alone. (*p<0.05,**p<0.01, *** p<0.001)

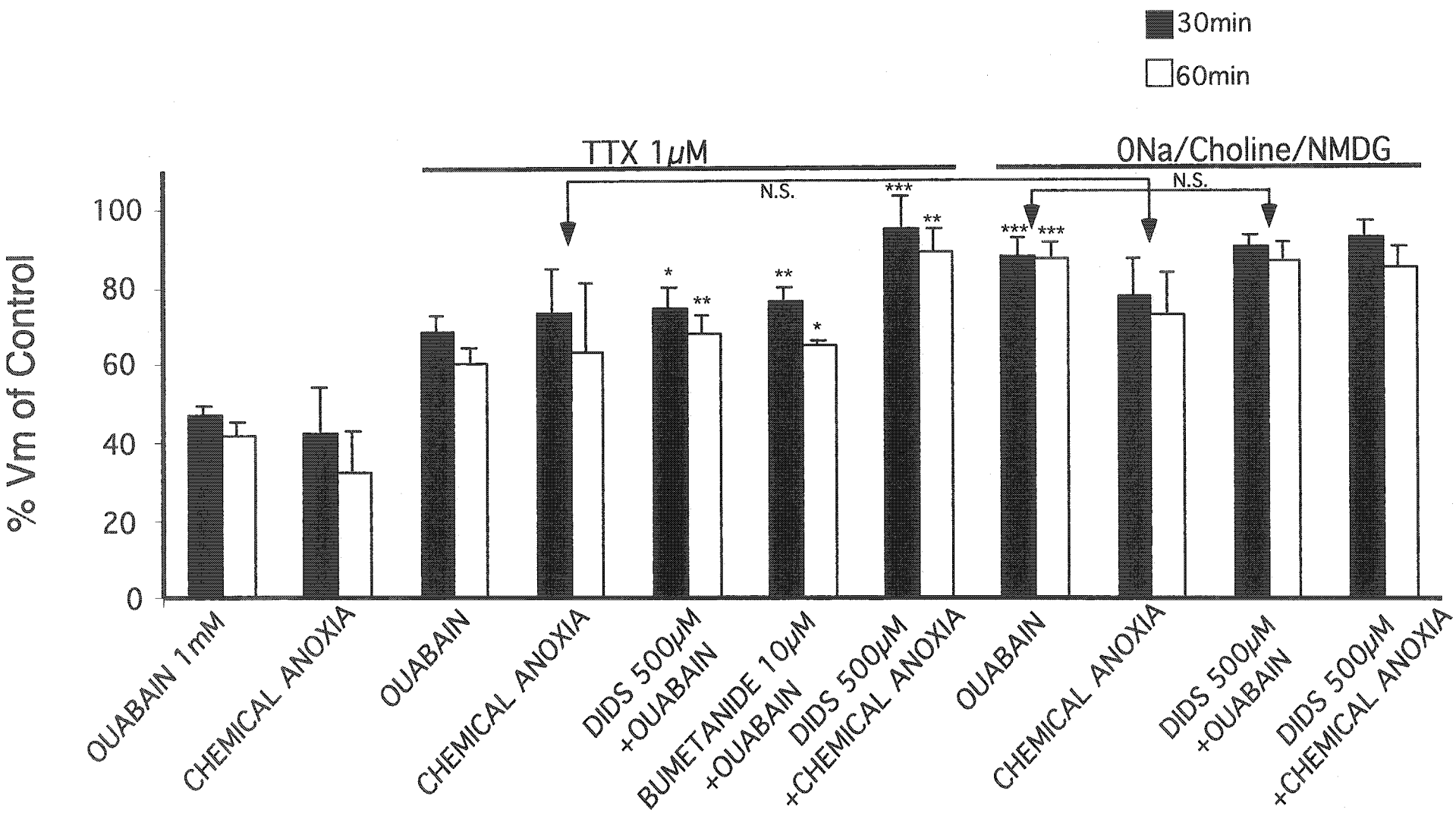
30min
60min
TTX 1μM
0Na/Choline/NMDG
N.S.
N.S.
% Vm of Control
100
80
60
40
20
0
OUABAIN 1mM
CHEMICAL ANOXIA
OUABAIN
CHEMICAL ANOXIA
DIDS 500μM +OUABAIN
BUMETANIDE 10μM +OUABAIN
DIDS 500μM +CHEMICAL ANOXIA
OUABAIN
CHEMICAL ANOXIA
DIDS 500μM +OUABAIN
DIDS 500μM +CHEMICAL ANOXIA

CHAPTER 4

Role Cl^- fluxes during Anoxia/Ischemia in the Rat Optic Nerve

4.1 Introduction

Anoxia/ischemia induces cellular ionic deregulation due to failure of regulatory mechanisms such as ATPases and coupled ion exchangers. As previously shown in CNS white matter, with the fall in energy substrates, axonal Na^+ overload occurs which in turn initiates Ca^{2+} accumulation in large part through reverse operation of the Na^+/Ca^{2+} exchanger (Stys *et al.* 1992b). Furthermore, in anoxic axons, Na^+ overload is largely balanced by an equivalent efflux of K^+ from the axoplasm (LoPachin and Stys 1995; Stys and Lopachin 1998) thus maintaining an electroneutral exchange of ions. One might therefore expect that restraining Na^+ influx into axoplasm during anoxia (e.g. by applying TTX or replacing bath Na^+ with an impermeant cation) would secondarily reduce K^+ loss. Unexpectedly, axoplasmic K^+ depletion is not restrained in anoxic optic nerve axons even when Na^+ overload is blocked by TTX (Stys and Lopachin 1998). Instead, K^+ loss is balanced by efflux of Cl^- and likely other organic anions (Stys and Lopachin 1998). Anion transporters including Na-K-2Cl cotransporter, Na^+-coupled Cl^-/HCO^-_3 exchange and the KCl-cotransporter (KCC) play an important role in intracellular Cl^- regulation in central neurons (Kaila 1994). Given its cotransport of K^+ and Cl^-, KCC would be a plausible candidate for mediating the observed parallel efflux of these ions during anoxia under conditions when Na^+ overload is restrained (as may occur during attempts at neuroprotection with Na^+ channel blockers or glutamate receptor antagonists). The emergence of K^+-Cl^- co-efflux under such conditions may have important implications for cellular integrity, because osmotically obligated water loss may have deleterious effects on cellular volume and therefore mechanical integrity, and in addition, this loss of water may in turn paradoxically concentrate remaining ions (such as Na^+) to toxic levels (see section 4.3 Discussion).

There are currently 4 known isoforms of the KCC (Gillen *et al.* 1996; Mount *et al.* 1999; Payne *et al.* 1996), which are part of the larger family of cation coupled cotransporter proteins also including the Na-K-2Cl cotransporter. Identified in 1996 by Payne and colleagues, the neuronal isoform (KCC2) appears to mainly extrude Cl^- out of the cell under physiological conditions (Payne *et al.* 1996). KCC3 has been shown to have a robust expression in the brain (Mount *et al.* 1999) with a cellular localization to white matter tracts (Pearson *et al.* 2001). Based on the fact that during anoxia and Na^+-

channel inhibition, there is persistent decay in membrane potential (Leppanen and Stys 1997b) probably as a result of K^+ efflux which proceeds in conjunction with Cl^- exit (Stys *et al.* 1997), we hypothesized that blockade of Cl^- loss during anoxia/Na^+-channel inhibition will impede K^+ efflux and protect white matter against anoxia better than Na^+-channel blockers alone. We confirmed that combined inhibition of Na^+ influx and K^+ + Cl^- efflux via the KCC reduced anoxic depolarization and improved compound action potential (CAP) recovery to a greater extent than Na^+ channel inhibitors alone. Moreover, quantitative evaluation of the CAP waveshape revealed that combined treatment also greatly improved not only CAP area but also the shape, suggesting a preservation of the underlying tissue architecture (eg. maintenance of axo-glial relationships or myelin integrity which would preserve conduction velocities of constituent fibers). We suggest therefore that, at least for white matter, combined Na^+ channel inhibition and reduction of secondary K^+ and Cl^- efflux represents an improved neuroprotective strategy.

4.2 Results

V_g recordings in aCSF typically stabilized 90 min after insertion into the grease gap chamber. Raw control resting potentials ranged from -45mV to -50mV. No consistent differences were noted between the first and second nerves studied sequentially. In order to compare responses over time and between different treatments, ratios of V_g's were calculated at different time points (typically 30 and 60 min) with respect to potentials at time zero (defined as a stable potential baseline before any experimental treatment).

4.2.1.Effects of Cl^- transport inhibition on membrane potential (V_m) during anoxia/Na^+-channel inhibition

For technical reasons, we were unable to obtain reproducible responses in the grease gap chamber using N_2/CO_2 as a means of inducing anoxia even with the use of oxygen scavengers, or oxygen/glucose deprivation to induce ischemia (data not shown). We elected instead to induce anoxia chemically, using either 2mM NaCN or NaN_3, inhibitors of complex IV of the respiratory chain (Kauppinen and Nicholls 1986; Tadic 1992) and chemical ischemia was induced by combining NaN_3 (2 mM) and iodoacetic

acid-Na^+ salt (IAA, 1 mM), an irreversible blocker of the glycolytic enzyme glyceraldehyde-3-phosphate dehydrogenase (Sabri and Ochs 1971). Regardless of the initiating injury (eg. nerve ischemia, anoxia, acrylamide intoxication, spinal cord impact trauma), similar patterns of ionic disruption in CNS and PNS myelinated axons are observed (for review see LoPachin and Lehning 1997; Stys 1997).

Fig. 4.1A shows a typical response to chemical anoxia induced by CN^-. Resting membrane potential depolarized within minutes, decaying to 44±14% and to 34±13% of control after 30 and 60 min. N_3^- produced very similar results (40±6% and 30±5% of control potential remaining after 30 and 60 min). Results from both treatments were therefore combined in subsequent analyses. Chemical ischemia produced a decay of V_m to values comparable to those observed with chemical anoxia alone (41 ± 5% and 31± 6% at 30 and 60min, respectively; n=10, Fig. 4.1B).

Previous reports have demonstrated the effectiveness of Na^+ channel inhibition as a neuroprotective strategy in anoxic white matter (Fern *et al.* 1993; Leppanen and Stys 1997b; Stys *et al.* 1992a; Stys *et al.* 1992b). The effects of TTX (1 μM) on optic nerve resting membrane potential during anoxia or ischemia are illustrated in Fig. 4.2 and quantitatively in Fig 4.4. Application of TTX under normoxic conditions caused a hyperpolarization as previously observed (Leppanen and Stys 1997a; b; Stys *et al.* 1993). Depolarization was less pronounced in anoxic nerves exposed to TTX (73 ± 11% of control V_m remaining after 30 min in TTX + anoxia vs. 42 ± 11% with anoxia alone, $p<0.01$; 63 ± 18% after 60 min, $p<0.001$; n=12). Replacement of Na^+ with an impermeant cation during chemical anoxia resulted in a blunted depolarization to 77 ± 9% of control membrane potential at 30 min ($p<0.01$ vs chemical anoxia) and to 73 ± 10% after 60min ($p<0.01$, n=3, Fig 4.4, Table 4.1). Because neither of the above manipulations completely prevented anoxic depolarization suggests that there exist other non-Na^+-dependent pathways promoting loss of resting potential in anoxic axons.

The role of anion transporters on resting membrane potential during anoxia was studied using DIDS, a broad spectrum anion transport blocker, that acts on the K^+-Cl^- cotransporter (Russell, 2000), volume sensitive Cl^- channels (Estevez *et al.* 1999), Cl^--HCO_3^- exchange (Clark *et al.* 1998; Sakai and Tosaka 1999) and hyperpolarization-activated Cl^- channels (Clark *et al.* 1998). In contrast, DIDS has no reported effect on

Na^+-K^+-$2Cl^-$ or Na^+-Cl^- cotransporters (Russell, 2000). DIDS (500 μM) alone did not alter the anoxic depolarization (43±8%, p=0.99 vs chemical anoxia at 30min; 40±9% at 60min, p=0.45, n=2; Fig 4.4, Table 4.4).

Previous results indicate that Na^+ channel inhibition promotes efflux of Cl^- in parallel with K^+ from anoxic optic axons (Stys and LoPachin 1998), thus concomitant blockade of Na^+-influx and Cl^--efflux pathways would be expected to spare K^+-efflux, and further reduce anoxic depolarization. Application of TTX (1 μM) together with DIDS 500 μM (Fig 4.3A, 4.4, Table 4.1) reduced the amount of depolarization to a greater degree than TTX alone (95 ± 8% vs 73 ± 10% in TTX alone at 30min, $p<0.001$; 89 ± 6% vs 63 ± 18% at 60min, $p<0.001$; n=13) (Fig 3A). DMSO (0.2% vol/vol used for DIDS stock solutions) had no effect on the anoxia-induced membrane potential changes (data not shown). $0Na^+$/choline/NMDG reduced anoxic depolarization to a similar extent as did TTX, and addition of DIDS (500μM) to the zero- Na^+ perfusate was even more effective (Fig 4.4, Table 4.1) (V_m maintained at 92 ± 3% of control after 30min in zero-Na^+ and DIDS vs. 77 ± 9% in zero-Na^+ alone).

Of the many anion transporters inhibited by DIDS, one potential route that could mediate both Cl^- and K^+ flux is the KCC. More selective inhibition of this transporter with furosemide (100 μM), a relatively specific blocker of KCC at this concentration (Cabantchik and Greger 1992; Payne 1997) reduced anoxic depolarization more than TTX alone (Figs. 4.3B and 4.4; 84±14% V_m remaining after 30 min in TTX+furosemide vs 73±10% in TTX alone at 30min, $p<0.01$; 79±16% vs 63±18% at 60min, $p<0.05$; n=20). However, the fact that DIDS reduced anoxic depolarization more than furosemide suggests that additional Cl^- transport pathways were operating in parallel (TTX+DIDS vs TTX+ Furosemide, $p<0.05$ at both 30 and 60min).

4.2.2.Effects of Cl^- transport inhibition on the compound propagated action potential

Fig 4.5A shows a typical control compound action potential (CAP) recorded from optic nerve under normoxic conditions, and 3hrs in normoxia following a 1 hr of anoxic insult. The area of the CAP recovered to 24 ± 12% (n=46) of control after 1hr anoxia/reoxygenation, in agreement with previous reports (Stys *et al.* 1992b). *In vitro*

ischemia (1 hr of OGD; Figs 4.5B and 4.9) allowed mean CAP area recovery of only 8 ± 3% of control after 3hr of reperfusion (n=9).

Previous reports have shown that axoplasmic Na^+-overload occurs mainly through TTX-sensitive channels during anoxia, ischemia and trauma is a primary event in the injury cascade (Stys 1998). Nerves subjected to 1 hr of anoxia in the presence of TTX 100nM (Fig 4.6a) recovered to 74±12% of control CAP area vs. 26±6% without TTX after 3 hrs of reoxygenation and wash in TTX-free aCSF ($p<0.001$, n=12; Figs. 4.6A and 4.9). This prolonged wash period was necessary to maximize removal of the blocker, which was still incomplete (control CAPs recovered to only 80% after a similar exposure to TTX/wash period without anoxia). As expected with the more severe ischemic insult (1 hr of OGD; Figs. 4.5B and 4.9), mean CAP area recovered to only 8±3% of control. Nevertheless TTX (100nM) partially rescued the nerves from ischemia as well (Figs. 4.6B and 4.9), allowing 56 ± 4% CAP area recovery after 3 hr of reperfusion/wash ($p<0.01$, n=3).

Anion transport blockade using DIDS 500μM caused an irreversible depression of the CAP to 16±17% after 1hr normoxic perfusion (Fig 4.7a, 4.9). At 2hr post anoxia, the CAP recovered to only 6±5% ($p<0.001$ vs anoxia, n=8). Hence we could not assess the effect of DIDS on CAP (in contrast to V_m). The effect of KCC inhibition on CAP recovery was assessed during normoxic, anoxic and ischemic conditions. Furosemide (10 μM), a relatively specific KCC inhibitor at these concentrations (Jarolimek *et al.* 1999), had no effect on the control CAP (Fig 4.9). However, this blocker partially prevented anoxic (mean CAP area recovery 40±4% vs. 26±6% without furosemide, $p<0.01$, n=8, Figs. 4.7B and 4.9) and ischemic (20±14% vs. 8±3%, $p<0.05$, n=9) injury as measured by CAP area.

The axoplasmic anoxia-induced Cl^- loss observed only in the presence of Na^+ channel inhibition (Stys and Lopachin 1998) suggests that a combination of Na^+-channel and KCC blockade may be more protective than either agent alone. Mean CAP area recovery was significantly improved following anoxia after the addition of furosemide to TTX (Fig 4.7C, 4.9), compared to TTX alone (91±9% vs 74±12% TTX alone, $p<0.001$, n=11). Moreover, furosemide substantially normalized the shapes of the post-anoxic CAPs (see next section). However, this drug combination was not more effective in

OGD, producing a recovery of only 50±19% ($p>0.05$ compared to 56 ± 4% in TTX alone, n=14, Fig 4.9).

Axoplasmic Ca^{2+} is known to increase during anoxia (Stys and Lopachin 1998) thus it was of interest to study potential Ca^{2+}-sensitive anion transporters such the Ca^{2+}-activated Cl^- channel during anoxia/ischemia. Inhibition of Ca^{2+}-activated Cl^- channels with niflumic acid 50μM (Currie *et al.* 1995; Scott *et al.* 1995), during 1 hr normoxic perfusion, caused a minor insignificant depression of the CAP. Niflumic acid unexpectedly worsened post-anoxic CAP recovery (6±1% vs. 26±6% in aCSF alone, $p<0.001$, n=6; Fig 4.8A, 4.9), in contrast to KCC inhibition, which improved outcome (see above). Similarly during *in vitro* ischemia CAP recovery was also worse with niflumic acid treatment (3±1% vs. 8 ± 3% in aCSF alone, $p<0.01$, n=3; Fig 4.8B, 4.9).

4.2.3.Compound Action Potential Waveshape Recovery.

Combined treatment with furosemide + TTX not only improved CAP area recovery post-anoxia, but also appeared to significantly improve the shape of the response, which in part reflects the preservation of normal conduction velocities of the constituent fibers. In order to quantify these observations we devised a measure of the shape of the CAP compared to the pre-injury control waveshape, independent of CAP magnitude. This "waveshape fidelity index" was calculated by first normalizing the areas between the pre-injury control CAP and post-treatment response, by scaling the smaller waveform so that areas are equal. Next a point-by-point squared difference was calculated between the two CAPs, and these squared differences averaged to yield a single numerical index. In mathematical terms:

$$F = \frac{\sum_{i}^{n} \left(w_{0i} - \frac{A_0}{A_1} w_{1i} \right)^2}{n}$$

where:

F is the "waveshape fidelity index"

w_0 and w_1 are control and post-treatment CAP waveforms, respectively

A_0 and A_1 are control and post-treatment CAP areas

n is the number of points in each waveform

An index of zero denotes a post-treatment waveshape that is identical to control, regardless of its size. An increasing index indicates a waveshape that differs more and more from control (again independent of magnitude). Selected normalized waveforms are shown in Fig 4.10(A-D) while indices for various treatments are summarized in Fig4.10E. Of the various treatments tested, combined application of TTX and furosemide was the most successful in restoring CAP shape after anoxic exposure; indeed, waveshapes were not statistically different between this treatment group and time matched normoxic controls, indicating that not only did this combination of drugs allow recovery of CAP area, but the configuration of the CAP was restored to near normal. This is in contrast to TTX alone, which was very effective at protecting CAP area, but resulted in distorted waveshapes reflected by a higher waveshape fidelity index.

4.2.4.Immunolocalization of K-Cl Cotransporter in the Rat Optic Nerve

Fig. 4.11 shows representative confocal microscopic images of rat optic nerve immunostained for different KCC isoforms. The red channel outlines axons stained with neurofilament while green shows KCC stained with isoform specific antibodies. Strong KCC3a signal was found on optic nerve astrocytes and their processes (Fig. 4.11A, B). Weaker KCC3a signal was found in the myelin of many larger axons (Fig. 4.11A inset). There was more modest but reproducible, often punctate, KCC3 signal in the myelin sheaths of larger axons (Fig. 4.11C, D). KCC2 appeared more widespread, with signal in cell bodies of oligodendrocytes, and also within axon cylinders (hence the orangy hue in Fig.4.11E, representing colocalization of green KCC2 fluorescence and red NF160). KCC1 staining was very weak, diffusely localized and not consistently stronger than controls so no conclusions about its presence or localization could be drawn (not shown).

4.3 Discussion

In adult mammalian neurons, the Cl^- gradient is influenced by a number of systems, including the K-Cl (KCC) and Na-K-2Cl (NKCC) co-transporters (for a review see Alvarez-Leefmans, 1990). KCC2, the neuronal isoform, appears to mainly extrude Cl^- out of the cell (Payne *et al.* 1996).By lowering the internal $[Cl^-]$ during development, there is a switch in the GABA response from depolarizing to hyperpolarizing (Rivera *et al.* 1999). Indeed, three types of Cl^- channels were found on myelinated peripheral *Xenopus* sciatic nerve axons by single channel recordings (Wu and Shrager 1994), though direct evidence of such channels in CNS axons is lacking. Stys *et al.* (1997) showed that Cl^- is not passively distributed, instead has a concentration significantly above its predicted passive level of 7 mM; resting axoplasmic $[Cl^-]_i$ is in the range of 40-50 mM, indicating active accumulation into fibers, likely mediated at least in part by Na-K-2Cl co-transport that favours a predicted resting $[Cl^-]_i$ of 55mM (Stys *et al.* 1997) (see Fig. 4.12). Using immunohistochemistry, Alvarez-Leefmans *et al.* (2001) confirmed the presence of Na-K-2Cl co-transporter on the membranes of both axons and Schwann cells in peripheral nerves. Using *in situ* hybridization, others have demonstrated Na-K-2Cl co-transporter mRNA in both grey and white matter areas in rat CNS, indicating that this Cl^- regulator appears widely distributed in the mammalian nervous system (Kanaka *et al.* 2001). In central axons, $[Cl^-]$ appears to be determined by a coordinated interplay of accumulating (eg. Na-K-2Cl co-transport) systems and passive and/or coupled efflux, mediated in part by channels and other Cl^- regulatory pathways such as the KCC. A speculative explanation could be that such type of Cl^- distribution creates a favourable gradient for proper functioning of Cl^--dependent mechanisms such volume regulatory pathways.

4.3.1 Na-channel blockade

Previous studies on white matter anoxia, ischemia and trauma established the importance of axonal Na^+ influx as a major event in the injury cascade (for review see Stys, 1998). Our results agree with others whose general finding was that blockade of TTX-sensitive Na^+-channels during injury was protective as assessed by electrophysiological, biochemical and structural methods (Agrawal and Fehlings 1996;

Fern *et al.* 1993; Imaizumi *et al.* 1997; Jiang and Stys 2000; Leppanen and Stys 1997a; b; Teng and Wrathall 1997). The normal adult optic nerve CAP configuration arises from an ordered segregation of fiber conduction velocities, in turn dependent on fiber diameters and myelination in the maturing animal (Foster *et al.* 1982). One might expect the partially protective effects of TTX to be manifested in elements that possess substantial densities of Na^+ channels, ie. axons, rather than glia or the myelin sheath. Ultrastructural examination of anoxic optic nerve suggests that glial damage may be due more to volume disruption rather than cytoskeletal dissolution as occurs in the axon cylinder (Waxman *et al.* 1994). This implies that volume changes in glial elements, potentially including the myelin sheath, may play an important role in causing serious alterations in fiber conduction velocities, which would adversely affect information coding in white matter tracts, or result in complete propagation failure in fibers with more severely disrupted axo-glial architecture. Since Cl^- has been shown to participate in a variety of regulatory volume processes (O'Neill 1999), modulation of such pathways during injury might reduce such deleterious volume changes, helping to preserve normal conduction velocity distributions. In our study, the ability of furosemide to normalize CAP waveshape after anoxia and ischemia is consistent with the idea that KCC mediates pathological Cl^- flux (especially under conditions of Na^+-channel inhibition); the resultant osmotic and water shifts are likely responsible for mechanical perturbation of subcellular architecture and disturbances of action potential propagation. We attempted to determine whether other Cl^- transporters contributed to this process by applying DIDS, a broad spectrum anion transport blocker. Unfortunately this compound caused a severe and irreversible depression of CAP amplitude, possibly because of its blocking effect on voltage-gated Na^+ channels (Liu *et al.* 1998), so we were unable to assess any putative protective effect on CAP recovery. However, the incremental sparing of anoxic depolarization observed with DIDS compared to furosemide (both in the presence of TTX; Fig. 4.4) suggests that additional anion transporters may play a role as well.

4.3.2 Cl^- shifts in RON during anoxia

Under pathophysiological conditions such as anoxia/ischemia, $[Cl^-]_i$ often increases in grey matter. For example, hypoglossal neurons of rat brain slices subjected to

anoxia showed an increase in $[Cl^-]_i$ by ≈20 mM (Jiang *et al.* 1992). Taylor *et al.* (1999) showed an increase in $[Cl^-]_i$ in CA1 area cell bodies in adult hippocampal slices exposed to OGD. Others have shown the effects of Cl^- deregulation on hypoxic depolarization. CA1 pyramidal cells subjected to hypoxia displayed a delayed hypoxic depolarization in the presence of Cl^- transport inhibitors (Muller 2000). Fig. 4.12 summarizes theoretical calculations of equilibrium Cl^- concentrations under normal and anoxic conditions based on data from optic nerve (Stys *et al.* 1997). Under normal conditions (single solid arrowheads in Fig. 4.12), KCC attempts to maintain $[Cl^-]_i$ at low levels, well below 10 mM, whereas Na-K-2Cl co-transport will accumulate Cl^- towards an equilibrium concentration of ≈55 mM. Actual resting axonal $[Cl^-]$ lies between these two values, reflecting a balance between these two opposing Cl^- transport systems. During anoxia, with a significant reduction of $[K^+]_i$ (LoPachin and Stys 1995; Stys and LoPachin 1998) a parallel rise in $[K^+]_o$ (Ransom and Philbin 1992), both transporters will be biased towards strong Cl^- accumulation (double arrow, Fig. 4.12) and likely cause significant cellular volume deregulation. Surprisingly, in contrast to grey matter, there is little change in axonal or glial $[Cl^-]_i$ during anoxia in white matter (LoPachin and Stys 1995; Stys and LoPachin 1998). One Cl^- efflux mechanism that may have compensated for such expected Cl^- accumulation is the opening of a Cl^- channel, such as $Cl^-_{Ca^{2+}}$ (Frings *et al.* 2000; Scott *et al.* 1995). Calculations (based on data from LoPachin and Stys 1995) reveal that axonal V_m remains more negative than E_{Cl^-}, even at the end of a 60 min anoxic insult (Fig. 4.1; axonal $V_m \approx$ -44 mV, vs. $E_{Cl^-} \approx -30$ mV). Glial V_m is also estimated to be more negative than E_{Cl^-}. This indicates that Cl^- flux through an uncoupled transporter such as a channel would be continuously directed outward. For this reason, Cl^-_{Ca} would be well poised to serve as a compensatory system because a rise in free $[Ca^{2+}]$ will almost always be a feature of a pathological state such as anoxia/ischemia. Consistent with this hypothesis was the finding of Duchen (1990) who showed an enhancement of $Cl^-_{Ca^{2+}}$ current during chemical anoxia in dissociated mouse DRG neurons. This would also explain the deleterious effects of $Cl^-_{Ca^{2+}}$ channel inhibition by niflumic acid, which likely hindered the optic nerve's ability to compensate for an abnormal influx of Cl^- mediated by coupled transporters as assessed from the CAP area recovery values (Fig 4.8,4.9) and waveshape (Fig 4.10). Other Cl^- channels (such as volume regulated channels which are

also blocked by niflumic acid (Leaney *et al.* 1997) could also participate in this mechanism.

4.3.3 Concomitant Blockade of specific Na^+ and Cl^- pathways

Stys and LoPachin (1998) suggested that KCl-cotransport may act as a parallel pathway for K^+ and Cl^- loss during anoxia with concomitant Na^+ channel blockade. Under these conditions, axonal volume was noted to decrease markedly (Waxman *et al.* 1994), along with water content (LoPachin and Stys 1995; Stys and LoPachin 1998). With the major Na^+ influx route blocked by TTX, it is likely that ionic rundown may switch from Na^+-K^+ exchange to a parallel efflux of K^+ and Cl^- (and likely other anions); both modes will maintain electroneutrality, but in contrast, the latter will drag water out of the cytosol, causing cell shrinkage and possibly mechanical damage (Waxman *et al.* 1994). Because the water loss will substantially concentrate remaining intracellular ions (axoplasmic $[K^+]$ estimated at ≈55 mM at the end of 60 min of anoxia in TTX-treated optic nerves vs. ≈15 mM in untreated anoxic nerves, despite a loss of 90% of total axoplasmic K^+ under both conditions (LoPachin and Stys 1995; Stys and LoPachin 1998), the KCC will remain biased in the Cl^- efflux mode (open arrowhead, Fig. 4.12), and would be positioned to remove K^+ and Cl^- from the cytoplasm. Indeed, while the Na-K-2Cl cotransporter would attempt to accumulate Cl^- back into cells under such conditions, its activity will be reduced by a fall in ATP levels (Russell, 2000), whereas an ATP decrease will *activate* KCC (Ortiz-Carranza *et al.* 1996); therefore under anoxic conditions the transport rate of the Na-K-2Cl cotransporter may be greatly diminished, unmasking the KCC- and Cl^- channel-mediated Cl^- extrusion, precisely what is observed with direct axonal $[Cl^-]$ measurements (Stys and LoPachin, 1998). This scenario might explain why blocking KCC with furosemide was protective during anoxia: with concomitant Na^+ channel blockade KCC inhibition reduced the excessive Cl^- export, while decreasing abnormal Cl^- influx under conditions where Na^+ channels were not blocked. Therefore, excessive Cl^- movements in either direction may have deleterious effects on volume regulation resulting in secondary mechanical injury. These findings may have implications for the design of neuroprotective strategies, whereby concomitant

inhibition of Na^+ channels and KCC could result in better outcome than with blockade of either pathway alone.

Figure 4.1. Effect of chemical anoxia and ischemia on the membrane potential of rat optic nerve. V_g represents recorded gap potential and V_m represents membrane potential. Time 0 in this and all subsequent figures denotes application of insult (**A**) NaCN (2mM) caused a rapid loss of membrane potential decaying to approximately 42±11and 32±10 % of control at 30 and 60min respectively of chemical anoxia. (**B**) Chemical ischemia, NaN_3 2mM + IAA 1mM, caused a decay of 41±5% and 31± 6% after 30 and 60min of perfusion.

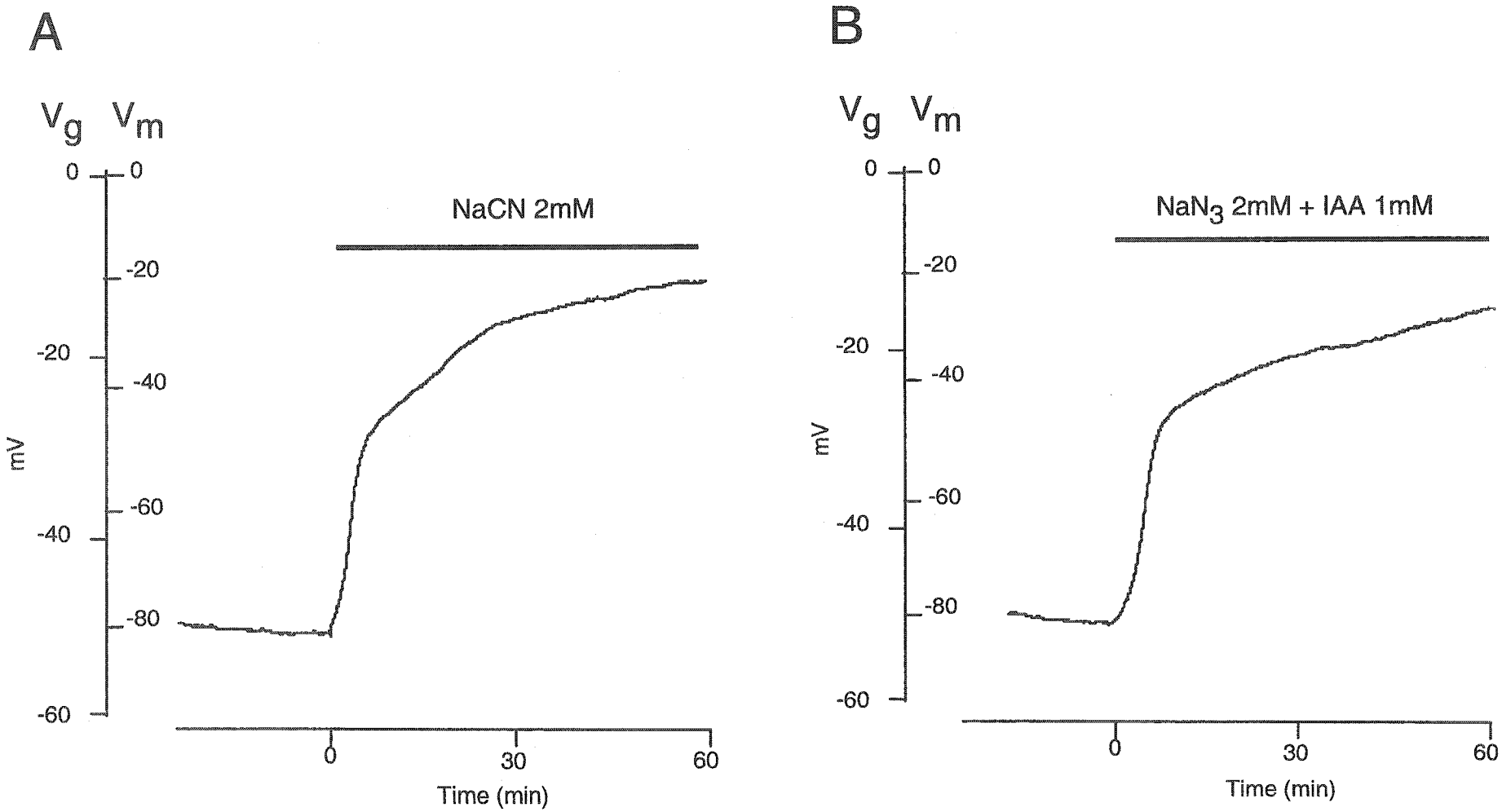
A
Vg Vm
0
0
-20
-40
-60
-20
-40
-60
-80
mV
NaCN 2mM
0
30
60
Time (min)
B
Vg Vm
0
0
-20
-40
-60
-20
-40
-60
-80
mV
NaN3 2mM + IAA 1mM
0
30
60
Time (min)

Figure 4.2. Effect of Na^+-channel inhibition on the membrane potential of rat optic nerve. TTX 1mM preapplied for 1h before chemical anoxia, caused a brief hyperpolarization of Vm; thus indicating the presence of a Na^+ conductance at rest. During chemical anoxia, TTX 1mM blunted the rapid phase of the characteristic depolarization (73 ± 11% of control Vm remaining after 30 min in TTX + anoxia vs. 42 ± 11% with anoxia alone, $p<0.005$; 63 ± 18% after 60 min, $p<0.001$; $n=12$) suggesting that Na^+ influx through TTX-sensitive channels constitutes one of the primary events in producing the anoxic depolarization.

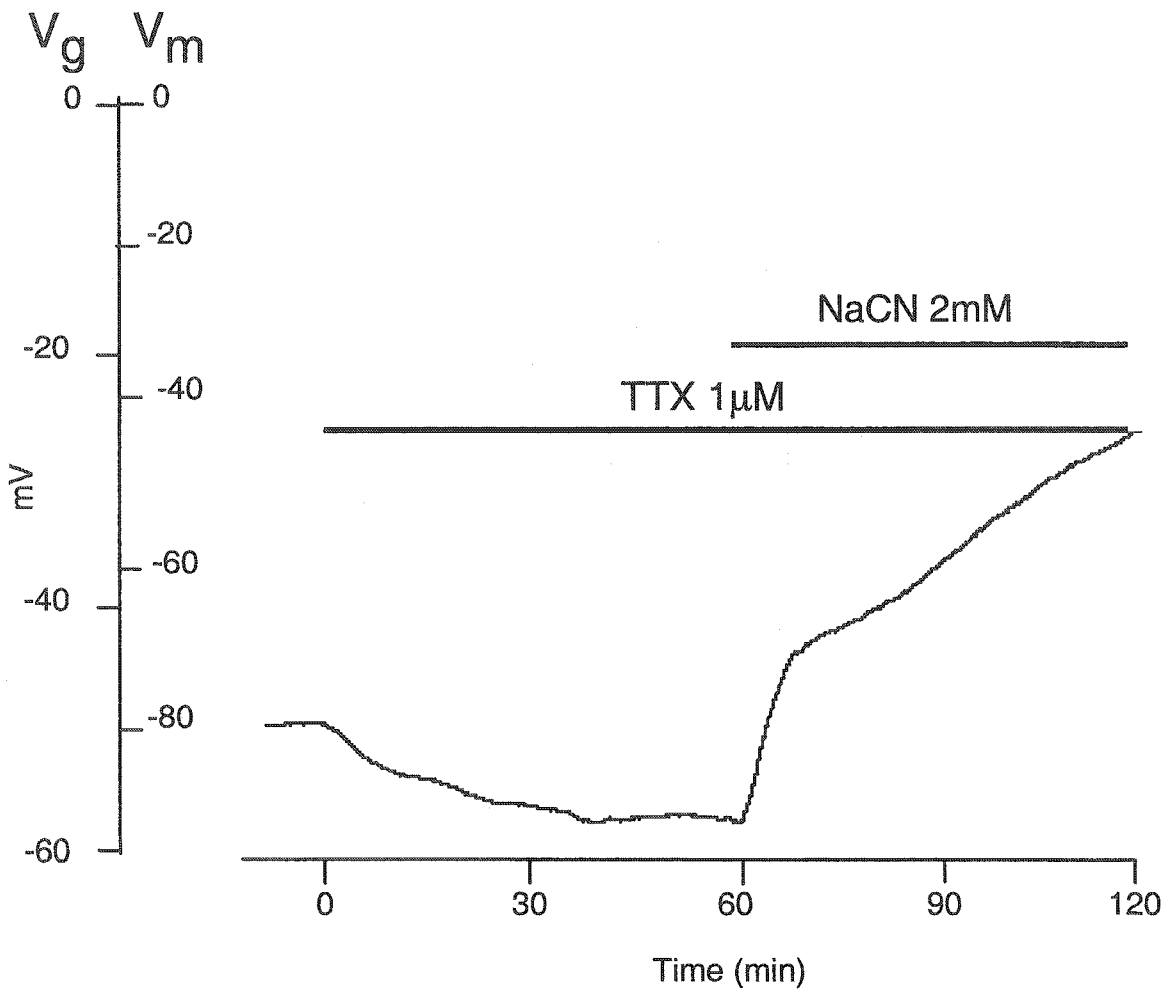
Vg
Vm
0
0
-20
-20
-40
-40
-60
-60
-80
mV
NaCN 2mM
TTX 1μM
0
30
60
90
120
Time (min)

Figure 4.3. Effect of anion transport and Na^+-channel co-blockade, on the membrane potential of rat optic nerve, during chemical anoxia. (A)DIDS 500μM, broad spectrum anion transport blocker, applied during normoxic conditions, had no effect on TTX 1μM hyperpolarization. During chemical anoxia, the combined treatment allowed for maximum maintenance of V_m (95±8% vs 73±10% in TTX alone at 30min, $p<0.001$; 89±6% vs 63±18% at 60min, $p<0.001$; n=13) suggesting an anion component for the depolarization. (B) Furosemide 100μM, a relatively specific blocker for KCC, produced a blunting of the residual depolarization seen with TTX+CN^- (84±14% Vm remaining after 30 min in TTX+furosemide vs 73±10% in TTX alone at 30min, $p<0.05$; 79±16% vs 63±18%, $p<0.05$; n=20). This suggests that the DIDS effect is mediated largely , but not exclusively , via KCC.

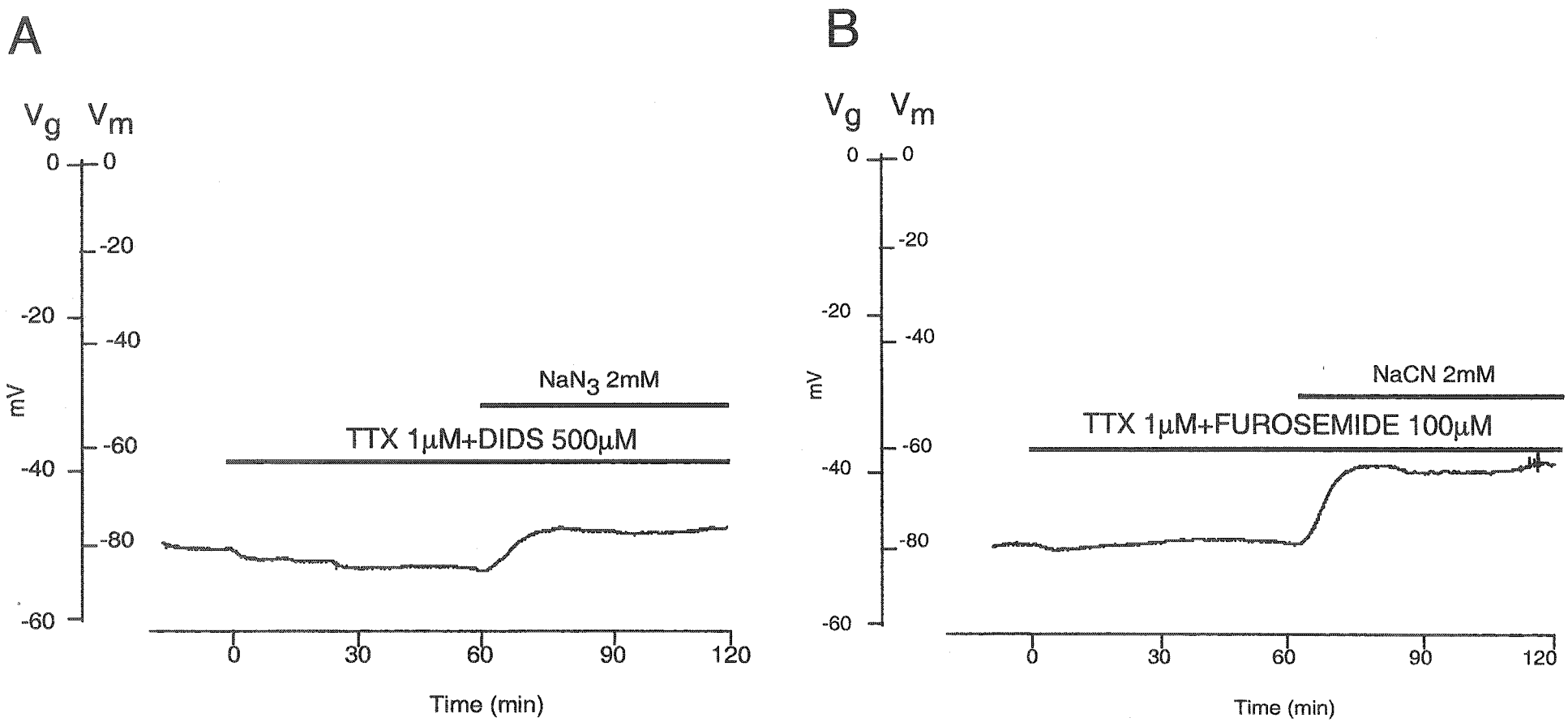
A
Vg Vm
0
0
-20
-20
-40
-40
-60
-60
-80
mV
NaN3 2mM
TTX 1μM+DIDS 500μM
0
30
60
90
120
Time (min)
B
Vg Vm
0
0
-20
-20
-40
-40
-60
-60
-80
mV
NaCN 2mM
TTX 1μM+FUROSEMIDE 100μM
0
30
60
90
120
Time (min)

Figure 4.4 Summary of different pharmacological manipulations and their effects on V_m of RON. Error bars denote standard deviation. Both chemical anoxia and ischemia caused comparable decay profiles . Anion transport blockers, DIDS 500μM and Furosemide 10μM, when used alone during chemical anoxia were in effective in maintaining V_m at pre-anoxic levels. Na^+-channel blockade, TTX 1μM, was more effective in preserving to a large extent V_m during chemical anoxia. Nevertheless, there existed a residual portion of the depolarization which was Na^+-independent as seen from either inhibition of Na^+-channels or Na^+-replacement. Co-blockade of Na^+-channel (TTX 1μM) and anion transport (DIDS 500μM) or Na^+-replacement (NMDG) in combination with DIDS 500μM produced a robust maintenance of V_m. Furosemide 100μM, a KCC blocker, co-applied with TTX 1μM, improved V_m maintenance as compared to TTX alone. However, the levels were not as comparable as those of DIDS presumably because there are other pathways involved in mediating residual V_m depolarization during TTX/chemical anoxia perfusion. (*p<0.05,**p<0.01, *** p<0.001)

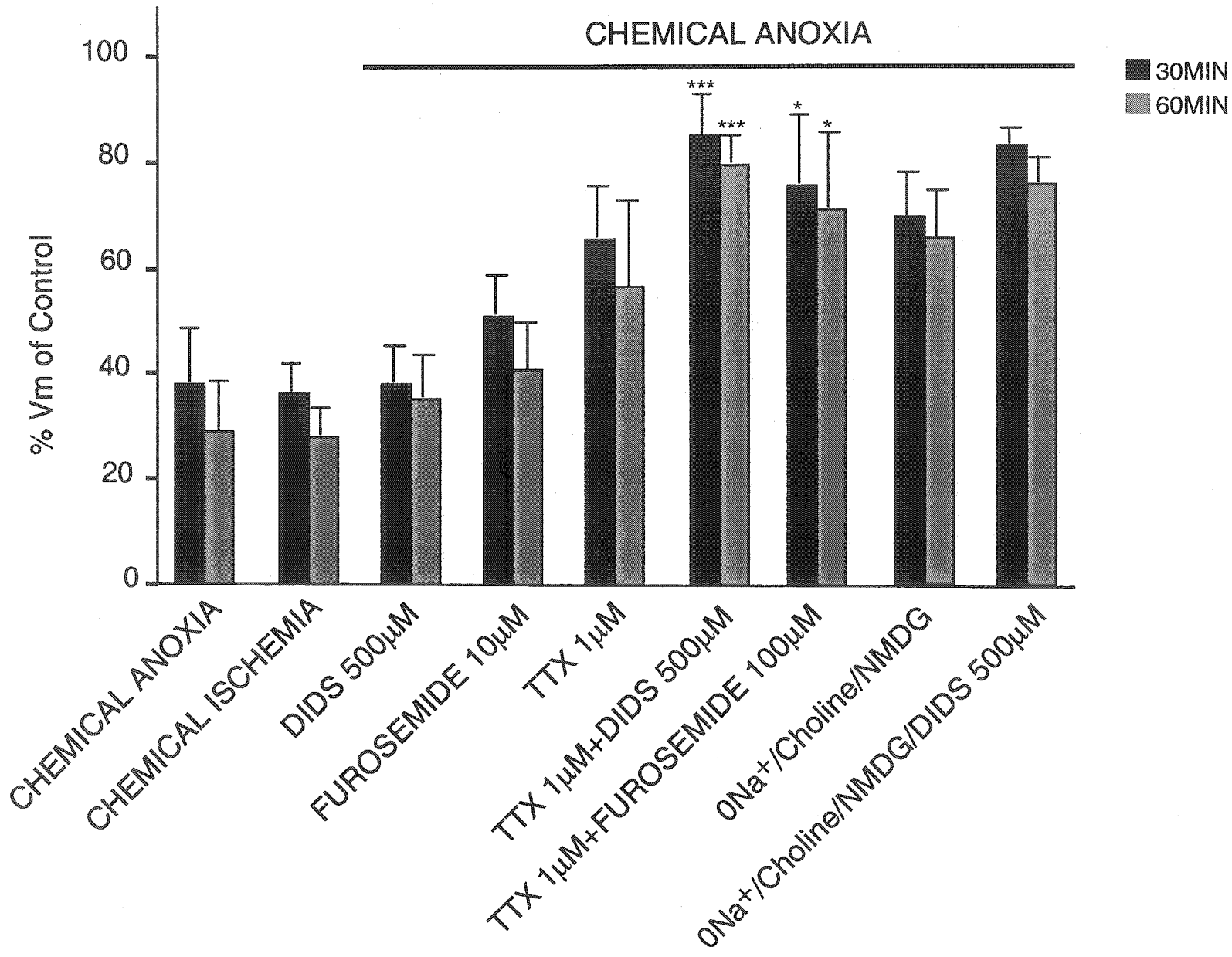
CHEMICAL ANOXIA
30MIN
60MIN
% Vm of Control
100
80
60
40
20
0
***
***
*
*
CHEMICAL ANOXIA
CHEMICAL ISCHEMIA
DIDS 500μM
FUROSEMIDE 10μM
TTX 1μM
TTX 1μM+DIDS 500μM
TTX 1μM+FUROSEMIDE 100μM
0Na+/Choline/NMDG
0Na+/Choline/NMDG/DIDS 500μM

Figure 4.5 Effects of anoxia versus oxygen/glucose deprivation(OGD) on the Compound action potential of the rat optic nerve. (**A**). Recovery of the CAP area after 60min anoxic insult, in normal aCSF was 26±6%of control at 3hr post mark. (**B**). With the stronger insult of 60min OGD, the recovery was only 8±4 % of control also at 3hr post.

A

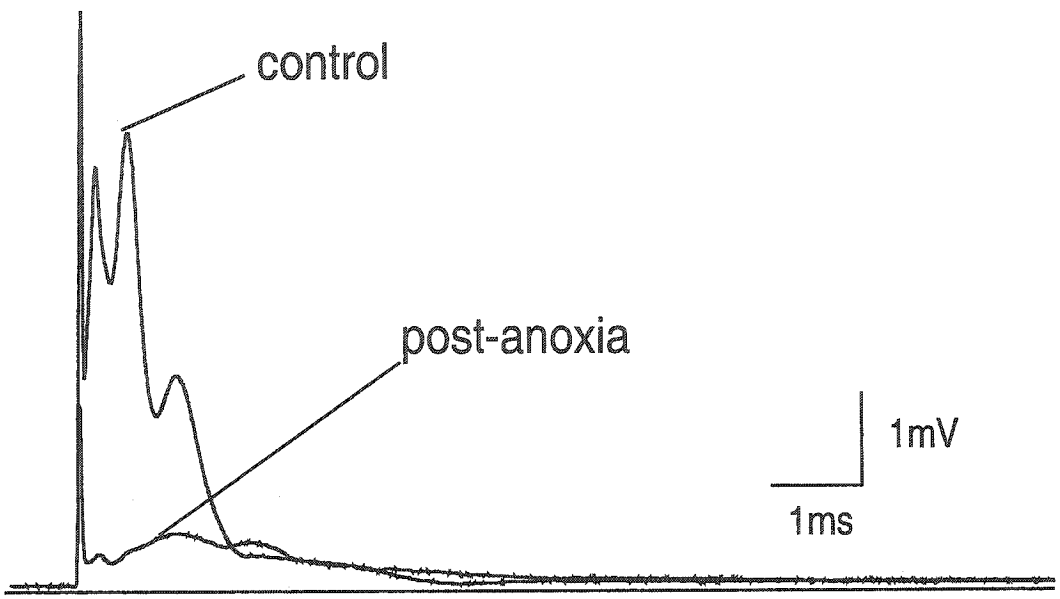

B

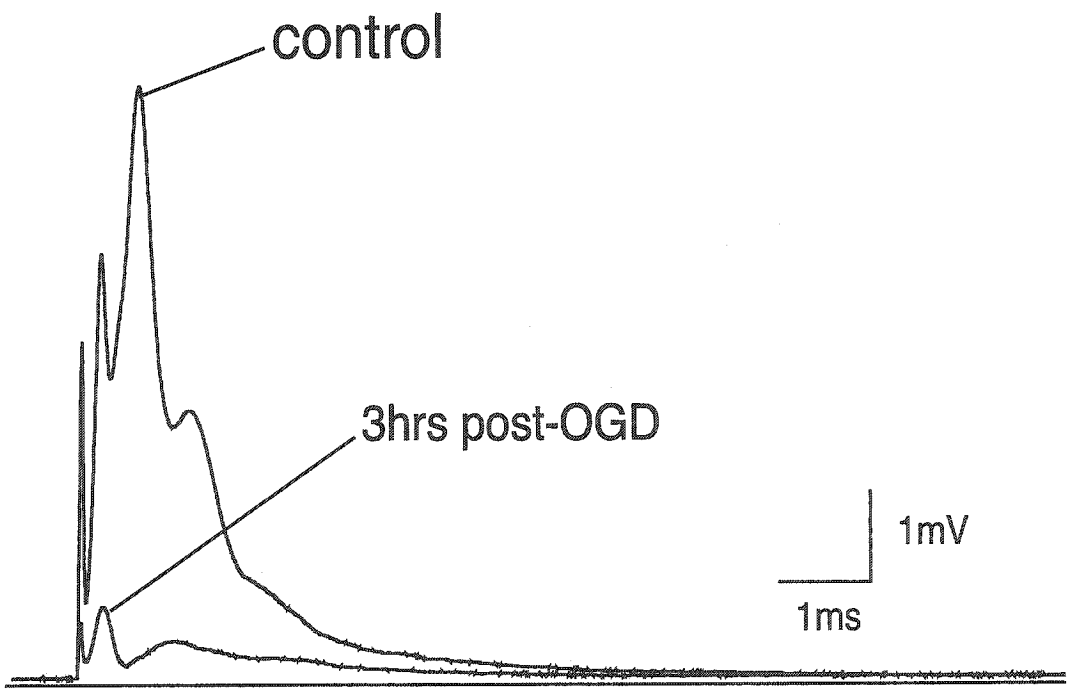

Figure 4.6 Effect of Na^+-channel blockers on CAP recovery during either anoxia or OGD. (A) TTX 100nM, significantly improved recovery. A 1hr preanoxic application abolished CAP. TTX was then continued for 30min after anoxic insult of 60min. CAP area recovered to 75±12% ($p<0.001$, $n=12$) of control at the 3hr post-anoxia mark. (B) A 30min pre-OGD application was continued for another 30min after a 60min OGD insult. CAP area recovered significantly to 56±4% in comparison to OGD alone (8±3%, $p<0.001$, $n=3$).

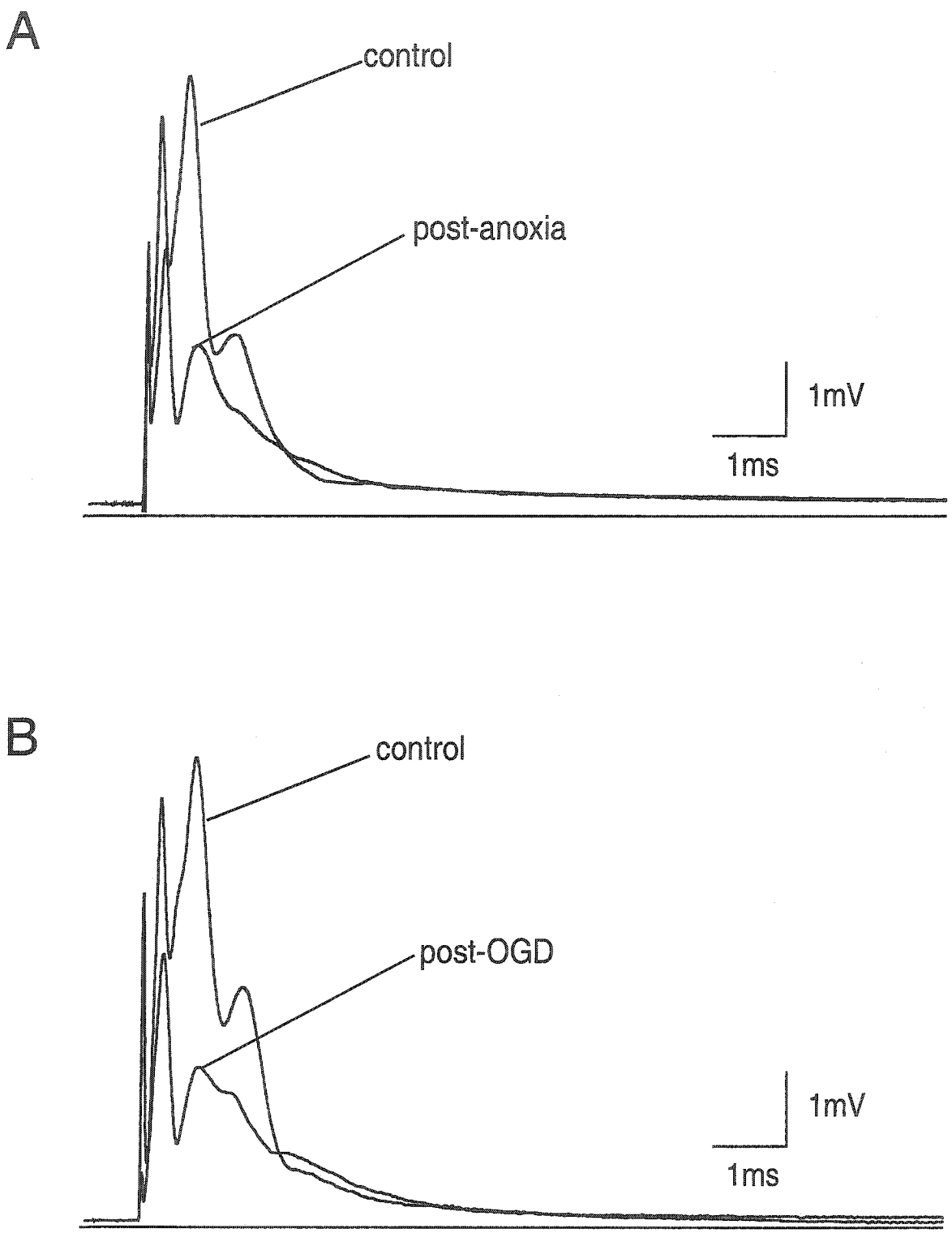
A
control
post-anoxia
1mV
1ms
B
control
post-OGD
1mV
1ms

Figure 4.7 Effect on Anion transport blockade on compound action potential during *in vitro* anoxia. (**A**) DIDS 500μM applied for 1hr during normoxic conditions and continued up to 30min post anoxia, caused a severe depression of CAP after normoxic perfusion. Furthermore, CAP recovered t o 6±5% compared to 24±13% at 2hr post mark ($p<0.001$ vs anoxia, n=8). Such an effect is presumably due to the interaction of DIDS with Na^+-channel (Liu *et al.* 1998). (**B**) Furosemide 10μM, applied for 1hr and also continued up to 30min post anoxia, had no effect on normoxic CAP while causing a recovery of 40±4% at 3hr post ($p<0.01$ vs anoxia , n=8). This suggests that KCC plays a role anoxic injury as assessed by CAP. (**C**) Effect of combined Na^+-channel and K-Cl cotransport blockade on the compound action potential of the rat optic nerve during anoxia. TTX 100nM and Furosemide 10μM was more protective than either agent alone (TTX+furosemide 91±8% vs 74±12% TTX alone; $p<0.001$; n=11). In addition, CAP shape was normalized to normoxic levels since fidelity index for normoxia and TTX+Furosemide when analyzed statistically was not significant.

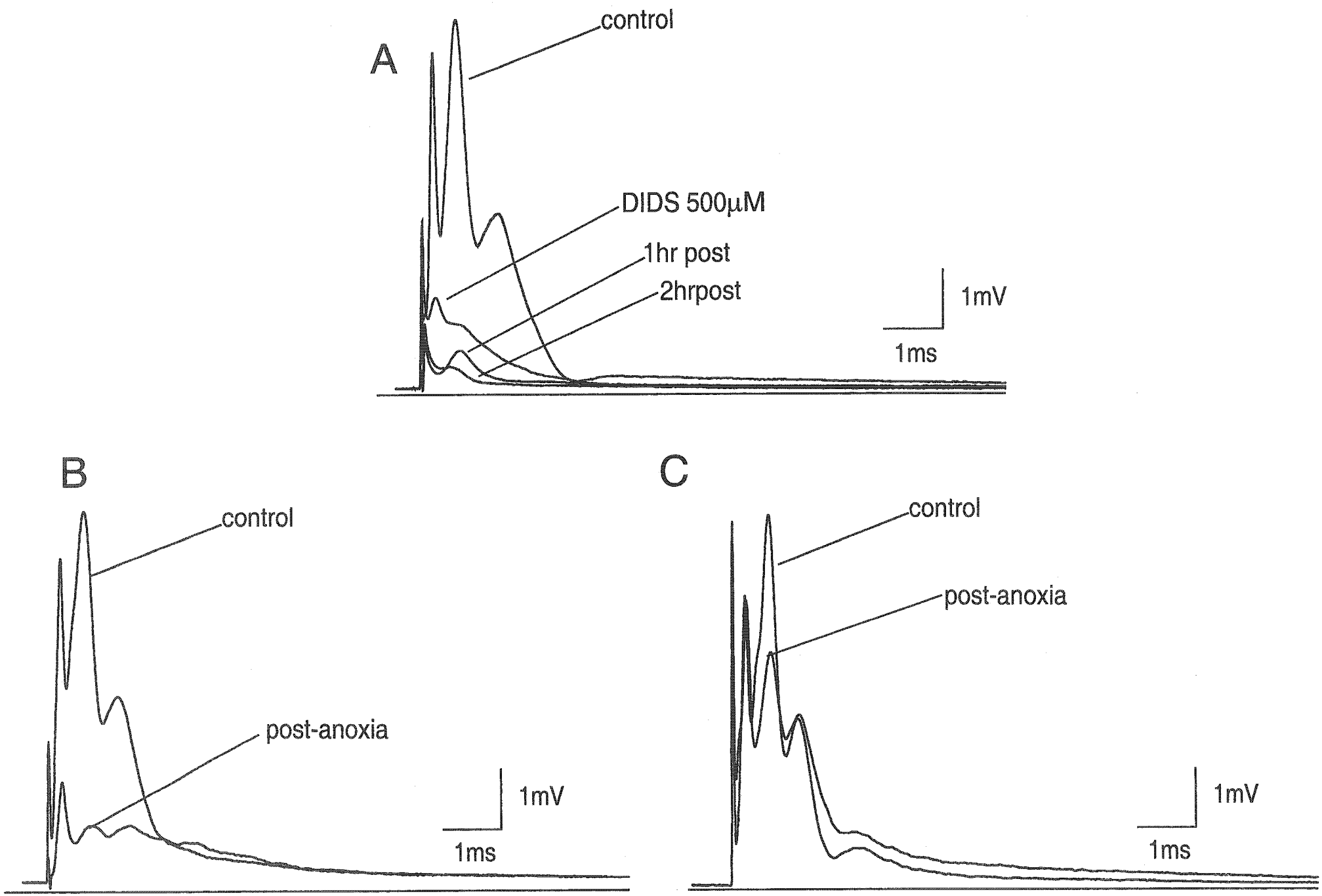
A
control
DIDS 500μM
1hr post
2hrpost
1mV
1ms
B
control
post-anoxia
1mV
1ms
C
control
post-anoxia
1mV
1ms

Figure 4.8 Evaluation of Ca^{2+}-activated Cl^- channel during *in vitro* anoxia and ischemia. (**A**) Niflumic acid 50μM (NFA) caused a statistically insignificant depression of normoxic CAP when perfused for 1hr. Even at 3hr post anoxia, NFA 50μM allowed for deterioration of CAP recovery to values lower than those with anoxia alone (6.0±0.7% vs 26±6% at 3hrs post, $p<0.01$, $n=6$). (**B**) Similarly post OGD, the recovery worsened to 3±1% vs 8±3% at 3hr ($p<0.05$, $n=3$). Taken together these results promote the idea that Ca^{2+}-activated Cl^- channels act as an imperative auto protective mechanism allowing volume modulation, via Cl^- efflux as dictated by V_m, during anoxic/ischemic conditions.

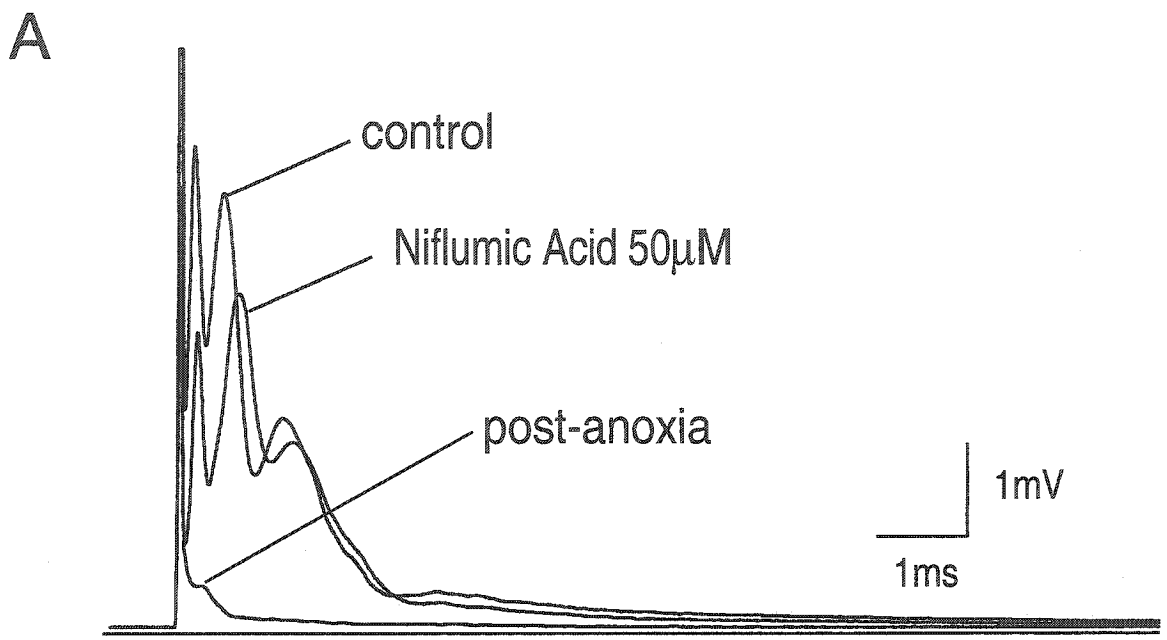
A
control
Niflumic Acid 50μM
post-anoxia
1mV
1ms

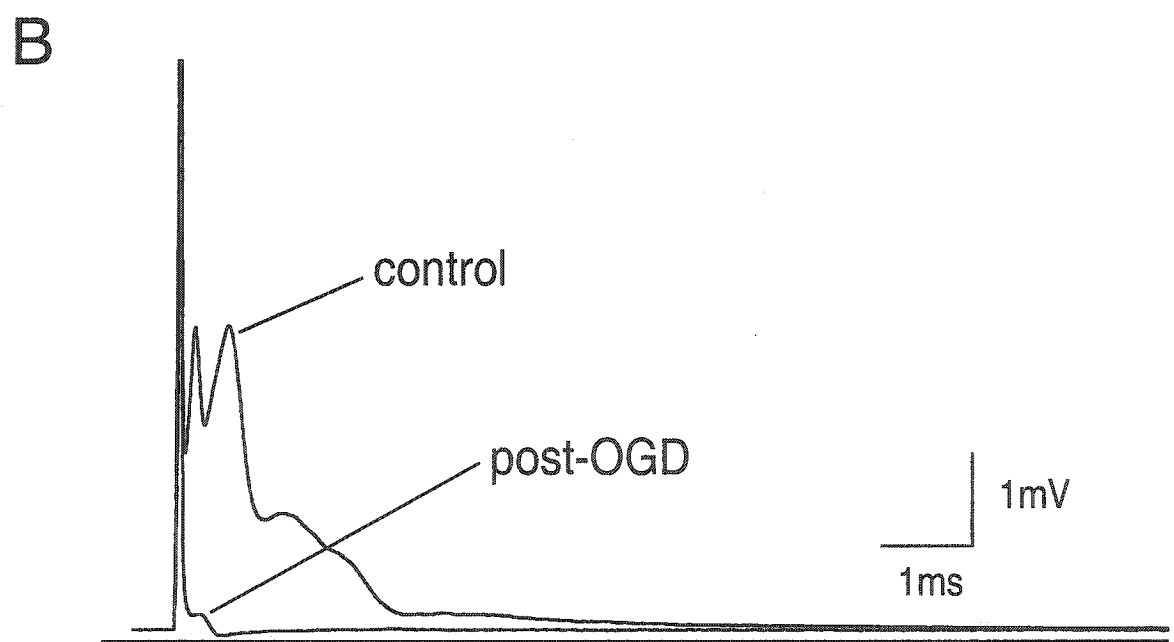
B
control
post-OGD
1mV
1ms

Figure 4.9 Quantitative effects of different pharmacological manipulations on CAP of RON. Error bars denote standard deviation. (Normoxia) TTX 100nM caused a reversible depression of CAP as seen by the wash timeline. Neither furosemide 10μM nor NFA 50μM had any effect on CAP during normoxia. (Anoxia) A marked improvement of CAP was seen with TTX 100nM perfusion with a maximum recovery of 74±12% at 3hr post . KCC blockade , allowed for 40±4% recovery vs 26±6% with anoxia ($p<0.01$). This reflects the aberrant activity of the transporter during anoxia. DIDS 500μM, on the other hand, due to its nonspecficity caused depression of the CAP during normoxic application (16±17%). At the 2hr post mark, the CAP recovered partially to only 6±5% which is far below the value observed with anoxia alone at this time point (23±13%, $p<0.001$, n=8). The combination of Na^+-channel and KCC blockade was the most effective manipulation in producing maximal recovery of CAP following anoxia (91±9% vs 74±12% TTX alone, $p<0.001$, n=11). On the other hand, Ca^{2+}-activated Cl^--channel blockade caused a deterioration of the CAP with a recovery of 5±2%, 5±2% and 6.0±0.9% at 1,2,3hr post anoxia ($p<0.01$, n=6 at 3hr post vs anoxia). (OGD) Under this paradigm, only 8±3% of control CAP area was rescued when measured at 3hr post mark (n=9). As with anoxia, a robust recovery was seen with Na^+-channel blockade with TTX100nM (56±4% vs 8±3% 3hr post, $p<0.01$, n=3). Similarly, KCC inhibition through furosemide 10μM, recovered 20±14% of control CAP area measured at 3hr post OGD ($p<0.05$, n=9). Thus it seems that KCC, during anoxic/ischemic conditions, operates in an injury causing mode by presumably allowing increase in Cl_i which will impact cellular volume. The compensatory process for this rise is the opening of $Cl^-_{Ca}{}^{2+}$ and the subsequent activation of an I_{Cl-} outward as dictated by differences in E_{Cl-} and V_m with the latter being more positive than E_{Cl-} . Therefore blockade of such channels will cause more injury to the tissue as evident from the CAP area recovery measurements (3±1% 3hr post vs 8±3%, $p<0.05$, n=3). Combining Na^+-channel and KCC blockade (TTX 100nM +Furosemide 10μM) under this paradigm was not as effective in improving CAP area recovery over and above levels seen with TTX alone (50±19% , n=14). (*$p<0.05$,**$p<0.01$, *** $p<0.001$)

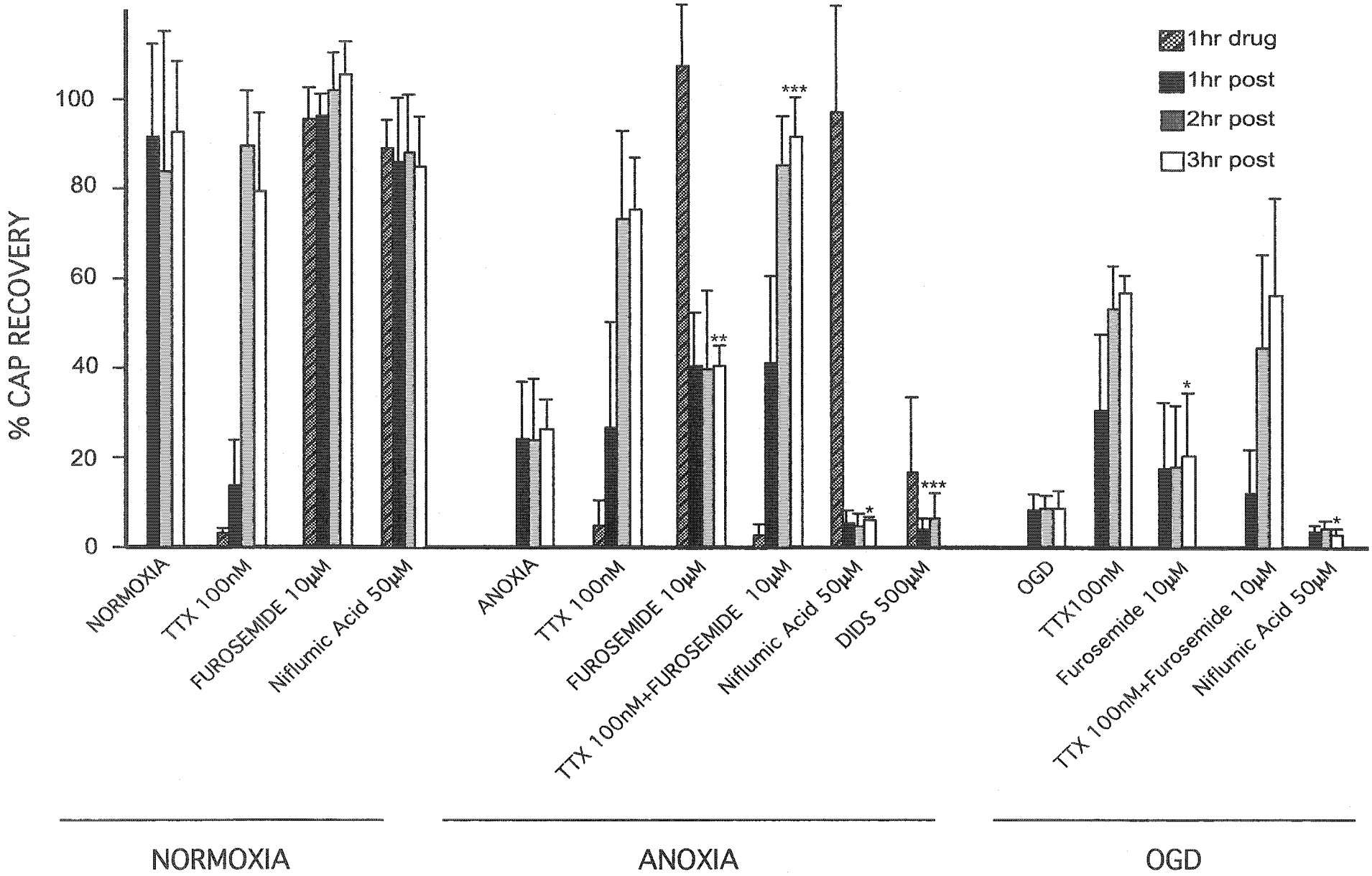
% CAP RECOVERY
0
20
40
60
80
100
1hr drug
1hr post
2hr post
3hr post
NORMOXIA
TTX 100nM
FUROSEMIDE 10µM
Niflumic Acid 50µM
ANOXIA
TTX 100nM
FUROSEMIDE 10µM
TTX 100nM+FUROSEMIDE 10µM
Niflumic Acid 50µM
DIDS 500µM
OGD
TTX100nM
Furosemide 10µM
TTX 100nM+Furosemide 10µM
Niflumic Acid 50µM
*
**
***
NORMOXIA
ANOXIA
OGD

Figure 4.10 Panels **A, B, C, D** show representative tracings **(NORMALIZED WITH RESPECT TO CAP AREA)**, of normoxic, untreated anoxic, post-anoxic/washed nerves treated with TTX 100nM, and TTX+furosemide 10μM respectively. As expected with normoxia there is very little change in the waveshape over time. However, with anoxia/reoxygenation, the waveshape becomes very distorted. TTX results in a significant recovery of CAP area, but the waveshapes (particularly latencies of the slower peaks), remained significantly distorted. With addition of furosemide, a relatively specific blocker of the K-Cl cotransporter, the waveform shape is further improved, and the fidelity index is not different than time-matched normoxic controls (P=0.20). The peak latencies of the pre-anoxic and post-anoxic waves now coincide, indicating a return of not only the number of fibers able to conduct, but also normalization of the conduction velocities of constituent fibers **(E)** Summary of waveshape fidelity indices. Error bars denote standard deviation .The lowest index was obtained with time-matched normoxic controls indicating little change in waveshape. While TTX provided a robust recovery of CAP area, the waveshape remains noticeably distorted (prolonged peak 2 latency, absence of peak 3), reflected by an index not much smaller than what was calculated for anoxic nerves alone (without TTX). In contrast, furosemide not only improved CAP area recovery, but substantially improved waveshapes as well, reducing the mean index to a value not different from *normoxic* controls. Niflumic acid, by worsening the CAP area recovery, not surprisingly increased waveshape distortion as well. (*$p<0.05$,**$p<0.01$)

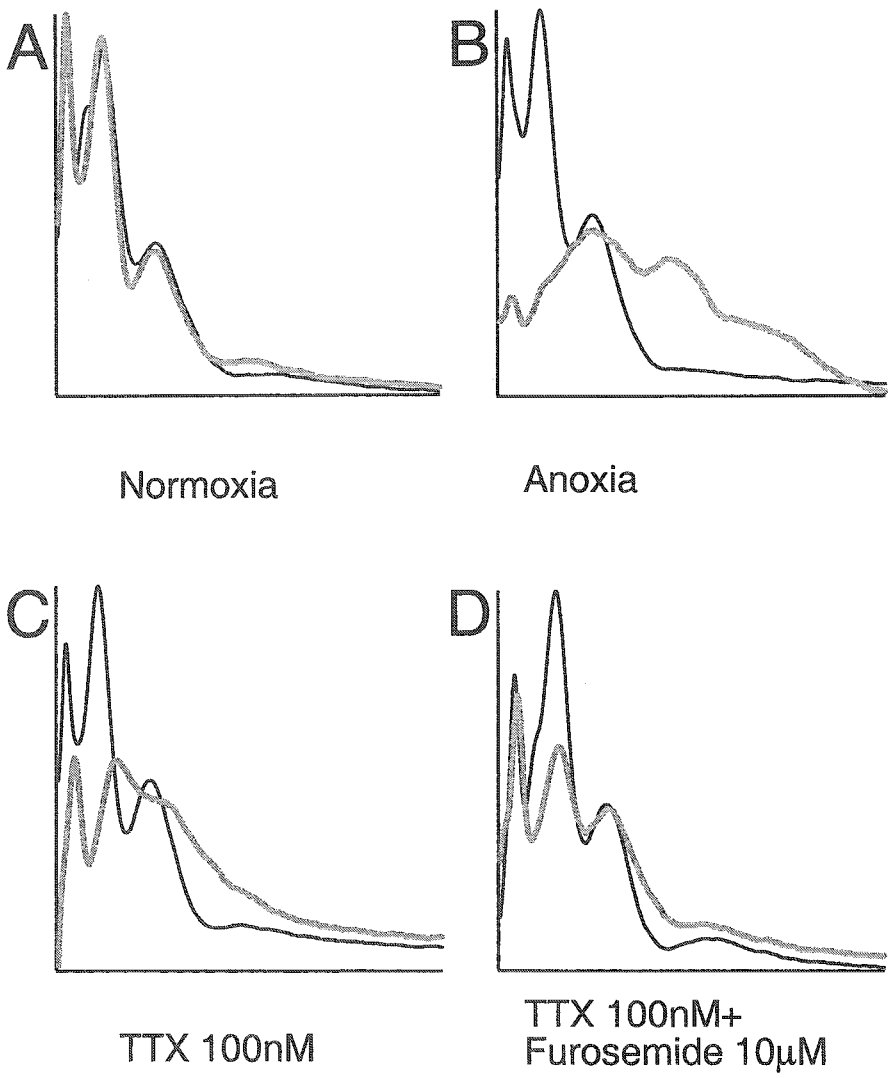
A
B
Normoxia
Anoxia
C
D
TTX 100nM
TTX 100nM+
Furosemide 10μM

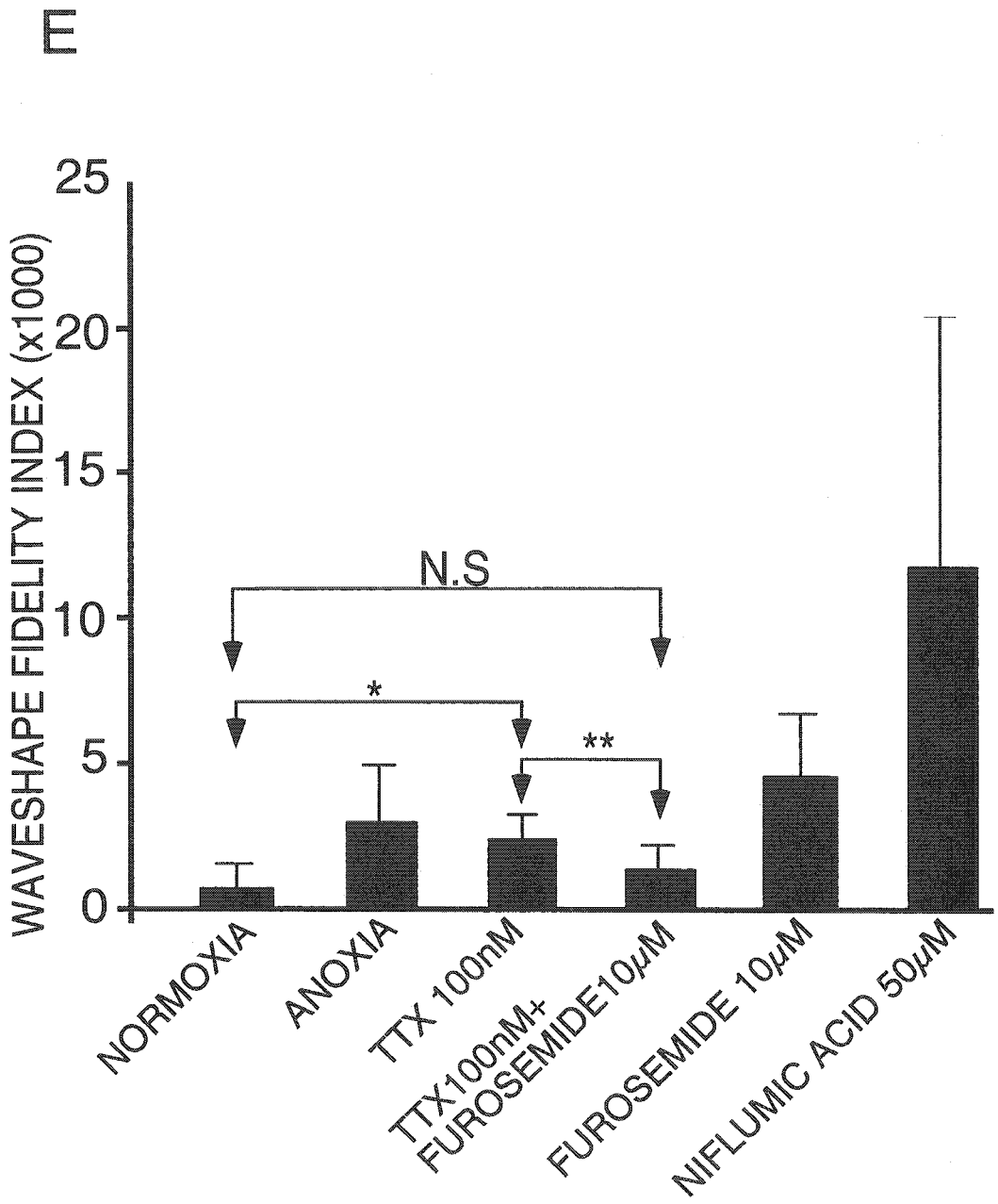
E
WAVESHAPE FIDELITY INDEX (x1000)
25
20
15
10
5
0
N.S
*
**
NORMOXIA
ANOXIA
TTX 100nM
TTX100nM+
FUROSEMIDE10μM
FUROSEMIDE 10μM
NIFLUMIC ACID 50μM

Figure 4.11 Immunohistochemical localization of different KCC isoforms in rat optic nerve. Laser scanning confocal micrographs showing immunohistochemical localization of different KCC isoforms (green) in rat optic nerve (axons stained with NF160 in red). A, B: There was strong KCC3a signal in astrocytes, and occasional signal in the myelin of larger axons (inset, arrowhead). C, D: Less intense but reproducible, often punctate, KCC3 signal was observed in the myelin sheath of larger axons. Because all axons are myelinated in mature optic nerve, fluorescence immediately adjacent to axon cylinders as seen here is consistently localized to the sheath rather than glial processes. E: KCC2 was clearly present in cell bodies of oligodendrocytes (arrows), and also diffusely in the optic nerve, including signal within axon cylinders (appearing as a more orangy hue due to colocalization with red NF160 signal; compare with a more pure red neurofilament signal in the other panels). F: controls with 1° antisera omitted were clean.

KCC3a + NF160
KCC3 + NF160
KCC2 + NF160
A
B
C
D
E
F
10 μm
2 μm
10 μm
5 μm
5 μm
10 μm
No primary control

Figure 4.12 Mathematical model depicting KCC and NKCC activity during normoxia and anoxia. Graph shows calculated theoretical Cl- equilibrium concentrations that would be achieved by the KCC and Na-K-2Cl co-transport (NKCC) as a function of axoplasmic [K+] under various conditions. Arrows highlight values, which have been experimentally measured by Stys *et al.* (1997). The theoretical values were based upon previous work by Alvarez-Leefmans (1990). In normal axons, the high transmembrane K+ gradient favors a low $[Cl^-]_i$ maintained by KCC, and approximately 55 mM Cl^- by NKCC (solid arrows). During anoxia, with collapse of the K^+ gradient, both KCC and NKCC will attempt to import Cl^- to very high concentrations (double solid arrow). Anoxia in the presence of TTX sees residual K^+_i concentrated back up to ≈55 mM because of water loss, thereby maintaining the KCC in a Cl^- efflux mode (open arrow). Bottom panels illustrate hypothetical Cl^- fluxes in anoxic optic nerve axons under various conditions. i) In normal axons, an equilibrium between Cl^- efflux (KCC and various Cl^- channels) and influx (NKCC) maintains $[Cl^-]$ above what would be expected from passive distribution. ii) The collapse of the K^+ gradient during anoxia will drive the KCC to accumulate Cl^-, which is largely compensated for by activation of Cl^- channels; blocking these with niflumic acid worsens outcome (see Results). Na^+ and K^+ exchange across the axolemma in an electroneutral manner through various channels. The drop in ATP levels may reduce NKCC activity. iii) Blocking Na^+ influx into anoxic axons with TTX prevents Na^+ from entering; instead electroneutrality is maintained by Cl^- egress, through KCC (the loss of water concentrates axoplasmic Na such that KCC remains biased in the Cl^--efflux direction [open arrow, graph]) and Cl^- channels (Cl^- is also concentrated such that ECl remains much more positive than the resting membrane potential favoring Cl^- loss) resulting in shrinkage and mechanical disruption. iv) Addition of furosemide to block KCC reduces Cl^- loss and tissue damage, possibly by helping preserve volume and mechanical integrity. Anoxic depolarization is also reduced perhaps by decreasing K^+ loss because of the lower capacity for electroneutral co-efflux of Cl^- anions

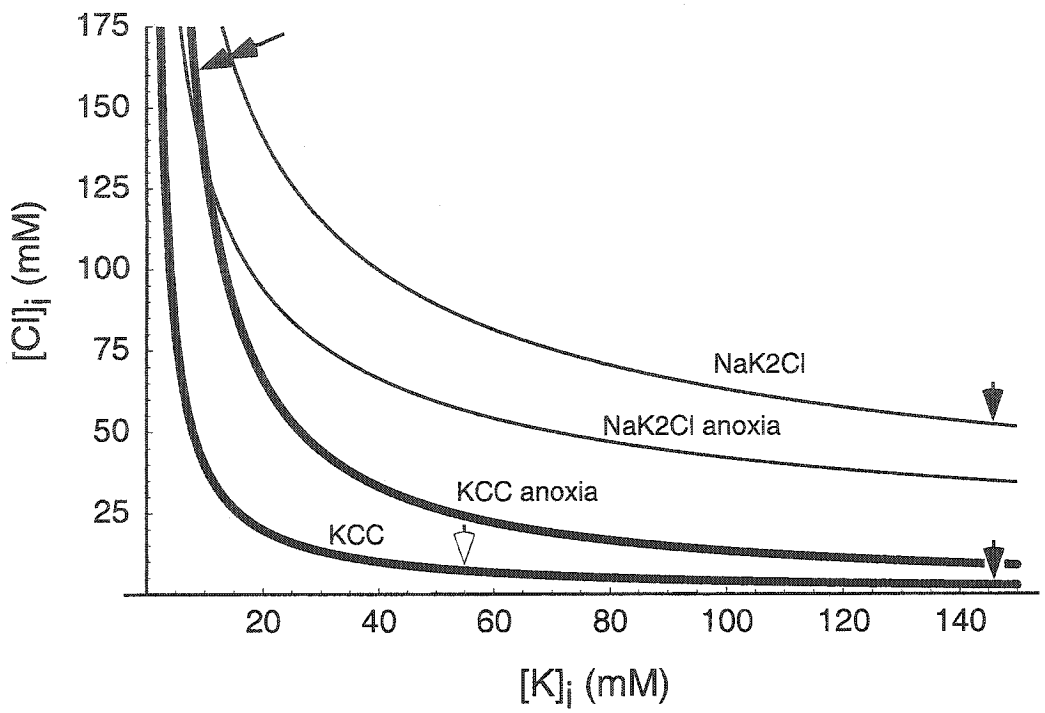
175
150
125
100
75
50
25
$[Cl]_i$ (mM)
NaK2Cl
NaK2Cl anoxia
KCC anoxia
KCC
20
40
60
80
100
120
140
$[K]_i$ (mM)

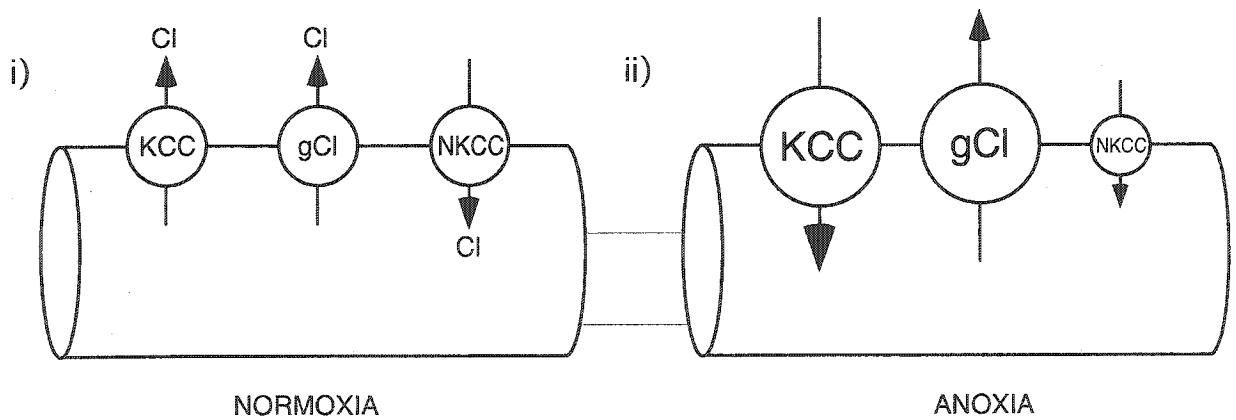
i)
Cl
Cl
KCC
gCl
NKCC
Cl
NORMOXIA
ii)
KCC
gCl
NKCC
ANOXIA

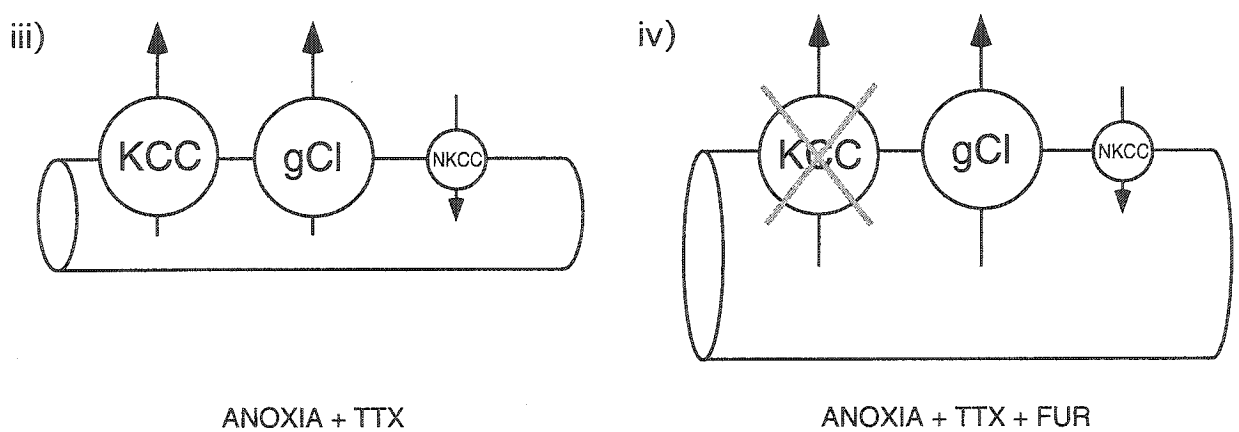
iii)
KCC
gCl
NKCC
ANOXIA + TTX
iv)
KCC
gCl
NKCC
ANOXIA + TTX + FUR

CHAPTER 5

GENERAL DISCUSSION

5.1 General Summary

5.1.1 Summary of Findings

Stroke is 4th leading cause of death in Canada, with an incidence of 40-50 thousand strokes in Canada/yr and about 300,000 are living with its effects. This in turn costs the Canadian economy $2.7 billion/yr with average acute care costs $30,000/stroke. Our interest was the study of ionic events occurring during white matter injury with a primary focus on anion transport in the context of either Na-K-ATPase inhibition alone or anoxia/ischemia. To answer the question regarding Cl^- activity in white matter injury, we used:

The Grease Gap technique allowed us to elucidate mechanisms with effects on V_m. We were able to measure a stable fraction of the true compound V_m in the rat optic nerve at 37°C for several hours. Prolonged stability of the readings allowed us to conclude that effects of pharmacological manipulations on V_m were authentic.

Dependence of the V_m on the Na-K-ATPase activity was demonstrated by the abrupt depolarization seen with ouabain application. Equally as important was the effect of chemical anoxia causing a severe loss of V_m. Consequently, blunting of both depolarizations with TTX, underscores the importance of Na^+-channel blockers in attenuating V_m decay. However a dichotomy was created upon anion transport analysis. Broad spectrum Cl^- transport blocker, DIDS, was unsuccessful by itself in blunting V_m loss during chemical anoxia. Nevertheless, when combined with TTX, almost complete maintenance was observed during chemical anoxia but less effective during Na-K-ATPase inhibition. Hence, DIDS alone was unable to reduce anoxia-induced depolarization by itself probably because it was masked by the TTX-sensitive pathway. In fact when Na^+-channels were blocked by TTX, DIDS blocked the observed residual depolarization. Further experiments with more relatively specific blockers established KCC as the main pathway responsible for the residual depolarization observed during

Na^+-channel blockade/chemical anoxia as Furosemide mimicked the effect of DIDS during chemical anoxia in presence of TTX.

Compound Action Potential recordings were used to assess the functionality of the RON. In this case, KCC blockade alone was sufficient to improve CAP area recovery following 1hr anoxic insult to levels over those seen without the drug. This suggests that KCC were activated during anoxia despite the fact that we did not observe any effect on V_m during chemical anoxia in presence of either DIDS or Furosemide alone. Yet unexpectedly, blockade of Cl^- channels by NFA, be it Ca^{2+}, volume or voltage activated worsened the recovery of the RON.

Based on our mathematical model, we were able to reconcile the previous outlined data through the following explanation. Anoxic conditions dictates that KCC produces Cl^-_i accumulation because of K^+_o increases. Cl^-_i levels have been shown to be remain unchanged during anoxia and hence we proposed that a Cl^- channel opens inorder to counteract this accumulation. The precise trigger for channel opening was not determined that is be it volume changes or increases in Ca^{2+}_i.

Co-blockade of Na^+-channels and KCC during anoxia provided the best strategy for total CAP area and waveshape recovery. In fact levels were comparable to those recorded prior to insult administration and the CAP latencies were well maintained with this drug combination. The CAP area reflects to a large extent the integrity and functionality of the axon, while the shape and latency are indicators for the preservation of the axo-glial interaction.

5.1.2 Implications for Drug Development

The ultimate implication of our study is the suggestion that concomitant anion transport blockade (specifically KCC inhibition), together with another neuroprotectant (such as a Na channel blocker in our case) may be more beneficial than either alone in *in vivo* stroke and neurotrauma. Furosemide as a drug has been prescribed as a loop diuretic and thus its human toxicity profile is well established. Yet at the present time, there is a lack of data concerning its efficacy in *in vivo* models of stroke. The field examining the deleterious effects of Cl^- during anoxia/ischemia in white matter is still at its infancy, with more questions to be posed for future studies.

5.2 Conclusion

Na^+ and K^+ gradient run down is a hallmark of anoxic/ischemic cellular injury and Na-K-ATPase blockade. However, we suggest that only during anoxia, concomitant blockade of voltage-gated Na^+ channels together with K-Cl co-efflux pathway, which likely proceeds at least partially through KCC, will allow for better retention of ionic gradients and membrane polarization. The added result of presumed normalization of $[Cl^-]_i$ produced not only a robust recovery of the CAP area, but significantly improved waveshape; the latter could be attributed to protection of glia whose volume changes affect axon-myelin connectivity and ultimately influence conduction velocities. These findings may have implications for the design of neuroprotective strategies, whereby concomitant inhibition of Na^+ channels and KCC could result in better outcome than with blockade of either pathway alone.

5.3 Future Considerations

To this point we have established the role of only a few Cl^- transport pathways activated during anoxia/ischemia. Yet, there are still unanswered questions concerning this phenomenon and it is vital to address them possibly through the following experiments.

5.3.1 Future Directions:Volume vs pH

The complexity of anion and specifically Cl^- transport is inherent in the homeostatic mechanisms modulated by this ion, which are volume and pH. We did not address the question of volume shifts quantitatively, but we only speculated on the possible mechanisms. A specialized study of this phenomenon in white matter has to be undertaken. The primary experiment to be conducted is the effect of Cl^- replacement on cellular volume during normoxia and the injury, either glycolytic inhibition, anoxia, ischemia. Subsequently this will provide the basis to further study the specific pathways mediating volume changes and to quantify these effects. Nevertheless, our system is complicated by the presence of extra-neuronal compartments such as astrocytes, oligodendrocytes and myelin and their effects during volume changes cannot be neglected. One approach is to eliminate axonal effects and study these elements in

isolation through the use of enucleate optic nerves. The other important Cl^- sensitive mechanism is pH regulation.

Cl^-/HCO^-_3 exchanger presents a potential anion transport pathway for study. There is currently no specific pharmacology to isolate this transporter. Nevertheless, one can still study the protein within the context of pH_i-modulation through Cl^- mediated transport. Future experiments should address the issue of pH-shifts in white matter tracts pertaining to the different injury paradigms of glycolytic inhibition, anoxia and ischemia.

5.3.2 Advanced Techniques

With the improvement in optical imaging techniques in terms of ionic dyes and microscopy, it would be of interest to re-examine the proposed hypothesis using fluorescence Cl_i-imaging (Sah and Schwartz-Bloom 1999). Changes in dye fluorescence will certainly strengthen our findings and improve our understanding through direct real-time observation of Cl^- changes in various cells of white matter.

Another approach worth considering is the Electron Probe Microanalysis for Cl^- in different injury models and using a number of blockers to assess the shifts occurring at the different cellular compartments, that is either axon, oligodendrocyte/myelin or astrocytes, and which specific condition. These experiments will lay the foundation for studying other pertinent Cl^- pathways, besides the ones mentioned in this study.

References

Agrawal SK,Fehlings MG (1996). Mechanisms of secondary injury to spinal cord axons in vitro: role of Na+, Na(+)-K(+)-ATPase, the Na(+)-H+ exchanger, and the Na(+)-Ca2+ exchanger. *J Neurosci* 16(2): 545-52.

Alvarez-Leefmans F.J. (1990) Intracellular Cl^- regulation and synaptic inhibition in vertebrate and invertebrate neurons. In: Chloride channels and carriers of nerve, muscle and glial cells. (eds FJ Alvarez-Leefmans and J.M. Russell)New York: Plenum; p.109-58.

Alvarez-Leefmans FJ, Gamino SM, Giraldez F,Nogueron I (1988). Intracellular chloride regulation in amphibian dorsal root ganglion neurones studied with ion-selective microelectrodes. *J Physiol* 406: 225-46.

Alvarez-Leefmans FJ, Leon-Olea M, Mendoza-Sotelo J, Alvarez FJ, Anton B,Garduno R (2001). Immunolocalization of the Na(+)-K(+)-2Cl(-) cotransporter in peripheral nervous tissue of vertebrates. *Neuroscience* 104(2): 569-82.

Ariyasu RG,Ellisman MH (1987). The distribution of (Na+ + K+)ATPase is continuous along the axolemma of unensheathed axons from spinal roots of 'dystrophic' mice. *J Neurocytol* 16(2): 239-48.

Ayar A,Scott RH (1999). The actions of ryanodine on Ca2+-activated conductances in rat cultured DRG neurones; evidence for Ca2+-induced Ca2+ release. *Naunyn Schmiedebergs Arch Pharmacol* 359(2): 81-91.

Baker M, Bostock H, Grafe P,Martius P (1987). Function and distribution of three types of rectifying channel in rat spinal root myelinated axons. *J Physiol* 383: 45-67.

Ballanyi K,Grafe P (1985). An intracellular analysis of gamma-aminobutyric-acid-associated ion movements in rat sympathetic neurones. *J Physiol* 365: 41-58.

Barr L, Berger W. (1969) Use of rubber membranes to improve sucrose-gap and other electrical recording techniques. J. Appl. Physiol.; 26(3):378-382.

Black JA, Sontheimer H, Oh Y, Waxman SG (1995) The Oligodendrocyte, the perinodal astrocyte, and the central node of Ranvier. In: The Axon (eds SG Waxman, JD Kocsis, PK Stys) Oxford University Press, New York p.116-43.

Ben-Ari Y, Tseeb V, Raggozzino D, Khazipov R,Gaiarsa JL (1994). gamma-Aminobutyric acid (GABA): a fast excitatory transmitter which may regulate the development of hippocampal neurones in early postnatal life. *Prog Brain Res* 102: 261-73.

Birch BD, Kocsis JD, Di Gregorio F, Bhisitkul RB,Waxman SG (1991). A voltage- and time-dependent rectification in rat dorsal spinal root axons. *J Neurophysiol* 66(3): 719-28.

Black JA, Foster RE,Waxman SG (1982). Rat optic nerve: freeze-fracture studies during development of myelinated axons. *Brain Res* 250(1): 1-20.

Bormann J,Kettenmann H (1988). Patch-clamp study of gamma-aminobutyric acid receptor Cl- channels in cultured astrocytes. *Proc Natl Acad Sci U S A* 85(23): 9336-40.

Boron WF,De Weer P (1976). Intracellular pH transients in squid giant axons caused by CO2, NH3, and metabolic inhibitors. *J Gen Physiol* 67(1): 91-112.

Boron WF,Knakal RC (1989). Intracellular pH-regulating mechanism of the squid axon. Interaction between DNDS and extracellular Na+ and HCO3. *J Gen Physiol* 93(1): 123-50.

Boron WF,Russell JM (1983). Stoichiometry and ion dependencies of the intracellular-pH-regulating mechanism in squid giant axons. *J Gen Physiol* 81(3): 373-99.

Bowe CM, Kocsis JD,Waxman SG (1985). Differences between mammalian ventral and dorsal spinal roots in response to blockade of potassium channels during maturation. *Proc R Soc Lond B Biol Sci* 224(1236): 355-66.

Bowes MP, Swanson S,Zivin JA (1996). The AMPA antagonist LY293558 improves functional neurological outcome following reversible spinal cord ischemia in rabbits. *J Cereb Blood Flow Metab* 16(5): 967-72.

Breitwieser GE, Altamirano AA,Russell JM (1990). Osmotic stimulation of Na(+)-K(+)-Cl- cotransport in squid giant axon is [Cl-]i dependent. *Am J Physiol* 258(4 Pt 1): C749-53.

Brines ML, Dare AO,de Lanerolle NC (1995). The cardiac glycoside ouabain potentiates excitotoxic injury of adult neurons in rat hippocampus. *Neurosci Lett* 191(3): 145-8.

Brown AM, Westenbroek RE, Catterall WA,Ransom BR (2001). Axonal L-type Ca2+ channels and anoxic injury in rat CNS white matter. *J Neurophysiol* 85(2): 900-11.

Cabantchik ZI,Greger R (1992). Chemical probes for anion transporters of mammalian cell membranes. *Am J Physiol* 262(4 Pt 1): C803-27.

Cala PM. (1990) Principles of cell volume regulation: Ion flux pathways and the roles of Anions . In: Chloride channels and carriers of nerve, muscle and glial cells. (eds FJ Alvarez-Leefmans and J.M. Russell)New York: Plenum; p.67-81

Cherubini E, Gaiarsa JL,Ben-Ari Y (1991). GABA: an excitatory transmitter in early postnatal life. *Trends Neurosci* 14(12): 515-9.

Chesnoy-Marchais D (1983). Characterization of a chloride conductance activated by hyperpolarization in Aplysia neurones. *J Physiol* 342: 277-308.

Chiu SY,Ritchie JM (1980). Potassium channels in nodal and internodal axonal membrane of mammalian myelinated fibres. *Nature* 284(5752): 170-1.

Chiu SY,Ritchie JM (1981). Evidence for the presence of potassium channels in the paranodal region of acutely demyelinated mammalian single nerve fibres. *J Physiol* 313: 415-37.

Choi DW, Koh JY,Peters S (1988). Pharmacology of glutamate neurotoxicity in cortical cell culture: attenuation by NMDA antagonists. *J Neurosci* 8(1): 185-96.

Clark S, Jordt SE, Jentsch TJ,Mathie A (1998). Characterization of the hyperpolarization-activated chloride current in dissociated rat sympathetic neurons. *J Physiol* 506 (Pt 3): 665-78.

Connors BW,Ransom BR (1984). Chloride conductance and extracellular potassium concentration interact to modify the excitability of rat optic nerve fibres. *J Physiol* 355: 619-33.

Cummins TR, Donnelly DF,Haddad GG (1991). Effect of metabolic inhibition on the excitability of isolated hippocampal CA1 neurons: developmental aspects. *J Neurophysiol* 66(5): 1471-82.

Currie KP, Wootton JF,Scott RH (1995). Activation of Ca(2+)-dependent Cl- currents in cultured rat sensory neurones by flash photolysis of DM-nitrophen. *J Physiol* 482 (Pt 2): 291-307.

De Juan J, Cuenca N, Iniguez C,Fernandez E (1992). Axon types classified by morphometric and multivariate analysis in the rat optic nerve. *Brain Res* 585(1-2): 431-4.

De Weer P,Geduldig D (1973). Electrogenic sodium pump in squid giant axon. *Science* 179(80): 1326-8.

Delpire E, Rauchman MI, Beier DR, Hebert SC,Gullans SR (1994). Molecular cloning and chromosome localization of a putative basolateral Na(+)-K(+)-2Cl- cotransporter from mouse inner medullary collecting duct (mIMCD-3) cells. *J Biol Chem* 269(41): 25677-83.

Dichter MA,Fischbach GD (1977). The action potential of chick dorsal root ganglion neurones maintained in cell culture. *J Physiol* 267(2): 281-98.

Dick GM, Kong ID,Sanders KM (1999). Effects of anion channel antagonists in canine colonic myocytes: comparative pharmacology of Cl-, Ca2+ and K+ currents. *Br J Pharmacol* 127(8): 1819-31.

Dinudom A, Young JA,Cook DI (1993). Na+ and Cl- conductances are controlled by cytosolic Cl- concentration in the intralobular duct cells of mouse mandibular glands. *J Membr Biol* 135(3): 289-95.

Doroshenko P (1999). High intracellular chloride delays the activation of the volume-sensitive chloride conductance in mouse L-fibroblasts. *J Physiol* 514 (Pt 2): 437-46.

Dringen R,Hamprecht B (1992). Glucose, insulin, and insulin-like growth factor I regulate the glycogen content of astroglia-rich primary cultures. *J Neurochem* 58(2): 511-7.

Duchen MR (1990). Effects of metabolic inhibition on the membrane properties of isolated mouse primary sensory neurones. *J Physiol* 424: 387-409.

Duchen MR, Valdeolmillos M, O'Neill SC,Eisner DA (1990). Effects of metabolic blockade on the regulation of intracellular calcium in dissociated mouse sensory neurones. *J Physiol* 424: 411-26.

Dyer CA,Benjamins JA (1990). Glycolipids and transmembrane signaling: antibodies to galactocerebroside cause an influx of calcium in oligodendrocytes. *J Cell Biol* 111(2): 625-33.

Eng DL, Gordon TR, Kocsis JD,Waxman SG (1990). Current-clamp analysis of a time-dependent rectification in rat optic nerve. *J Physiol* 421: 185-202.

Erecinska M,Silver IA (1989). ATP and brain function. *J Cereb Blood Flow Metab* 9(1): 2-19.

Erecinska M,Silver IA (1994). Ions and energy in mammalian brain. *Prog Neurobiol* 43(1): 37-71.

Estevez AY, Bond T,Strange K (2001). Regulation of I(Cl,swell) in neuroblastoma cells by G protein signaling pathways. *Am J Physiol Cell Physiol* 281(1): C89-98.

Estevez AY, O'Regan MH, Song D,Phillis JW (1999). Effects of anion channel blockers on hyposmotically induced amino acid release from the in vivo rat cerebral cortex. *Neurochem Res* 24(3): 447-52.

Fern R, Ransom BR, Stys PK,Waxman SG (1993). Pharmacological protection of CNS white matter during anoxia: actions of phenytoin, carbamazepine and diazepam. *J Pharmacol Exp Ther* 266(3): 1549-55.

Fern R, Ransom BR,Waxman SG (1995). Voltage-gated calcium channels in CNS white matter: role in anoxic injury. *J Neurophysiol* 74(1): 369-77.

Ferroni S, Marchini C, Schubert P,Rapisarda C (1995). Two distinct inwardly rectifying conductances are expressed in long term dibutyryl-cyclic-AMP treated rat cultured cortical astrocytes. *FEBS Lett* 367(3): 319-25.

Firestein S,Shepherd GM (1995). Interaction of anionic and cationic currents leads to a voltage dependence in the odor response of olfactory receptor neurons. *J Neurophysiol* 73(2): 562-7.

Foster RE, Connors BW, Waxman SG (1982). Rat optic nerve: electrophysiological, pharmacological and anatomical studies during development. *Brain Res* 255(3): 371-86.

Frings S, Reuter D, Kleene SJ (2000). Neuronal Ca2+ -activated Cl- channels--homing in on an elusive channel species. *Prog Neurobiol* 60(3): 247-89.

Gallant PE (1988). Effects of the external ions and metabolic poisoning on the constriction of the squid giant axon after axotomy. *J Neurosci* 8(5): 1479-84.

Garthwaite G, Brown G, Batchelor AM, Goodwin DA, Garthwaite J (1999) Mechanisms of ischaemic damage to central white matter axons: a quantitative histological analysis using rat optic nerve. *Neuroscience* 94(4): 1219-30.

Genazzani AA, Empson RM,Galione A (1996). Unique inactivation properties of NAADP-sensitive Ca2+ release. *J Biol Chem* 271(20): 11599-602.

George EB, Glass JD,Griffin JW (1995). Axotomy-induced axonal degeneration is mediated by calcium influx through ion-specific channels. *J Neurosci* 15(10): 6445-52.

Gillen CM, Brill S, Payne JA,Forbush B, 3rd (1996). Molecular cloning and functional expression of the K-Cl cotransporter from rabbit, rat, and human. A new member of the cation-chloride cotransporter family. *J Biol Chem* 271(27): 16237-44.

Goldberg MP,Choi DW (1993). Combined oxygen and glucose deprivation in cortical cell culture: calcium-dependent and calcium-independent mechanisms of neuronal injury. *J Neurosci* 13(8): 3510-24.

Goldin AL (1999). Diversity of mammalian voltage-gated sodium channels. *Ann N Y Acad Sci* 868: 38-50.

Gordon TR, Kocsis JD,Waxman SG (1988). Evidence for the presence of two types of potassium channels in the rat optic nerve. *Brain Res* 447(1): 1-9.

Haun SE, Murphy EJ, Bates CM,Horrocks LA (1992). Extracellular calcium is a mediator of astroglial injury during combined glucose-oxygen deprivation. *Brain Res* 593(1): 45-50.

Hiki K, D'Andrea RJ, Furze J, Crawford J, Woollatt E, Sutherland GR, Vadas MA,Gamble JR (1999). Cloning, characterization, and chromosomal location of a novel human K+-Cl- cotransporter. *J Biol Chem* 274(15): 10661-7.

Hirano A (1968). A confirmation of the oligodendroglial origin of myelin in the adult rat. *J Cell Biol* 38(3): 637-40.

Hollmann M,Heinemann S (1994). Cloned glutamate receptors. *Annu Rev Neurosci* 17: 31-108.

Honmou O, Utzschneider DA, Rizzo MA, Bowe CM, Waxman SG,Kocsis JD (1994). Delayed depolarization and slow sodium currents in cutaneous afferents. *J Neurophysiol* 71(5): 1627-37.

Imaizumi T, Kocsis JD,Waxman SG (1997). Anoxic injury in the rat spinal cord: pharmacological evidence for multiple steps in Ca(2+)-dependent injury of the dorsal columns. *J Neurotrauma* 14(5): 299-311

Jarolimek W, Lewen A,Misgeld U (1999). A furosemide-sensitive K+-Cl- cotransporter counteracts intracellular Cl- accumulation and depletion in cultured rat midbrain neurons. *J Neurosci* 19(12): 4695-704.

Jentsch TJ, Stein V, Weinreich F,Zdebik AA (2002). Molecular structure and physiological function of chloride channels. *Physiol Rev* 82(2): 503-68.

Jiang C, Agulian S,Haddad GG (1992). Cl- and Na+ homeostasis during anoxia in rat hypoglossal neurons: intracellular and extracellular in vitro studies. *J Physiol* 448: 697-708.

Jiang Q,Stys PK (2000). Calpain inhibitors confer biochemical, but not electrophysiological, protection against anoxia in rat optic nerves. *J Neurochem* 74(5): 2101-7.

Julian FJ, Moore JW, Goldman DE (1962) Membrane potentials of the lobster giant axon obtained by use of the sucrose-gap technique. *J. Gen. Physiol* 45: 1195-1216.

Kaila K (1994). Ionic basis of GABAA receptor channel function in the nervous system. *Prog Neurobiol* 42(4): 489-537.

Kakazu Y, Akaike N, Komiyama S,Nabekura J (1999). Regulation of intracellular chloride by cotransporters in developing lateral superior olive neurons. *J Neurosci* 19(8): 2843-51.

Kanaka C, Ohno K, Okabe A, Kuriyama K, Itoh T, Fukuda A,Sato K (2001). The differential expression patterns of messenger RNAs encoding K-Cl cotransporters (KCC1,2) and Na-K-2Cl cotransporter (NKCC1) in the rat nervous system. *Neuroscience* 104(4): 933-46.

Katchman AN, Vicini S,Hershkowitz N (1994). Mechanism of early anoxia-induced suppression of the GABAA-mediated inhibitory postsynaptic current. *J Neurophysiol* 71(3): 1128-38.

Kauppinen RA,Nicholls DG (1986). Failure to maintain glycolysis in anoxic nerve terminals. *J Neurochem* 47(6): 1864-9.

Kettenmann H (1987). K+ and Cl- uptake by cultured oligodendrocytes. *Can J Physiol Pharmacol* 65(5): 1033-7.

Kimelberg HK (1981). Active accumulation and exchange transport of chloride in astroglial cells in culture. *Biochim Biophys Acta* 646(1): 179-84.

Kocsis JD, Waxman SG, Hildebrand C,Ruiz JA (1982). Regenerating mammalian nerve fibres: changes in action potential waveform and firing characteristics following blockage of potassium conductance. *Proc R Soc Lond B Biol Sci* 217(1206): 77-87.

Krnjevic K,Schwartz S (1967). The action of gamma-aminobutyric acid on cortical neurones. *Exp Brain Res* 3(4): 320-36.

Kuffler SW, Nicholls JG,Orkand RK (1966). Physiological properties of glial cells in the central nervous system of amphibia. *J Neurophysiol* 29(4): 768-87.

Lancaster E, Oh EJ, Gover T,Weinreich D (2002). Calcium and calcium-activated currents in vagotomized rat primary vagal afferent neurons. *J Physiol* 540(Pt 2): 543-56.

Lascola CD,Kraig RP (1996). Whole-cell chloride currents in rat astrocytes accompany changes in cell morphology. *J Neurosci* 16(8): 2532-45.

Lascola CD, Nelson DJ,Kraig RP (1998). Cytoskeletal actin gates a Cl- channel in neocortical astrocytes. *J Neurosci* 18(5): 1679-92.

Leaney JL, Marsh SJ,Brown DA (1997). A swelling-activated chloride current in rat sympathetic neurones. *J Physiol* 501 (Pt 3): 555-64.

Lees GJ, Lehmann A, Sandberg M,Hamberger A (1990). The neurotoxicity of ouabain, a sodium-potassium ATPase inhibitor, in the rat hippocampus. *Neurosci Lett* 120(2): 159-62.

Lehning EJ, Doshi R, Stys PK,LoPachin RM, Jr. (1995). Mechanisms of injury-induced calcium entry into peripheral nerve myelinated axons: in vitro anoxia and ouabain exposure. *Brain Res* 694(1-2): 158-66.

Leppanen L, Stys PK (1997a). Ion transport and membrane potential in CNS myelinated axons I. Normoxic conditions. *J Neurophysiol* 78(4): 2086-94.

Leppanen L, Stys PK (1997b). Ion transport and membrane potential in CNS myelinated axons. II. Effects of metabolic inhibition. *J Neurophysiol* 78(4): 2095-107.

Li S, Mealing GA, Morley P, Stys PK (1999). Novel injury mechanism in anoxia and trauma of spinal cord white matter: glutamate release via reverse Na+-dependent glutamate transport. *J Neurosci* 19(14): RC16.

Li S, Stys PK (2000). Mechanisms of ionotropic glutamate receptor-mediated excitotoxicity in isolated spinal cord white matter. *J Neurosci* 20(3): 1190-8.

Li S, Stys PK (2001). Na(+)-K(+)-ATPase inhibition and depolarization induce glutamate release via reverse Na(+)-dependent transport in spinal cord white matter. *Neuroscience* 107(4): 675-83.

Lipton P (1999). Ischemic cell death in brain neurons. *Physiol Rev* 79(4): 1431-568.

Liu J, Lai ZF, Wang XD, Tokutomi N,Nishi K (1998). Inhibition of sodium current by chloride channel blocker 4,4'-diisothiocyanatostilbene-2,2'-disulfonic acid (DIDS) in guinea pig cardiac ventricular cells. *J Cardiovasc Pharmacol* 31(4): 558-67.

LoPachin RM, Lehning E (1997). Mechanism of Calcium entry during axon injury and degeneration. *Toxicol Appl Pharmacol.*143:233-44.

LoPachin RM, Jr., Saubermann AJ (1990). Disruption of cellular elements and water in neurotoxicity: studies using electron probe X-ray microanalysis. *Toxicol Appl Pharmacol* 106(3): 355-74.

LoPachin RM, Jr., Stys PK (1995). Elemental composition and water content of rat optic nerve myelinated axons and glial cells: effects of in vitro anoxia and reoxygenation. *J Neurosci* 15(10): 6735-46.

Lu J, Karadsheh M, Delpire E (1999). Developmental regulation of the neuronal-specific isoform of K-Cl cotransporter KCC2 in postnatal rat brains. *J Neurobiol* 39(4): 558-68.

Lux HD, Loracher C, Neher E (1970). The action of ammonium on postsynaptic inhibition of cat spinal motoneurons. *Exp Brain Res* 11(5): 431-47.

Lytle C (1997). Activation of the avian erythrocyte Na-K-Cl cotransport protein by cell shrinkage, cAMP, fluoride, and calyculin-A involves phosphorylation at common sites. *J Biol Chem* 272(24): 15069-77.

MacVicar BA, Feighan D, Brown A,Ransom B (2002). Intrinsic optical signals in the rat optic nerve: role for K(+) uptake via NKCC1 and swelling of astrocytes. *Glia* 37(2): 114-23.

Madden KP, Clark WM,Zivin JA (1993). Delayed therapy of experimental ischemia with competitive N-methyl-D-aspartate antagonists in rabbits. *Stroke* 24(7): 1068-71.

Mata M, Fink DJ, Ernst SA, Siegel GJ (1991). Immunocytochemical demonstration of Na+,K(+)-ATPase in internodal axolemma of myelinated fibers of rat sciatic and optic nerves. *J Neurochem* 57(1): 184-92.

Mayer ML (1985). A calcium-activated chloride current generates the after-depolarization of rat sensory neurones in culture. *J Physiol* 364: 217-39.

Mayer ML, Owen DG, Barker JL. (1990) Calcium-dependent chloride in vetebrate central neurons. In: Chloride channels and carriers of nerve, muscle and glial cells. (eds FJ Alvarez-Leefmans and J.M. Russell)New York: Plenum; p.355-364

McCarren M,Alger BE (1987). Sodium-potassium pump inhibitors increase neuronal excitability in the rat hippocampal slice: role of a Ca2+-dependent conductance. *J Neurophysiol* 57(2): 496-509.

McDonough AA, Geering K,Farley RA (1990). The sodium pump needs its beta subunit. *Faseb J* 4(6): 1598-605.

Mercado A, Song L, Vazquez N, Mount DB,Gamba G (2000). Functional comparison of the K+-Cl- cotransporters KCC1 and KCC4. *J Biol Chem* 275(39): 30326-34.

Misgeld U, Deisz RA, Dodt HU,Lux HD (1986). The role of chloride transport in postsynaptic inhibition of hippocampal neurons. *Science* 232(4756): 1413-5.

Mount DB, Mercado A, Song L, Xu J, George AL, Jr., Delpire E,Gamba G (1999). Cloning and characterization of KCC3 and KCC4, new members of the cation-chloride cotransporter gene family. *J Biol Chem* 274(23): 16355-62.

Muller M (2000). Effects of chloride transport inhibition and chloride substitution on neuron function and on hypoxic spreading-depression-like depolarization in rat hippocampal slices. *Neuroscience* 97(1): 33-45.

Nabekura J, Ueno T, Okabe A, Furuta A, Iwaki T, Shimizu-Okabe C, Fukuda A,Akaike N (2002). Reduction of KCC2 expression and GABAA receptor-mediated excitation after in vivo axonal injury. *J Neurosci* 22(11): 4412-7.

Nakao M,Gadsby DC (1989). [Na] and [K] dependence of the Na/K pump current-voltage relationship in guinea pig ventricular myocytes. *J Gen Physiol* 94(3): 539-65.

Neumcke B,Stampfli R (1982). Sodium currents and sodium-current fluctuations in rat myelinated nerve fibres. *J Physiol* 329: 163-84.

Nicholls DG,Budd SL (2000). Mitochondria and neuronal survival. *Physiol Rev* 80(1): 315-60.

Novakovic SD, Deerinck TJ, Levinson SR, Shrager P,Ellisman MH (1996). Clusters of axonal Na+ channels adjacent to remyelinating Schwann cells. *J Neurocytol* 25(6): 403-12.

Omar AI, Senatorov VV,Hu B (2001). Sodium-potassium adenosine triphosphatase inhibition enhances membrane accumulation of DiI in rat hippocampus in vivo. *Neuroscience* 102(2): 353-9.

O'Neill WC (1999). Physiological significance of volume-regulatory transporters. *Am J Physiol* 276(5 Pt 1): C995-C1011.

Orrenius S, Ankarcrona M,Nicotera P (1996). Mechanisms of calcium-related cell death. *Adv Neurol* 71: 137-49; discussion 149-51.

Ortiz-Carranza O, Adragna NC,Lauf PK (1996). Modulation of K-Cl cotransport in volume-clamped low-K sheep erythrocytes by pH, magnesium, and ATP. *Am J Physiol* 271(4 Pt 1): C1049-58.

Owen DG, Segal M,Barker JL (1986). Voltage-clamp analysis of a Ca2+- and voltage-dependent chloride conductance in cultured mouse spinal neurons. *J Neurophysiol* 55(6): 1115-35.

Owens DF, Boyce LH, Davis MB,Kriegstein AR (1996). Excitatory GABA responses in embryonic and neonatal cortical slices demonstrated by gramicidin perforated-patch recordings and calcium imaging. *J Neurosci* 16(20): 6414-23.

Park K, Arreola J, Begenisich T,Melvin JE (1998). Comparison of voltage-activated Cl-channels in rat parotid acinar cells with ClC-2 in a mammalian expression system. *J Membr Biol* 163(2): 87-95.

Payne JA (1997). Functional characterization of the neuronal-specific K-Cl cotransporter: implications for [K+]o regulation. *Am J Physiol* 273(5 Pt 1): C1516-25.

Payne JA,Forbush B, 3rd (1995). Molecular characterization of the epithelial Na-K-Cl cotransporter isoforms. *Curr Opin Cell Biol* 7(4): 493-503.

Payne JA, Stevenson TJ,Donaldson LF (1996). Molecular characterization of a putative K-Cl cotransporter in rat brain. A neuronal-specific isoform. *J Biol Chem* 271(27): 16245-52.

Pearson MM, Lu J, Mount DB,Delpire E (2001). Localization of the K(+)-Cl(-) cotransporter, KCC3, in the central and peripheral nervous systems: expression in the choroid plexus, large neurons and white matter tracts. *Neuroscience* 103(2): 481-91.

Plotkin MD, Kaplan MR, Peterson LN, Gullans SR, Hebert SC,Delpire E (1997a). Expression of the Na(+)-K(+)-2Cl- cotransporter BSC2 in the nervous system. *Am J Physiol* 272(1 Pt 1): C173-83.

Plotkin MD, Snyder EY, Hebert SC,Delpire E (1997b). Expression of the Na-K-2Cl cotransporter is developmentally regulated in postnatal rat brains: a possible mechanism underlying GABA's excitatory role in immature brain. *J Neurobiol* 33(6): 781-95.

Race JE, Makhlouf FN, Logue PJ, Wilson FH, Dunham PB,Holtzman EJ (1999). Molecular cloning and functional characterization of KCC3, a new K-Cl cotransporter. *Am J Physiol* 277(6 Pt 1): C1210-9.

Raman IM, Sprunger LK, Meisler MH,Bean BP (1997). Altered subthreshold sodium currents and disrupted firing patterns in Purkinje neurons of Scn8a mutant mice. *Neuron* 19(4): 881-91.

Ransom BR and Fern R (1996) Anoxic-Ischemic Glial Cell Injury. In: Tissue Oxygen Deprivation: From molecular to integrated function (eds. GG Haddad, G Lister) NY M Dekker. pp:617-652.

Ransom BR,Philbin DM, Jr. (1992). Anoxia-induced extracellular ionic changes in CNS white matter: the role of glial cells. *Can J Physiol Pharmacol* 70 Suppl: S181-9.

Ransom CB, Ransom BR,Sontheimer H (2000). Activity-dependent extracellular K+ accumulation in rat optic nerve: the role of glial and axonal Na+ pumps. *J Physiol* 522 Pt 3: 427-42.

Rasband MN, Trimmer JS, Peles E, Levinson SR,Shrager P (1999). K+ channel distribution and clustering in developing and hypomyelinated axons of the optic nerve. *J Neurocytol* 28(4-5): 319-31.

Ritchie JM (1995) Physiology of Axons. In: The Axon (eds SG Waxman, JD Kocsis, PK Stys) Oxford University Press, New York p.68-96.

Rivera C, Voipio J, Payne JA, Ruusuvuori E, Lahtinen H, Lamsa K, Pirvola U, Saarma M,Kaila K (1999). The K+/Cl- co-transporter KCC2 renders GABA hyperpolarizing during neuronal maturation. *Nature* 397(6716): 251-5.

Roper J,Schwarz JR (1989). Heterogeneous distribution of fast and slow potassium channels in myelinated rat nerve fibres. *J Physiol* 416: 93-110.

Rose CR,Ransom BR (1997). Regulation of intracellular sodium in cultured rat hippocampal neurones. *J Physiol* 499 (Pt 3): 573-87.

Ross ST,Soltesz I (2000). Selective depolarization of interneurons in the early posttraumatic dentate gyrus: involvement of the Na(+)/K(+)-ATPase. *J Neurophysiol* 83(5): 2916-30.

Russell JM (1979). Chloride and sodium influx: a coupled uptake mechanism in the squid giant axon. *J Gen Physiol* 73(6): 801-18.

Russell JM (2000). Sodium-potassium-chloride cotransport. *Physiol Rev* 80(1): 211-76.
Sabri MI,Ochs S (1971). Inhibition of glyceraldehyde-3-phosphate dehydrogenase in mammalian nerve by iodoacetic acid. *J Neurochem* 18(8): 1509-14.

Russell JM and Boron WF. (1990) Chloride Tranport in the Squid Giant Axon In: Chloride channels and carriers of nerve, muscle and glial cells. (eds FJ Alvarez-Leefmans and J.M. Russell)New York: Plenum; p.85-106.

Safronov BV, Kampe K,Vogel W (1993). Single voltage-dependent potassium channels in rat peripheral nerve membrane. *J Physiol* 460: 675-91.

Sah R, Schwartz-Bloom RD (1999) Optical Imaging reveals elevated intracellular chloride in hippocampal pyramidal neurons after oxidative stress. *J. Neurosci.* 19(2):9209-17.

Sakai S,Tosaka T (1999). Analysis of hyposmolarity-induced taurine efflux pathways in the bullfrog sympathetic ganglia. *Neurochem Int* 34(3): 203-12.

Sanfeliu C, Hunt A,Patel AJ (1990). Exposure to N-methyl-D-aspartate increases release of arachidonic acid in primary cultures of rat hippocampal neurons and not in astrocytes. *Brain Res* 526(2): 241-8.

Schanne FA, Kane AB, Young EE,Farber JL (1979). Calcium dependence of toxic cell death: a final common pathway. *Science* 206(4419): 700-2.

Schwiebert EM, Cid-Soto LP, Stafford D, Carter M, Blaisdell CJ, Zeitlin PL, Guggino WB,Cutting GR (1998). Analysis of ClC-2 channels as an alternative pathway for chloride conduction in cystic fibrosis airway cells. *Proc Natl Acad Sci U S A* 95(7): 3879-84.

Schwiening CJ,Boron WF (1994). Regulation of intracellular pH in pyramidal neurones from the rat hippocampus by Na(+)-dependent Cl(-)-HCO3- exchange. *J Physiol* 475(1): 59-67.

Scott RH, Sutton KG, Griffin A, Stapleton SR,Currie KP (1995). Aspects of calcium-activated chloride currents: a neuronal perspective. *Pharmacol Ther* 66(3): 535-65.

Sher PK (1988). Neurochemical correlates of cyanide-induced hypoxic neuronal damage in vitro. *Neurochem Res* 13(2): 159-63.

Shoukimas JJ,French RJ (1980). Incomplete inactivation of sodium currents in nonperfused squid axon. *Biophys J* 32(2): 857-62.

Shrager P (1989). Sodium channels in single demyelinated mammalian axons. *Brain Res* 483(1): 149-54.

Siesjo BK (1986). Cellular calcium metabolism, seizures, and ischemia. *Mayo Clin Proc* 61(4): 299-302.

Sik A, Smith RL,Freund TF (2000). Distribution of chloride channel-2-immunoreactive neuronal and astrocytic processes in the hippocampus. *Neuroscience* 101(1): 51-65.

Sivilotti L,Nistri A (1991). GABA receptor mechanisms in the central nervous system. *Prog Neurobiol* 36(1): 35-92.

Smith MR, Smith RD, Plummer NW, Meisler MH,Goldin AL (1998). Functional analysis of the mouse Scn8a sodium channel. *J Neurosci* 18(16): 6093-102.

Smith RL, Clayton GH, Wilcox CL, Escudero KW,Staley KJ (1995). Differential expression of an inwardly rectifying chloride conductance in rat brain neurons: a potential mechanism for cell-specific modulation of postsynaptic inhibition. *J Neurosci* 15(5 Pt 2): 4057-67.

Soliven B, Takeda M, Shandy T,Nelson DJ (1993). Arachidonic acid and its metabolites increase Cai in cultured rat oligodendrocytes. *Am J Physiol* 264(3 Pt 1): C632-40.

Srinivasan Y, Elmer L, Davis J, Bennett V,Angelides K (1988). Ankyrin and spectrin associate with voltage-dependent sodium channels in brain. *Nature* 333(6169): 177-80.

Stämpfli R (1954) A new method for measuring membrane potentials with external electrodes. *Experientia* 10:508-9.

Staley K (1994). The role of an inwardly rectifying chloride conductance in postsynaptic inhibition. *J Neurophysiol* 72(1): 273-84.

Steffensen I, Waxman SG, Mills L,Stys PK (1997). Immunolocalization of the Na(+)-Ca2+ exchanger in mammalian myelinated axons. *Brain Res* 776(1-2): 1-9.

Strange K, Singer TD, Morrison R,Delpire E (2000). Dependence of KCC2 K-Cl cotransporter activity on a conserved carboxy terminus tyrosine residue. *Am J Physiol Cell Physiol* 279(3): C860-7.

Stryer L (1988) Biochemistry. New York: WH Freeman. pp:356-362, 410-413, 503

Stys PK (1998). Anoxic and ischemic injury of myelinated axons in CNS white matter: from mechanistic concepts to therapeutics. *J Cereb Blood Flow Metab* 18(1): 2-25.
Stys PK (1994) WaveTrak: A data acquisition system and waveform database for Macintosh. *Sci. Comput. Automation* 10:19-24

Stys PK, Lehning E, Saubermann AJ,LoPachin RM, Jr. (1997). Intracellular concentrations of major ions in rat myelinated axons and glia: calculations based on electron probe X-ray microanalyses. *J Neurochem* 68(5): 1920-8.

Stys PK, Lopachin RM (1998). Mechanisms of calcium and sodium fluxes in anoxic myelinated central nervous system axons. *Neuroscience* 82(1): 21-32.

Stys PK, Ransom BR, Waxman SG (1990). Effects of polyvalent cations and dihydropyridine calcium channel blockers on recovery of CNS white matter from anoxia. *Neurosci Lett* 115(2-3): 293-9.

Stys PK, Ransom BR, Waxman SG (1991). Compound action potential of nerve recorded by suction electrode: a theoretical and experimental analysis. *Brain Res* 546(1): 18-32.

Stys PK, Ransom BR,Waxman SG (1992a). Tertiary and quaternary local anesthetics protect CNS white matter from anoxic injury at concentrations that do not block excitability. *J Neurophysiol* 67(1): 236-40.

Stys PK, Sontheimer H, Ransom BR,Waxman SG (1993). Noninactivating, tetrodotoxin-sensitive Na+ conductance in rat optic nerve axons. *Proc Natl Acad Sci U S A* 90(15): 6976-80.

Stys PK, Waxman SG,Ransom BR (1992b). Ionic mechanisms of anoxic injury in mammalian CNS white matter: role of Na+ channels and Na(+)-Ca2+ exchanger. *J Neurosci* 12(2): 430-9.

Sun D,Murali SG (1999). Na+-K+-2Cl- cotransporter in immature cortical neurons: A role in intracellular Cl- regulation. *J Neurophysiol* 81(4): 1939-48.

Tadic V (1992). The in vivo effects of cyanide and its antidotes on rat brain cytochrome oxidase activity. *Toxicology* 76(1): 59-67.

Taylor CP, Weber ML, Gaughan CL, Lehning EJ,LoPachin RM (1999). Oxygen/glucose deprivation in hippocampal slices: altered intraneuronal elemental composition predicts structural and functional damage. *J Neurosci* 19(2): 619-29.

Teng YD,Wrathall JR (1997). Local blockade of sodium channels by tetrodotoxin ameliorates tissue loss and long-term functional deficits resulting from experimental spinal cord injury. *J Neurosci* 17(11): 4359-66.

Thiemann A, Grunder S, Pusch M,Jentsch TJ (1992). A chloride channel widely expressed in epithelial and non-epithelial cells. *Nature* 356(6364): 57-60.

Thomas RC (1972a). Electrogenic sodium pump in nerve and muscle cells. *Physiol Rev* 52(3): 563-94.

Thomas RC (1972b). Intracellular sodium activity and the sodium pump in snail neurones. *J Physiol* 220(1): 55-71.

Thompson SM, Deisz RA,Prince DA (1988). Relative contributions of passive equilibrium and active transport to the distribution of chloride in mammalian cortical neurons. *J Neurophysiol* 60(1): 105-24.

Tian GF,Baker AJ (2000). Glycolysis prevents anoxia-induced synaptic transmission damage in rat hippocampal slices. *J Neurophysiol* 83(4): 1830-9.

Ullrich N,Sontheimer H (1996). Biophysical and pharmacological characterization of chloride currents in human astrocytoma cells. *Am J Physiol* 270(5 Pt 1): C1511-21.

Vabnick I, Novakovic SD, Levinson SR, Schachner M,Shrager P (1996). The clustering of axonal sodium channels during development of the peripheral nervous system. *J Neurosci* 16(16): 4914-22.

van den Pol AN, Obrietan K,Chen G (1996). Excitatory actions of GABA after neuronal trauma. *J Neurosci* 16(13): 4283-92.

Verbny Y, Zhang CL,Chiu SY (2002). Coupling of calcium homeostasis to axonal sodium in axons of mouse optic nerve. *J Neurophysiol* 88(2): 802-16.

Vogel W, Schwarz JR (1995) Voltage-clamp studies in axons: macroscopic and single channel currents. In: The Axon (eds SG Waxman, JD Kocsis, PK Stys) Oxford University Press, New York p.257-80.

Walz W (1992). Role of Na/K/Cl cotransport in astrocytes. *Can J Physiol Pharmacol* 70 Suppl: S260-2.

Walz W (2002). Chloride/anion channels in glial cell membranes. *Glia* 40(1): 1-10.

Walz W,Schlue WR (1982). External ions and membrane potential of leech neuropile glial cells. *Brain Res* 239(1): 119-38.

Waxman SG (1995) Voltage-gated ion channels in axons: Localization, function and development. In: The Axon (eds SG Waxman, JD Kocsis, PK Stys) Oxford University Press, New York p.116-43.

Waxman SG, Black JA, Ransom BR,Stys PK (1994). Anoxic injury of rat optic nerve: ultrastructural evidence for coupling between Na+ influx and Ca(2+)-mediated injury in myelinated CNS axons. *Brain Res* 644(2): 197-204.

Waxman SG, Black JA, Stys PK,Ransom BR (1992). Ultrastructural concomitants of anoxic injury and early post-anoxic recovery in rat optic nerve. *Brain Res* 574(1-2): 105-19.

Waxman SG,Ritchie JM (1993). Molecular dissection of the myelinated axon. *Ann Neurol* 33(2): 121-36.

Waxman SG,Sims TJ (1984). Specificity in central myelination: evidence for local regulation of myelin thickness. *Brain Res* 292(1): 179-85.

Williams JR, Sharp JW, Kumari VG, Wilson M,Payne JA (1999). The neuron-specific K-Cl cotransporter, KCC2. Antibody development and initial characterization of the protein. *J Biol Chem* 274(18): 12656-64.

Wolf JA, Stys PK, Lusardi T, Meaney D,Smith DH (2001). Traumatic axonal injury induces calcium influx modulated by tetrodotoxin-sensitive sodium channels. *J Neurosci* 21(6): 1923-30.

Wood JG, Jean DH, Whitaker JN, McLaughlin BJ,Albers RW (1977). Immunocytochemical localization of the sodium, potassium activated ATPase in knifefish brain. *J Neurocytol* 6(5): 571-81.

Wu JV,Shrager P (1994). Resolving three types of chloride channels in demyelinated Xenopus axons. *J Neurosci Res* 38(6): 613-20.

Xu JC, Lytle C, Zhu TT, Payne JA, Benz E, Jr.,Forbush B, 3rd (1994). Molecular cloning and functional expression of the bumetanide-sensitive Na-K-Cl cotransporter. *Proc Natl Acad Sci U S A* 91(6): 2201-5.

Yan Y, Dempsey RJ,Sun D (2001). Expression of Na(+)-K(+)-Cl(-) cotransporter in rat brain during development and its localization in mature astrocytes. *Brain Res* 911(1): 43-55.

Yu AC, Gregory GA,Chan PH (1989). Hypoxia-induced dysfunctions and injury of astrocytes in primary cell cultures. *J Cereb Blood Flow Metab* 9(1): 20-8.

Zalc B, Collet A, Monge M, Ollier-Hartmann MP, Jacque C, Hartmann L,Baumann NA (1984). Tamm-Horsfall protein, a kidney marker is expressed on brain sulfogalactosylceramide-positive astroglial structures. *Brain Res* 291(1): 182-7.